GENETIC DISSECTION AND FUNCTIONAL ANALYSIS OF SUPPRESSORS OF RECEPTOR-LIKE KINASE BAK1 FAMILY-MEDIATED CELL DEATH

A Dissertation

by

GUANGYUAN XU

Submitted to the Office of Graduate and Professional Studies of
Texas A&M University
in partial fulfillment of the requirements for the degree of

DOCTOR OF PHILOSOPHY

Chair of Committee,	Ping He
Co-chair of Committee	Libo Shan
Committee Members,	Wayne Versaw
	Keyan Zhu-Salzman
Interdisciplinary Faculty Chair,	Dirk B. Hays

August 2016

Major Subject: Molecular and Environmental Plant Sciences

ABSTRACT

Precise control of cell death is critical for all organismal survival. *Arabidopsis* receptor-like kinase BAK1 and SERK4 redundantly and negatively regulate cell death with elusive mechanisms. By deploying a genetic screen for suppressors of cell death triggered by virus-induced gene silencing of *BAK1/SERK4* on *Arabidopsis* knockout mutant collections, we identified STT3a, which is involved in *N*-glycosylation modification and cyclic nucleotide-gated channel 20, a nonselective cation channel, as important regulators as *bak1/serk4* cell death. Systematic investigation of glycosylation pathway and ER quality control (ERQC) components revealed distinct and overlapping mechanisms operating BAK1/SERK4- and their interacting protein BIR1-regulated cell death. Genome-wide transcriptional analysis revealed the activation of members of cysteine-rich receptor-like kinase (*CRK*) genes in the *bak1/serk4* mutant. Ectopic expression of *CRK4* induced STT3a/*N*-glycosylation-dependent cell death in *Arabidopsis* and *Nicotiana benthamiana*. Therefore, *N*-glycosylation and specific ERQC components are essential to activate *bak1/serk4* cell death, and CRK4 is likely among client proteins of protein glycosylation involved in BAK1/SERK4-regulated cell death. In addition, our genetic screen revealed that CNGC20 plays an important role in *bak1/serk4* cell death. Interestingly, *in vivo* and *in vitro* assays indicated that BAK1 directly interacts with and phosphorylates membrane-resident CNGC20. Mass spectrometry and mutagenesis analysis revealed that specific phosphorylation sites of CNGC20 by BAK1 are indispensable for its function in cell death control. In conclusion,

our findings unravel novel components and provide mechanistic insights into plant cell death regulation.

ACKNOWLEDGEMENTS

Time flies so fast, and my five-year's graduate study is ending. When I recall this experience, I have a lot to be thankful for. First, special thanks to my advisors, Dr. Ping He and Dr. Libo Shan for their support, encouragement, guidance and supervision over the course of my research and life. I learned a lot from them: they taught me how to do research objectively, how to present logically and how to write scientifically. They also consistently encourage me to never give up my scientist faith. Their serious attitudes toward science impress me a lot and will have a deep imprint in my future work. I also appreciate their care for my family. Thanks for holding the baby shower for my daughter and inviting my family to parities and picnics. Many thanks also go to my committee members, Dr. Wayne Versaw and Dr. Keyan Zhu-Salzman, for their guidance and support.

I am extremely thankful to Dr. Marcos V. V. de Oliveira who helped me a lot in my research. He frequently discussed scientific questions with me, which helped me grow a lot. Many thanks to Dr. Bo Li, who helped me do a lot of biochemical work in the CNGC20 project. In addition, I would like to thank all the lab members for the help, not only with the scientific discussion but also for providing a lot of help in my private life. Because of all of you, my graduate life was filled with so much love and fun. I appreciate all of your help and wish all of us a good future.

I also want to extend my gratitude to the China Scholarship Council for the scholarship. Without the support, I cannot have the chance to study in the USA. I wish my country become more prosperous and thriving.

The last but not least, I want to thank my parents and my wife who gave me endless encouragement and deep love. I cannot have finished my Ph.D study without them. I also want to thank my sweet daughter for bringing me so much happiness. I love you forever and wish you to grow happily all the time.

NOMENCLATURE

BAK1	BRI1-associated Receptor Kinase 1
BAM1	Barely Any Meristem 1
BKI1	BRI1 Kinase Inhibitor
BR	Brassinosteroid
BRI1	Brassinosteroid Insensitive 1
CaMBD	Calmodulin Binding Domain
CERK1	Chitin-Elicitor Receptor Kinase
CLV1	CLAVATA1
CNBD	Cyclic Nucleotide Binding Domain
CNGC	Cyclic Nucleotide-gated Channel
cNMPs	Cyclic nucleotide Monophosphates
CRK	Cysteine-rich Receptor-like Kinase
DAMP	Danger-Associated Molecular Pattern
DND	Defense, no death
PCD	Programmed Cell Death
dPCD/ePCD	Development-related PCD/environment-related PCD
EDS1	Enhanced Disease Susceptibility 1
EF-Tu	Elongation Factor-Tu
EFR	EF-Tu Receptor
ERL1	ER-like1
ERQC	ER Quality Control

FLS2	Flagellin Sensitive 2
HAE	HAESA
HR	Hypersensitive Response
HSL2	HAESA-like 2
LORE	LipoOligosaccharide-specific Reduced Elicitation
LPS	Lipopolysaccharide
LRR	Leucine-rich Repeat
lsd1	*l*esion *s*imulating *d*isease 1
MAPK	Mitogen-Activated Protein Kinase
MDIS1	Male Discoverer 1
MIK1	MDIS1-interacting Receptor-like Kinase1
NDR1	Non-race-specific Disease Resistance 1
NLPs	Necrosis and Ethylene-inducing Peptide 1-like Proteins
PAD4	Phytoalexin Deficient 4
PAMPs/MAMP	Pathogen-or Microbe-associated molecular patterns
PBC	Phosphate Binding Cassette
ReMAX	Receptor of eMAX /RLP1
RFO2	Resistance to Fusarium Oxysporum-2
RLK	Receptor-like Kinase
RLP	Receptor-like Protein
ROS	Reactive Oxygen Species
SA	Salicylic Acid

SAG101	Senescence-associated Gene 101
SERK	Somatic Embryogenesis Receptor Kinase
SNC2	Suppressor of NPR1, Constitutive-2
SOBIR1	Suppressor Of BIR1-1
UPR	Unfold Protein Response

TABLE OF CONTENTS

Page

LIST OF FIGURES

Page

LIST OF TABLES

Page

1 INTRODUCTION AND LITERATURE REVIEW

1.1 Plant receptor-like kinases (RLKs)/receptor-like proteins (RLPs) in diverse signaling

Plants are decorated with bunch of receptor-like kinases (RLKs) and receptor-like proteins (RLPs) at cell surface to perceive external environment cues and internal signals, relaying signaling cascades to target genes and proteins that are central to plant growth and development, innate immunity and stress adaptation. Typically, RLKs are composed of extracellular domain, a single membrane-spanning region and a cytoplasmic kinase domain. RLPs have similar compositions with RLKs except lacking cytosolic kinase domain. The *Arabidopsis* genome encodes around 600 RLKs and 57 RLPs (Shiu and Bleecker, 2001; Wang et al., 2008a). The largest subgroup of RLKs/RLPs are leucine-rich repeat (LRR-RLKs/RLPs) as they contain conserved consensus sequence LxxLxxLxLxxNxLt/sgxIpxxLG in their extracellular domains (Jones and Jones, 1997; Li and Tax, 2013). Members of LRR-RLKs/RLPs have been suggested to function as receptors to perceive plant growth hormone molecules, various microbial component-derived peptide ligands or endogenous peptide ligands.

1.1.1 RLKs/RLPs and plant development

RLKs/RLPs play important roles in a wide range of physical responses during plant life cycle, from zygotic embryogenesis to flowering. For example, brassinosteroid insensitive 1 (BRI1) regulates brassinosteroids (BRs) perception and signal initiation (Karlova et al., 2006; Li et al., 2002; Nam and Li, 2002); PSKR mediate plant architecture, cell proliferation and organ growth (Wang et al., 2015a); ER, ER-LIKE 1

(ERL1), ERL2 control stomatal development (Lee et al., 2012; Meng et al., 2015; Shpak et al., 2005); CLAVATA1 (CLV1), BARELY ANY MERISTEM 1 (BAM1), BAM2, and BAM3 are involved in apical meristem maintenance and development (Clark et al., 1997; DeYoung et al., 2006). HAESA (HAE) and HAESA LIKE 2 (HSL2) function redundantly to regulate floral organ abscission (Jinn et al., 2000; Stenvik et al., 2008). Recently, MALE DISCOVERER1 (MDIS1) and MDIS2, and MDIS1-INTERACTING RECEPTOR LIKE KINASE1 (MIK1) and MIK2, were found to recognize peptide LURE1 to initial the sexual reproduction in *Arabidopsis* (Wang et al., 2016).

1.1.2 RLKs/RLPs and plant defense response

In addition to development, several RLKs/RLPs participate in plant innate immunity. For example, FLAGELLIN SENSITIVE 2 (FLS2) confers immunity against bacterial flagellin or flg22 (a 22-amino-acid peptide corresponding to the amino (N)-terminus of flagellin) and initiates downstream immune responses (Chinchilla et al., 2006); EFR (EF-Tu receptor) initiates elongation factor-Tu (EF-Tu)-triggered immune responses (Zipfel et al., 2006). PEPR1 and PEPR2 recognize endogenous peptide pep1 known as danger-associated molecular pattern (DAMP) and released from plant cell due to pathogen infection, to amplify the immune responses (Huffaker et al., 2006; Huffaker and Ryan, 2007). *Arabidopsis* CERK1 (Chitin-Elicitor Receptor Kinase) directly binds chitin, a component from fungal cell walls to activate plant immune responses (Liu et al., 2012). Lipopolysaccharide (LPS) from gram-negative bacteria can be recognized by newly identified RLK LipoOligosaccharide-specific Reduced Elicitation (LORE) (Ranf et al., 2015). Among RLPs, RLP30 is required for the defense responses triggered by a

partially purified proteinaceous elicitor called sclerotinia culture filtrate elicitor 1 (SCFE1) from the necrotrophic fungal pathogen *Sclerotinia sclerotiorum* (Zhang et al., 2013). Another RLP SUPPRESSOR OF NPR1, CONSTITUTIVE-2 (SNC2) is a negative regulator in immune responses, as the *snc2* mutant exhibit constitutive defense response (Zhang et al., 2010). Recently, the *Arabidopsis* RESISTANCE TO FUSARIUM OXYSPORUM-2 (RFO2) was shown to be involved in resistance to the fungus *Fusarium oxysporum* (Shen and Diener, 2013) and RECEPTOR OF eMAX (ReMAX)/RLP1 detects ENIGMATIC MAMP OF XANTHOMONAS (eMAX) from *Xanthomonas* (Jehle et al., 2013).

1.2 Distinctive functions of BAK1/SERK family

Recent studies have shown that most RLKs/RLPs mentioned above are able to heterodimerize with another LRR-RLK, BRI1-associated receptor kinase 1 (BAK1), also known as somatic embryogenesis receptor kinases 3 (SERK3) upon cognate ligand perception. BAK1/SERK3 belongs to a subfamily of LRR-RLKs with 5 members (Chinchilla et al., 2009). SERKs harbor a relatively short extracellular domain with 5 LRRs (Boller and Felix, 2009; Chinchilla et al., 2009). SERK5 in the Col-0 ecotype, commonly used for most of studies, bears an amino acid polymorphism at a conserved site in the kinase domain from the other SERKs, which likely renders a nonfunctional kinase (Gou et al., 2012). Accumulating evidence suggests that SERK members coordinate a diverse range of distinct cellular functions via interacting with the corresponding receptors.

1.2.1 Function of BAK1/SERK in development

BAK1 was first identified in BR signaling from two independent studies. BR, a class of polyhydroxysteroid hormone regulating plant growth and development, is perceived by its receptor BRI1 (Kinoshita et al., 2005). Using the BRI1 kinase domain as a bait, a yeast two-hybrid screen identified BAK1 as the BRI1 interaction protein (Nam and Li, 2002). The other study employed genetic suppressor screening of *bri1-5* which is a weak allele of *bri1*. Overexpression of BAK1 partially rescued the *bri1-5* mutant phenotype (Li et al., 2002). Upon BL perception, BRI1 releases BRI1 kinase inhibitor (BKI1), a negative regulator, and recruits BAK1, resulting in sequential reciprocal *trans*-phosphorylation between BRI1 and BAK1, thereby triggering BR-mediated signaling (Kim et al., 2009; Wang et al., 2008b). Besides BAK1, SERK1 and SERK4 have been shown to interact physically with BRI1 and play redundant yet less pronounced roles in BR signaling pathway (Jeong et al., 2010; Karlova et al., 2006). Further genetic study indicates that the *serk1bak1serk4* triple mutant is complete insensitivity to BR treatment (Gou et al., 2012).

Besides the role in BR signaling, BAK1/SERK also are important players in PSK-mediated growth regulation (Tang et al., 2015), EPF-regulated stomatal development (Meng et al., 2015) and floral organ abscission with HAE/HSL (Meng et al., 2016).

1.2.2 Essential roles of BAK1/SERK in plant innate immunity

BAK1 was shown to interact with other ligand-binding receptor-like kinases mediating plant innate immune response. The first line of the innate immune responses

is triggered by perception of conserved pathogen- or microbe-associated molecular patterns (PAMPs or MAMPs) or damage-associated molecular patterns (DAMPs) via pattern recognition receptors (PRRs) (Chisholm et al., 2006; Jones and Dangl, 2006). BAK1 was shown to form complex with several PRRs, such as FLS2 and EFR. (Monaghan and Zipfel, 2012; Schwessinger and Ronald, 2012). Ligand binding to the corresponding PRR induces their association with co-receptor BAK1 through phosphorylation. Subsequently, BAK1 phosphorylates cytoplasmic kinase BIK1, which is further released from the complex (Lu et al., 2011). Activation of PRR complex further elicits downstream immune responses, including reactive oxygen species (ROS) production, mitogen-activated protein kinase (MAPK) activation and transcriptional reprogramming.

Pep1, originally identified as DAMP in *Arabidopsis,* induces receptor PERP1 heterodimerization with BAK1 (Schulze et al., 2010; Tang et al., 2015). BAK1 was also required for RLP30-meidated resistance to fungal pathogen *Sclerotinia sclerotiorum* (Zhang et al., 2013). Genetic screening identified a novel receptor like protein (RLP) ELR responding to elicitor from potato pathogen *Phytophthora infestans*. Further study revealed that BAK1 was most likely the partner with ELR to transmit downstream signaling (Du et al., 2015). Recent study showed that BAK1 played an essential role in signal transduction mediated by nlp20 which is a conserved 20aa peptide derived from multiple necrosis and ethylene-inducing peptide 1-like proteins (NLPs) (Albert et al., 2015).

1.2.3 Involvement of BAK1/SERK in the cell death control

BAK1 and SERK4 redundantly and negatively regulate plant cell death with an enigmatic mechanism. The *bak1serk4* null mutant, but not the cognate single mutants, is postembryonic seedling lethal associated with spontaneous cell death and constitutive H_2O_2 production (He et al., 2007). The genome-wide transcriptome analysis showed that the genes with significant changes in *bak1serk4* do not overlap with those in the *bri1* mutant, suggesting that BAK1 and SERK4-mediated cell death is likely uncoupled from the BR-mediated signaling. In addition, the *bak1-5* mutant with a mutation in the subdomain preceding the catalytic loop, which exhibits reduced kinase activity and largely compromised defense responses, is not impaired in the cell death control, as the *bak1-5serk4-1* double mutant is viable (Schwessinger et al., 2011). However, the *bak1-5* mutant retains normal BR-mediated responses, reconciling uncoupled functions of BAK1 and SERK4 in the cell death control and BR-mediated signaling. Furthermore, the kinase activity of BAK1 appears critical in the *bak1serk4* cell death control, as the kinase-inactive variants of BAK1 cannot rescue the *bak1serk4* cell death (Wang et al., 2008b).

1.3 Programmed cell death (PCD)

PCD is genetically controlled process leading to cell suicide. PCD is essential for plant development and stress responses. PCD in animals are well characterized and molecular basis is well studied (Bruggeman et al., 2015). In contrast, PCD in plants are less clear. It's hallmarks include cytoplasmic shrinkage, chromatin condensation, mitochondrial swelling, and plant specific characteristics, such as vacuolization and

chloroplast disruption. (Coll et al., 2011). PCD can be divided into development-related PCD (dPCD) and environment-related PCD (ePCD). Recent study identified common transcriptional signatures in various dPCD contexts (Olvera-Carrillo et al., 2015).

1.3.1 Hypersensitive response (HR)

HR, a form of PCD occurring at or near pathogen infection site, is initiated by pathogen effector recognition. After recognizing the effectors directly or indirectly by nucleotide-binding domain-LRR (NB-LRR) disease resistance proteins, plants utilize two separate signaling modules transducing signaling downstream: non-race-specific disease resistance 1 (NDR1) regulates coil-coil (CC)-NB-LRR signaling, while the enhanced disease susceptibility 1 (EDS1)/ phytoalexin deficient 4 (PAD4)/senescence-associated gene 101 (SAG101) complex mediates Toll/interleukin-1 receptor (TIR)-NB-LRR signaling. These signaling leads to SA and ROS production which synergistically cause HR which play important role in limiting biotrophic pathogen proliferation (Coll et al., 2011).

The regulation of HR is relatively studied extensively. Insights are gained from mutants exhibiting HR-like phenotype, also known as lesion mimic mutants. For example, *lsd1* (*l*esion *s*imulating *d*isease resistance), a classic lesion mimic mutant, displayed a runaway cell death phenotype. Several components involved in HR were identified on the basis of *lsd1* mutant. EDS1, PAD4, NDR1 are required for *lsd*-mediated cell death in response to pathogen (Bonardi et al., 2011; Roberts et al., 2013). In addition, *At*MC1 and *At*MC2, two types of metacaspases, antagonistically regulate HR (Coll et al., 2010). Recent studies indicate cell cycle components regulate effector

triggered PCD process. It was demonstrated plant homologs of E2F and Retinoblastoma, mammalian cell-cycle regulators, are required for effector-triggered HR (Wang et al., 2014).

1.3.2 MEKK1/MKK1/2/MPK4-mediated cell death

In the pathogen-triggered defense responses, mitogen-activated protein kinase (MAPK) cascades have been implicated in transducing signals from upstream receptors to the downstream targets (Pitzschke et al., 2009a). Perception of MAMPs induces two branches of MAPK cascade activation, MEKK1-MKK4/MKK5-MPK3/MPK6 or MEKK1-MKK1/MKK2-MPK4. It was reported that *mekk1*, *mkk1/2* and *mpk4* mutant exhibited seedling lethal phenotype (Gao et al., 2008). Genetic screening for the suppressor of *mkk1/mkk2* double mutant identified two suppressors, *summ1* and *summ2*, mutation of MEKK2 and R protein. Further analysis indicates that MEKK2 function upstream of SUMM2 in MEKK1-MKK1/2-MPK4-mediated cell death signaling (Kong et al., 2012; Zhang et al., 2012).

1.3.3 BIR1-mediated cell death

BIR1, a BAK1-interacting receptor like kinase, negatively regulate defense response, since the *bir1* mutant displayed spontaneous cell death, which is suppressed by another LRR-RLK SOBIR1 (Suppressor Of BIR1-1) (Gao et al., 2009). In addition, overexpression of SOBIR1 led to activate defense response and cell death (Gao et al., 2009).

1.4 Cyclic Nucleotide Gated Channel (CNGC)

The secondary messengers play an essential role in physiology and signal transduction. One group secondary messenger is cyclic-nucleotide monophosphates (cNMPs) which includes 3',5'-cyclic adenyl monophosphate (cAMP), and 3',5'-cyclic guanyl monophosphate (cGMP) (Martinez-Atienza et al., 2007; Newton and Smith, 2004) while another important secondary messenger is Ca^{2+}. Plants use calcium channels to sense and respond the endogenous and environmental stimuli-mediated Ca^{2+} elevation, such as during plant–pathogen interaction (Qi et al., 2010) and development process (Frietsch et al., 2007). One reported channel which both binds cNMP and uptakes Ca^{2+} is cyclic nucleotide-gated channel (CNGC). CNGC is a non-selective ligand-gated channel protein and present in both animals and plants. Only 6 CNGC genes (CNGA1–4, CNGB1, and CNGB3) have been identified in animal genome and the biological importance and regulation have been well studied (Cukkemane et al., 2011). However, plant CNGCs have only been recently investigated and the regulation mechanism is still obscure.

Plant CNGC comprises 6 transmembrane segments (S1-S6) with a pore region (P loop) between S5 and S6, one cyclic nucleotide binding domain (CNBD) and one calmodulin binding domain (CaMD). In the CNBD, the most conserved region is a phosphate binding cassette (PBC), which binds phosphate moiety. The location of CNBD and CaMBD differs in mammalian and plant system. In mammals, CNBD locates in N-terminal domain and CaMBD locates in C-terminal domain. In plants, both CNBD and CaMBD reside in C-terminal overlapping regions (Hua et al., 2003). This

may suggest that the regulation mechanism for CNGC in animals and plants is different. It has been implicated that CNGC channel gated by cNMP can be blocked upon CaM binding to CaMBD (Nawaz et al., 2014).

The first plant CNGC, HvCBT1 [*Hordeum vulgare* Camodulin (CaM)-binding transporter], was identified in a screen for calmodulin (CaM) binding partners in barley (Schuurink et al., 1998), In *Arabidopsis*, there are totally 20 putative CNGCs which are classified into four subfamilies (I-IV) based on sequencing similarity. Group IV was further divided into two subgroups (IVA and IVB) (Maser et al., 2001). Several CNGCs have been implicated to play important roles in diverse physiological response.

1.4.1 Ion uptake and homeostasis

Using electrophysiological methods or heterologous system involved in cation-uptake deficient yeast (*Saccharomyces cerevisiae*) and *Escherichia coli* mutants, multiple CNGCs have been shown to involve in the ion uptake and homeostasis. CNGC2 is an inwardly-rectified cNMP-gated cation channel and permeable to many monovalent cations, but not to Na^+ (Chan et al., 2003). Another CNGC which mediates metal uptake is CNGC1, since *cngc1* mutant showed enhanced tolerance to toxic Pb^{2+}. This is consistent with that CNGC1 preferentially expressed in root (Ma et al., 2006). Furthermore, CNGC3 was reported to involve in ion homeostasis. Compared with wild type, *cngc3* mutant had lower germination rates when grown on 100-140mM NaCl, while there was no significant difference when grown on KCl or NH_4Cl. This suggests that CNGC3 can act as Na^+ channel. Recently it was reported that CNGC5 and CNGC6 are Ca^{2+} permeable channel in guard cell (Wang et al., 2013).

1.4.2 The role of CNGC in plant development

It has been reported that *CNGC2* is induced at the early stages of plant senescence, suggesting CNGC2 may play a positive role in developmental cell death control. Both *cngc2* and *cngc4* mutant exhibit slow growth and low fertility compared with wild type. It has been hypothesized that the phenotype may be caused by hypersensitivity to Ca^{2+} (Chan et al., 2003). Recently several reports indicate that CNGC7, CNGC8, CNGC16 and CNGC18 play essential roles in pollen tube tip growth (Tunc-Ozdemir et al., 2013a; Tunc-Ozdemir et al., 2013b; Wang et al., 2013; Zhou et al., 2014). *Arabidopsis* CNGC14 is required for root gravitropism and CNGC17 participates in PSK-mediated signaling (Shih et al., 2015).

1.4.3 Involvement of CNGC in plant defense response

Arabidopsis dnd1 and *dnd2* (defense, no death), screened from ethyl methane sulfonate (EMS) mutated population, were impaired in hypersensitive response (HR) which is induced by avirulent pathogens (Yu et al., 1998). The *dnd1* mutant carries mutation in *CNGC2* while the *dnd2* mutant bears mutations in *CNGC4*. Recently it was indicated that Ca^{2+} elevation induced by endogenous peptide, known as DAMP acting to induce plant immune response to pathogens, was compromised in *cngc2* (Ma et al., 2012). In addition to CNGC2 and CNGC4, CNGC11 and CNGC12 are also implicated in plant immune responses, because *cpr22* mutant, which carries a 3kb- deletion resulting in a chimeric fusion of CNGC11 and CNGC12, showed autoimmune response (Yoshioka et al., 2006).

1.4.4 Overview for CNGC20

There are three independent studies about CNGC20. One study mainly focused on CNGC20 localization in *Arabidopsis*. It was demonstrated that CNGC20 localizes on vacuole membrane (Yuen and Christopher, 2013). In contrast, another study showed that CNGC20 localizes to plasma membrane and the sequential organization of CaMBD and CNBD in CNGC20 differs from other CNGC members in *Arabidopsis* (Fischer et al., 2013). The last study mainly addressed the expression pattern of *CNGC20* and showed that *CNGC20* expresses in the epidermis and the mesophyll, mainly in petioles (Kugler et al., 2009).

1.5 Protein glycosylation and ERQC

Protein glycosylation is an essential post-translational modification of secretory and membrane proteins in all eukaryotes (Strasser, 2016). When nascent proteins enters ER after translation, they usually go through post-translational glycosylation. Asparagine (*N)*-linked glycosylation, one of the most common glycosylation, plays important roles in protein folding, ER quality control, protein stability and protein-protein interactions. It is catalyzed by oligosaccharyltransferase (OST) complex which transfers the lipid (dolichol)-linked *N*-glycan precursor $Glc_3Man_9GlcNAc_2$ (Glc: glucose; Man: mannose; GlcNAc: *N*-acetylglucosamine) to the acceptor proteins. After transferring of *N*-glycan precursor to acceptor proteins, the terminal two glucose residues of the oligosaccharides are subsequently removed by glucosidase I and glucosidase II (RSW3 in *Arabidopsis*), and then recognized by the ER chaperone-like lectins, calnexin (CNX) and calreticulin (CRT3) for proper protein folding and secretion. The incompletely- or mis-folded

proteins will be recognized by UDP-glucose:glycoprotein glucosyltransferase (UGGT) for additional CNX/CRT cycles and another round of folding. ER-localized HSP70 proteins, BiPs, and their associated factors ERdj3 and SDF2 also play important roles to prevent export of misfolded proteins, especially the nonglycosylated ones. Proteins with native conformation after ERQC will be exported to the Golgi apparatus for further modifications, such as formation of complex and hybrid *N*-glycans catalyzed by stepwise enzymatic reactions, including β1,2-*N*-acetylglucosaminyltransferase I (CGL1/GNTI), α-mannosidase II (HGL1/MANII), GNTII, β1,2-xylosyltransferase (XYLT), α1,3-fucosyltransferase (FUCTa and FUCTb), β1,3-galactosyltransferase (GALT) and α1,4-fucosyltransferase (FUCTc).

Protein glycosylation is a vital part of the ER protein quality control. Dysfunctional protein glycosylation and folding may trigger ER stress, termed as unfold protein response (UPR). The UPR is a strategy to maintain the ER hemostasis and it is exerted by decreasing the amount of expressed protein amount, increasing expression of molecular chaperones to remove misfolded protein, as well as employing ER-associated protein degradation (ERAD) to deal with misfolded proteins (Wang et al., 2015b). Several important ER-localized proteins are involved in the UPR process, such as activating transcription factor 6 (ATF6), protein kinase RNA-like ER kinase (PERK) and inositol-requiring protein 1α (IRE1α) (Liu et al., 2002; Wang et al., 2015b). With accumulation of unfolded proteins, the molecular chaperone BiP binding to the misfolded protein activates the kinase activity of IRE1α, regulating cleavage of the transcriptional factor XBP1 (Wang et al., 2015b). Another member of the UPR, PERK

phosphorylates eukaryotic translation initiation factor 2α (eIF2α) and weakens protein translation (Harding et al., 1999). While the third member, ATF6, is released from the ER and is cleaved by site 1 and site 2 proteases in Golgi (S1P and S2P), generating a cytoplasmic transcription factor that activates expression of chaperones involved in protein folding and degradation (Ye et al., 2000).

1.6 Objective and importance for the study

Programmed cell death (PCD) has essential role in plant growth and development, and adaption for the stresses. A detailed characterization and signal transduction for PCD will help us engineer the crops with high yield and durable resistance.

We aim to obtain suppressors of *bak1/serk4* cell death by virus-induced gene silencing of *BAK1/SERK4* on *Arabidopsis* knockout mutant collections. Furthermore, we want to understand mechanisms behind *bak1/serk4* cell death by combining genetic, biochemical studies on these suppressors.

2 SPECIFIC CONTROL OF ARABIDOPSIS BAK1/SERK4-REGULATED CELL DEATH BY PROTEIN GLYCOSYLATION*

2.1 Summary

Precise control of cell death is essential for all organismal survival. *Arabidopsis* BAK1 and SERK4 redundantly and negatively regulate cell death with elusive mechanisms. By deploying a genetic screen for suppressors of cell death triggered by virus-induced gene silencing of *BAK1/SERK4* on *Arabidopsis* knockout collections, we identified STT3a, a protein involved in *N*-glycosylation modification, as an important regulator of *bak1/serk4* cell death. Systematic investigation of glycosylation pathway and ER quality control (ERQC) components revealed distinct and overlapping mechanisms operating BAK1/SERK4- and their interacting protein BIR1-regulated cell death. Genome-wide transcriptional analysis revealed the activation of members of cysteine-rich receptor-like kinase (*CRK*) genes in the *bak1/serk4* mutant. Ectopic expression of *CRK4* induced STT3a/*N*-glycosylation-dependent cell death in *Arabidopsis* and *Nicotiana benthamiana*. Therefore, *N*-glycosylation and specific ERQC components are essential to activate *bak1/serk4* cell death and CRK4 is likely among client proteins of protein glycosylation involved in BAK1/SERK4-regulated cell death.

---

*Reprinted with permission from "Specific control of Arabidopsis BAK1/SERK4-regulated cell death by protein glycosylation" by Marcos V.V.de Oliveira#, Guangyuan Xu#, Bo Li#, Luciano de Souza Vespoli, Xiangzong Meng, Xin Chen, Xiao Yu, Suzane Ariádina de Souza, Aline C. Intorne, Ana Marcia E. de A. Manhães, Abbey L. Musinsky, Hisashi Koiwa, Gonçalo A. de Souza Filho, Libo Shan and Ping He, 2016. *Nature Plants*, 2, 15218, Copyright 2016 by Nature Publishing Group.

2.2 Introduction

Plant receptor-like kinases (RLKs) regulate diverse biological processes ranging from plant growth, developm SPECIFIC CONTROL OF *ARABIDOPSIS* BAK1/SERK4-REGULATED CELL DEATH BY PROTEIN GLYCOSYLATION ent, symbiosis to immunity (Belkhadir et al., 2014; Shiu and Bleecker, 2003). BRI1 is a receptor for plant brassinosteroid (BR) hormones involving in plant growth and development (Li and Chory, 1997) and FLS2 is a receptor for bacterial flagellin or flg22 (a 22-amino acid peptide derived from flagellin) involving in plant immunity (Gómez-Gómez and Boller, 2000). Both BRI1 and FLS2 interact with a subgroup of RLKs, named somatic embryogenesis receptor kinases (SERKs), which consist of five members in *Arabidopsis*. Except for SERK5, likely a nonfunctional kinase in Col-0 background (Gou et al., 2012), SERK1, SERK2, SERK3 and SERK4 are involved in a wide range of physiological responses (aan den Toorn et al., 2015). SERK1 and SERK2 play a crucial and redundant role in male gametophyte development (Albrecht et al., 2005; Colcombet et al., 2005). SERK3, also known as BAK1, and SERK4 function in plant immunity by association with FLS2 and other immune receptors (Chinchilla et al., 2007; Heese et al., 2007; Postel et al., 2010; Roux et al., 2011). SERK1, BAK1 and SERK4 function in BR signaling by association with BRI1 (Gou et al., 2012; Li et al., 2002; Nam and Li, 2002). SERK1, SERK2, BAK1 and SERK4 regulate stomatal patterning via EPF peptide ligand-induced association with ERECTA family RLKs (Meng et al., 2015). In addition, SERK1, SERK2 and BAK1 regulate PSK peptide hormone-mediated root growth via association with its receptor PSKR (Ladwig et al., 2015; Wang et al., 2015a).

In addition, BAK1 and SERK4 negatively regulate plant cell death process (He et al., 2007; Kemmerling et al., 2007). The *bak1-4/serk4-1* null mutant is postembryonic seedling lethal associated with spontaneous cell death and constitutive H_2O_2 production (He et al., 2007). In contrast to the well-defined signaling framework of BAK1/SERK-mediated plant growth and immunity, the mechanisms underlying BAK1/SERK4-regulated cell death control are poorly understood. Notably, BIR1, a BAK1-interacting RLK, also negatively regulates cell death and the *bir1* mutant exhibits postembryonic seedling lethality, which depends on another RLK SOBIR1 (Gao et al., 2009). It remains unknown whether same or distinct mechanisms operate *bir1* and *bak1/serk4* cell death. As no viable seeds produced by the *bak1-4/serk4-1* null mutant plants, the conventional forward genetic screen of *bak1/serk4* cell death suppressors is not feasible. Here, we have developed an *Agrobacterium*-mediated tobacco rattle virus (TRV)-based virus-induced gene silencing (VIGS) system (Burch-Smith et al., 2006) with TRV-RNA2 vector harboring fragments of both *BAK1* and *SERK4*. Mutants that suppress *bak1/serk4* cell death were identified via VIGS screening of *Arabidopsis* T-DNA insertion lines. We report that protein glycosylation pathway and specific ER quality control (ERQC) components are essential for *bak1/serk4* cell death. Transcriptomic analysis revealed that the plasma membrane-associated genes, including members of cysteine-rich receptor-like kinase (*CRK*) genes, were highly enriched among up-regulated genes in *bak1-4/serk4-1*. Further biochemical and genetic investigations suggest that CRK4 is one of the client proteins of protein glycosylation involved in the BAK1/SERK4-regulated cell death process.

2.3 Materials and methods

2.3.1 Plant materials and growth conditions

Arabidopsis accessions Col-0 and C24 (wild-type, WT), various mutants and transgenic plants used in this study were grown in soil (Metro Mix 366) in a growth room at 23°C, 60% relative humidity, 70 μE $m^{-2}s^{-1}$ light with a 12-hr light/12-hr dark photoperiod for two-weeks before VIGS assay or 30 days for protoplast isolation. The *bak1-4*, *serk4-1*, *sobir1-12*, *stt3a-1*, *hgl1-1*, *rsw3-1*, *fucTa/fucTb/xylT*, *erdjb3b-1*, *sdf2-2* and *crt3-1* mutants and *NahG* transgenic plants were reported previously (Kang et al., 2008; Koiwa et al., 2003; Meng et al., 2015; Sun et al., 2014). The *ire1a/ire1b* and *bzip60/bzip28* double mutants were obtained from Dr. Stephen H. Howell (Deng et al., 2013). The sets of confirmed *Arabidopsis* T-DNA insertion lines (CS27941, CS27943 and CS27944), *stt3a-2*, *ost3/6* (SALK_067271C), *stt3b-2* (SALK_078498C), *stt3b-3* (Salk_134449C), *alg3* (SALK_040296C), *alg10-1* (SAIL_515_F10), *alg12* (SALK_200867C) and *crk4* (CS859967) were obtained from the *Arabidopsis* Biological Resource Center (ABRC) and confirmed by PCR using primers listed in the table. Seedlings were grown on agar plates containing ½ Murashige and Skoog medium (½MS) with 0.5% sucrose, 0.8% agar and 2.5 mM MES at pH 5.7, in a growth chamber at 23°C or 30°C, 70 μE $m^{-2}s^{-1}$ light with a 12-hr light/12-hr dark photoperiod.

2.3.2 Plasmid construction and generation of transgenic plants

To generate VIGS *BAK1*/*SERK4* construct, fragments of *BAK1* (319 bp) and *SERK4* (310 bp) were PCR amplified from *Arabidopsis* Col-0 cDNA with primers listed in Table S5, digested with EcoRI and NcoI for the *SERK4* fragment, and NcoI and KpnI

for the *BAK1* fragment, and ligated with the *pYL156* (*pTRV-RNA2*) vector pre-cut with EcoRI and KpnI(Burch-Smith et al., 2006). To generate VIGS constructs for individual genes, fragments of *SERK4* (310 bp), *CLAI* (541 bp), *MEKK1* (520 bp) and *BIR1* (491 bp) were PCR amplified from *Arabidopsis* Col-0 cDNA using primers listed in Table S5, digested with EcoRI and KpnI, and ligated into the *pYL156* (*pTRV-RNA2*) vector pre-cut with EcoRI and KpnI. All the clones were confirmed by sequencing.

The *CRK4* and *CRK5* genes were amplified from Col-0 cDNA with primers containing BamHI or NcoI at N terminus and StuI at C terminus (Table S5), and ligated into a plant protoplast expression vector *pHBT* with a *CaMV 35S* promoter at N-terminus and HA epitope-tag at C-terminus. The point mutations of $CRK4^{N181Q}$ and $CRK4^{N286Q}$ were generated by site-directed mutagenesis with primers listed in Table S5. To construct the *pCB302* binary vector containing *CRKs* for *Agrobacterium*-mediated transient expression assay in *Nicotiana benthamiana*, the *CRKs* fragment was released from the *pHBT* vector digested with BamHI or NcoI and StuI and ligated into the *pCB302* binary vector. The *Est::CRK4* binary vector construct was generated by inserting the PCR products of *CRK4* open reading frame with an HA epitope-tag at its C-terminus from the *pHBT-CRK4-HA* vector into the *pER8* vector using XhoI and SpeI sites (Meng et al., 2015). All the clones were confirmed by sequencing.

STT3a complementation transgenic plants in the *stt3a-2* background were reported previously (Koiwa et al., 2003). *Arabidopsis* transgenic plants were generated using *Agrobacterium*-mediated transformation by the floral-dip method. For estradiol induction of *CRK4* expression, the detached leaves of *Est::CRK4* T1 transgenic plants

were treated with 10 μM estradiol for 24 hr and the transgene expression was detected using immunoblotting with α-HA antibody.

2.3.3 *Arabidopsis* protoplast and *Nicotiana benthamiana* transient assays

For *Arabidopsis* protoplast transient expression, protoplasts from WT or *stt3a* mutant were transfected with HA-tagged *CRKs* in the *pHBT* vector and incubated for 12 hr. Proteins were isolated with 2 x SDS loading buffer and subjected to immunoblot analysis with anti-HA antibody.

For *N. benthamiana* transient expression, *Agrobacterium tumefaciens* strain GV3101 containing *pCB302* vector was cultured in LB medium at 28ºC for overnight. Bacteria were harvested by centrifugation and re-suspended with buffer (10 mM MES, pH5.7, 10 mM $MgCl_2$, 200 μM acetosyringone) at OD_{600}=0.75. Leaves of four-week-old soil-grown *N. benthamiana* were hand-infiltrated using a needleless syringe with *Agrobacterium* cultures. Leaf samples were collected 36 hr after infiltration for protein isolation and immunoblot analysis. Cell death phenotype was observed and leaf pictures were taken 4 days after infiltration under UV light with a ChemiDoc system.

2.3.4 Trypan blue and DAB staining

Trypan blue staining and 3, 3'-diaminobenzidine (DAB) staining were performed according to procedures described previously with modifications (Gao et al., 2013). Briefly, the excised plant tissues were immersed in trypan blue staining solution (2.5 mg/mL trypan blue in lactophenol [lactic acid: glycerol: liquid phenol: H_2O = 1:1:1:1]) or DAB solution (1 mg/mL DAB in 10 mM Na_2HPO_4 and 0.05% Tween 20). Samples were vacuum-infiltrated for 30 min and then incubated for 8 hr at 25ºC with gentle

shaking at 75 rpm. Subsequently, samples were transferred to trypan blue destaining solution (ethanol: lactophenol = 2:1) or DAB destaining solution (ethanol: acetic acid: glycerol = 3:1:1) and incubated at 65ºC for 30 min. The samples were then incubated in fresh destaining solution at room temperature until complete destaining. Pictures were taken under a dissecting microscope with samples in 10% glycerol.

2.3.5 *Agrobacterium*-mediated virus-induced gene silencing (VIGS) assay

Plasmids containing binary TRV vectors *pTRV-RNA1* and *pTRV-RNA2* derivatives, *pYL156-BAK1/SERK4, pYL156-SERK4, pYL156-MEKK1, pYL156-BIR1, pYL156-GFP* (the vector control) or *pYL156-CLA1* were introduced into *Agrobacterium tumefaciens* strain GV3101 by electroporation. *Agrobacterium* cultures were first grown in LB medium containing 50 μg/ml kanamycin and 25 μg/ml gentamicin for overnight and then sub-cultured in fresh LB medium containing 50 μg/ml kanamycin and 25 μg/ml gentamicin supplemented with 10 mM MES and 20 μM acetosyringone for overnight at 28°C in a roller drum. Cells were pelleted by 4200 rpm centrifugation, re-suspended in a solution containing 10 mM $MgCl_2$, 10 mM MES and 200 μM acetosyringone, adjusted to OD_{600} of 1.5 and incubated at 25°C for at least 3 hr. *Agrobacterium* cultures containing *pTRV-RNA1* and *pTRV-RNA2* derivatives were mixed at a 1:1 ratio and inoculated into the first pair of true leaves of two-week-old soil-grown plants using a needleless syringe. The *pYL156-CLA1* construct, which leads to plant albino phenotype two weeks after *Agrobacterium* infiltration, was included as a visual marker for VIGS efficiency.

2.4 Results

Arabidopsis wild-type (WT) Col-0 plants silenced with *BAK1*/*SERK4* showed severe growth defects with chlorotic leaves and dwarfism two weeks after *Agrobacterium*-inoculation, which resembled *bak1-4* plants silenced with *SERK4* (Fig. 1a). RT-PCR analysis revealed the reduced transcripts of *BAK1* and *SERK4*, but not *SERK1* or *SERK2* in *BAK1/SERK4*-silenced plants (Fig. 1b). Trypan blue and 3,3'-diaminobenzidine (DAB) staining indicated that WT plants upon silencing of *BAK1*/*SERK4* or the *bak1-4* mutant silenced with *SERK4* displayed spontaneous cell death and the elevated H_2O_2 accumulation (Fig. 1c). In addition, these plants showed increased level of *PR1* and *PR2* gene expression (Fig. 1d). The *bak1-4/serk4-1* cell death is partially dependent on plant defense hormone salicylic acid (SA) (He et al., 2007). Consistently, the transgenic plants carrying the bacterial salicylate hydroxylase gene *NahG* and the *sid2* mutant which is deficient in SA biosynthesis partially suppressed the cell death and H_2O_2 production triggered by VIGS of *BAK1*/*SERK4* (Fig. 1e & 2a). Taken together, these results demonstrate that silencing of *BAK1*/*SERK4* via VIGS phenocopies cell death observed in the *bak1-4/serk4-1* null mutant.

We tested whether *bak1/serk4* cell death depends on SOBIR1, which is required for *bir1* cell death. Similar with the *bir1* null mutant, WT plants silenced of *BIR1* by VIGS showed the cell death (Fig. 1f). The dwarfism and leaf chlorosis associated with silencing of *BIR1* were almost completely suppressed in *sobir1-12* (Fig. 1f). Interestingly, the *sobir1-12* mutant did not affect the cell death triggered by VIGS of *BAK1*/*SERK4* (Fig. 1f). We further generated the *bak1-4*/*serk4-1*/*sobir1-12* triple

mutant, which showed the same level of seedling lethality, elevated cell death and H_2O_2 accumulation with *bak1-4*/*serk4-1* (Fig. 1g). Activation of resistance (R) protein-mediated defense is a common mechanism of plant cell death. However, the *pad4* and *ndr1* mutants, which had impaired R protein pathways, did not significantly suppress the cell death caused by VIGS of *BAK1*/*SERK4* (Fig. 1h), suggesting that activation of R protein-mediated defenses may not play a major role in *bak1/serk4* cell death. In contrast, the *pad4* mutant largely alleviated the cell death caused by silencing of *BIR1* (Fig. 2b). Consistently, the BAK1/SERK4-regulated cell death does not require R proteins RPS2 and RPM1 (Fig. 2c). Together, the data indicate distinct mechanisms underlying BAK1/SERK4- and BIR1-regulated cell death.

Figure 1. The *sobir1* mutant did not suppress *bak1/serk4* cell death.

(a) Silencing of *BAK1/SERK4* by VIGS causes plant dwarfism and leaf chlorosis. Plants were photographed two weeks after inoculation of *Agrobacterium* carrying indicated VIGS vectors in *bak1-4* or WT plants. Bar = 1 cm. (b) RT-PCR analysis of *BAK1/SERK4*-silenced plants upon VIGS. Expression of *BAK1, SERK4, SERK1* and *SERK2* was analyzed by RT-PCR from WT plants two weeks after VIGS. *UBQ1* was used as an internal control. (c) Silencing of *BAK1/SERK4* by VIGS triggers cell death and H_2O_2 production. Trypan blue staining for cell death (upper panel) and DAB staining for H_2O_2 production (lower panel) are shown from true leaves of *VIGS* plants. Bar = 2 mm. (d) Silencing of *BAK1/SERK4* by VIGS induces *PR1* and *PR2* expression. The data are shown as mean ± SE from three independent repeats. The different letters denote statistically significant difference according to one-way ANOVA followed by Tukey test ($p<0.05$). (e) The BAK1/SERK4-regulated cell death is partially SA-dependent. Plants silenced with *CLA1 (Cloroplastos alterados 1*) showed albino phenotype as a visual marker of VIGS efficiency. *NahG* and *sid2* plants upon VIGS of *BAK1/SERK4* remained greener with reduced leaf chlorosis than WT. Bar = 1 cm. (f) The BAK1/SERK4-regulated cell death is SOBIR1-independent. Bar = 1 cm. (g) The *sobir1-12* mutant did not suppress *bak1-4/serk4-1* cell death in the *bak1-4/serk4-1/sobir1-12* mutant. Seedlings were grown on ½MS plate and photographed at 16 days after germination (top panel, Bar = 1 cm). Cotyledons were stained with trypan blue for cell death (middle panel) and DAB for H_2O_2 accumulation (bottom panel). Bar = 1 mm in middle and bottom panels. (h) The BAK1/SERK4-regulated cell death is PAD4 and NDR1-independent. Bar = 1 cm.

The above experiments were repeated at least three times with similar results.

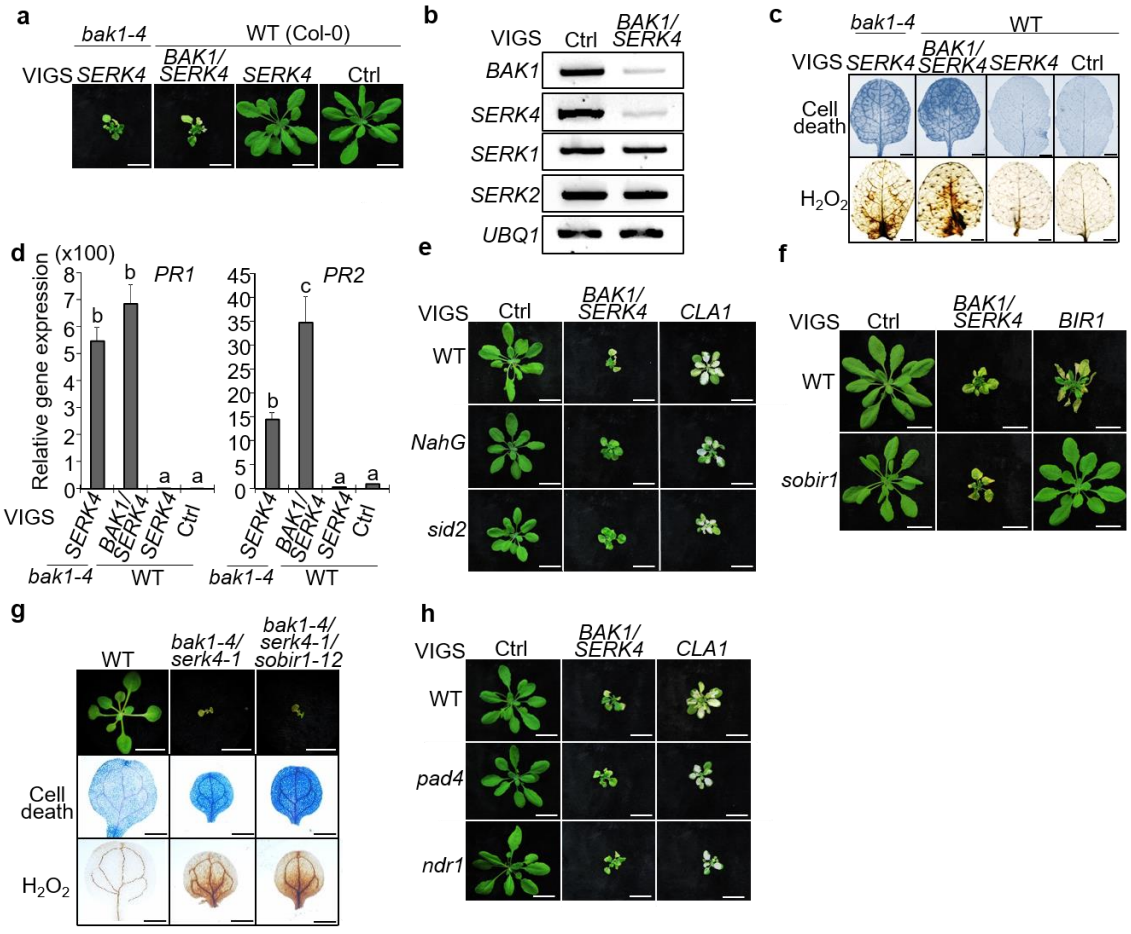
a
bak1-4
WT (Col-0)
VIGS
SERK4
BAK1/ SERK4
SERK4
Ctrl
b
VIGS
Ctrl
BAK1/ SERK4
BAK1
SERK4
SERK1
SERK2
UBQ1
c
bak1-4
WT
VIGS
SERK4
BAK1/ SERK4
SERK4
Ctrl
Cell death
H2O2
d
(x100)
Relative gene expression
PR1
PR2
VIGS
SERK4
BAK1/ SERK4
SERK4
Ctrl
bak1-4
WT
e
VIGS
Ctrl
BAK1/ SERK4
CLA1
WT
NahG
sid2
f
VIGS
Ctrl
BAK1/ SERK4
BIR1
WT
sobir1
g
WT
bak1-4/ serk4-1
bak1-4/ serk4-1/ sobir1-12
Cell death
H2O2
h
VIGS
Ctrl
BAK1/ SERK4
CLA1
WT
pad4
ndr1

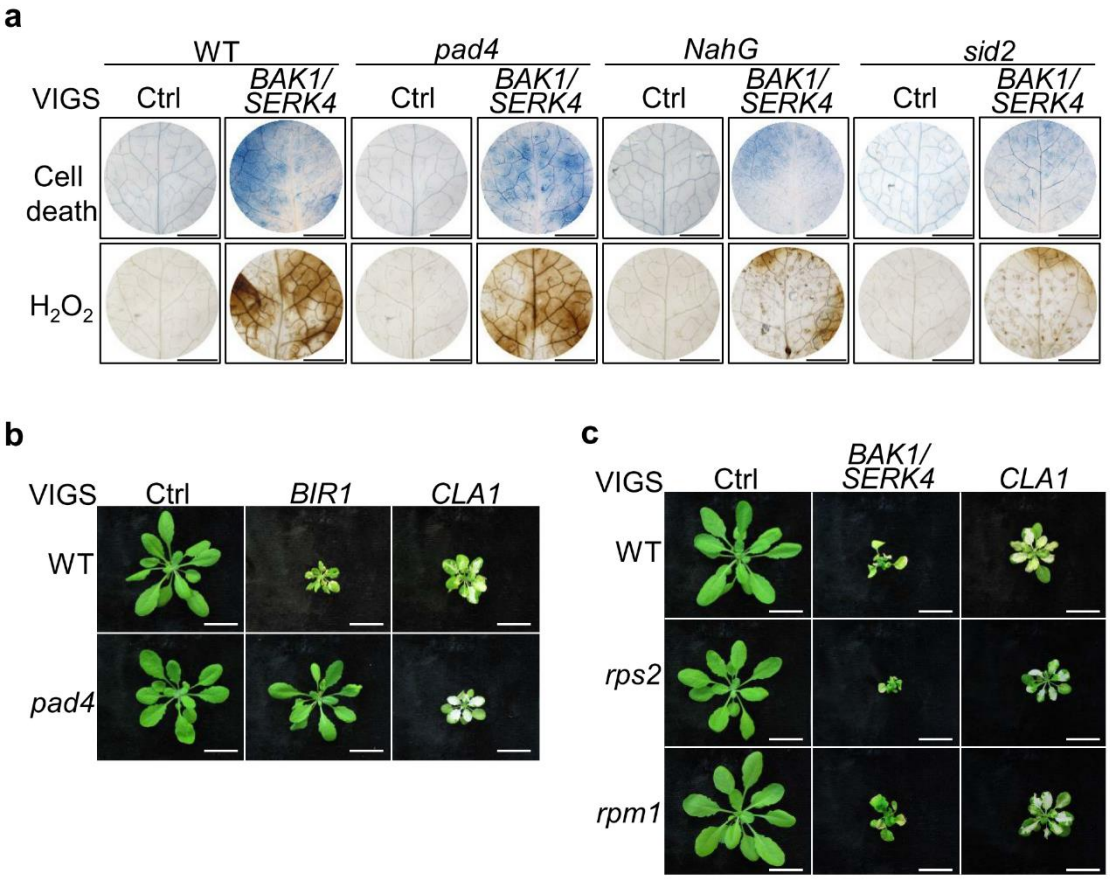

Figure 2. BAK1/SERK4-regulated cell death is partially suppressed in *NahG* and *sid2*, and independent of RPS2 and RPM1.

(a) *NahG* and *sid2* but not *pad4* partially suppress cell death and H_2O_2 production triggered by VIGS of *BAK1/SERK4*. True leaves of WT, *pad4*, *NahG* and *sid2* after VIGS of *BAK1/SERK4* or a vector control were stained with trypan blue for cell death (upper panel) and DAB for H_2O_2 accumulation (lower panel). Bar = 2 mm. (b) Plant phenotypes of Col-0 WT and *pad4* after VIGS of a vector control (Ctrl), *BIR1* or *CLA1*. Bar = 1 cm. (c) Plant phenotypes of WT, *rps2* and *rpm1* plants after VIGS of a vector control, *BAK1*/*SERK4* or *CLA1*. Bar = 1 cm.

To identify components involved in BAK1/SERK4-regulated cell death, we carried out a VIGS-based genetic screen of a sequence-indexed library of *Arabidopsis* T-DNA insertion lines. After screening ~6000 homozygous lines, a series of mutants were isolated based on the suppression of cell death by silencing of *BAK1/SERK4*. One

mutant (line CS800052 with an annotated T-DNA insertion at *STAUROSPORIN AND TEMPERATURE SENSITIVE3* [*STT3a*], *stt3a-2* [Fig. 4a]) largely suppressed the dwarfism and leaf chlorosis triggered by VIGS of *BAK1/SERK4* (Fig. 3a). MEKK1, a MAP kinase (MAPK) kinase kinase downstream of BAK1/SERK4 in flagellin signaling, is also involved in cell death regulation (Gao et al., 2008). Silencing of *MEKK1* by VIGS in WT plants resulted in severe dwarfism and cell death (Fig. 3a). However, the *stt3a-2* mutant did not suppress MEKK1-regulated cell death (Fig. 3a), suggesting different mechanisms underlying BAK1/SERK4- and MEKK1-regulated cell death. The data also suggest that *stt3a-2* did not affect the gene silencing machinery. RT-PCR analysis demonstrated a similar silencing efficiency of *BAK1/SERK4* by VIGS in WT and *stt3a-2* mutant (Fig. 4b). Furthermore, the cell death and elevated H_2O_2 accumulation caused by VIGS of *BAK1/SERK4* were almost completely abolished in *stt3a-2* (Fig. 3b). Compared with WT, *stt3a-2* showed much reduced accumulation of *PR1* and *PR2* genes upon VIGS of *BAK1*/*SERK4* (Fig. 3c). Another T-DNA insertion mutant s*tt3a-1*, which is in the ecotype C24 background, also suppressed the cell death by silencing of *BAK1*/*SERK4* (Fig. 3d). Furthermore, transformation of a genomic fragment containing the *STT3a* gene into *stt3a-2* restored BAK1/SERK4-regulated cell death (Fig. 3e & 4c). To investigate if *stt3a-2* could genetically suppress *bak1-4/serk4-1* seedling lethality and defense activation, we generated the *bak1-4/serk4-1/stt3a-2* triple mutant. The *bak1-4/serk4-1/stt3a-2* triple mutant overcame seedling lethality of *bak1-4/serk4-1* and resembled WT plants at two-week-old stage when grown on ½MS medium plates (Fig. 3f & 4d). In addition, cell death, H_2O_2 accumulation, and *PR1* and

PR2 expression were significantly ameliorated in *bak1-4/serk4-1/stt3a-2* compared with those in *bak1-4/serk4-1* (Fig. 3g & 3h). The *stt3a-2* mutant also partially suppressed VIGS of *BIR1*-induced cell death (Fig. 4e & 4f). The elevated expression of *PR1* and *PR2* was also significantly reduced in *stt3a-2* silenced with *BIR1* (Fig. 4g). This is consistent with that STT3a is required for the activation of defense responses in the *bir1* genetic mutant (Zhang et al., 2015).

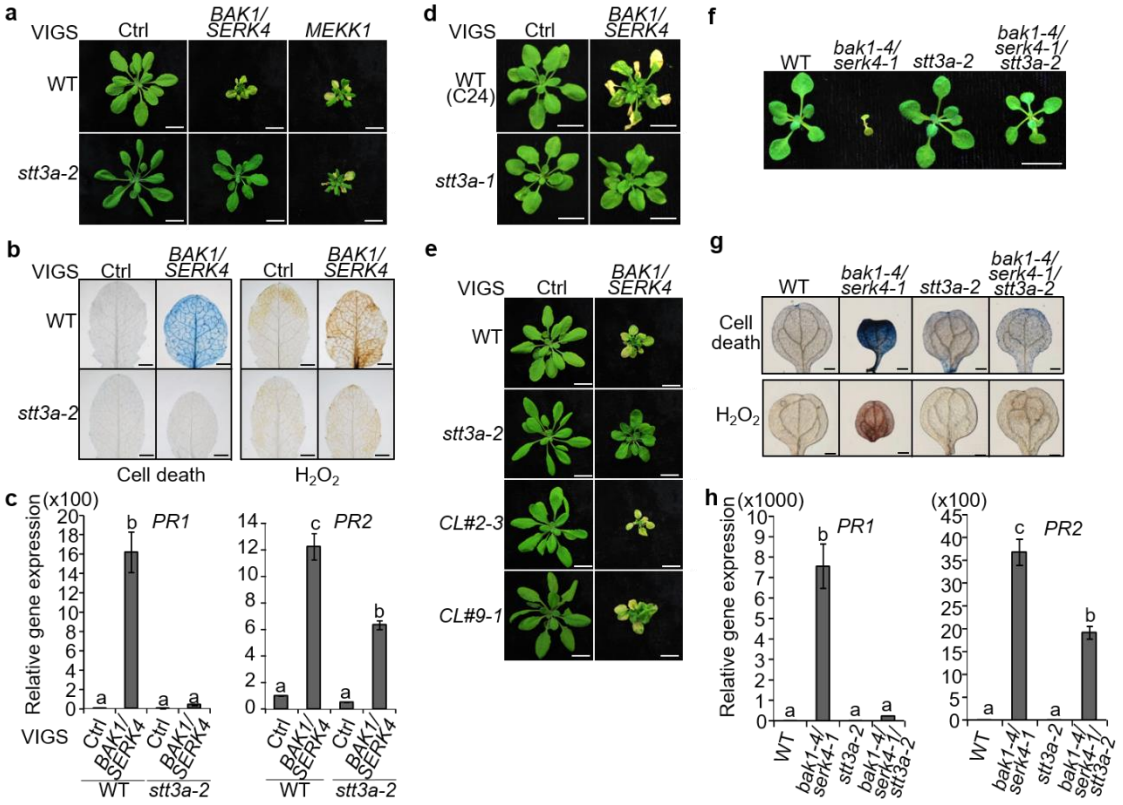

Figure 3. The *stt3a* mutants suppress BAK1/SERK4-regulated cell death.

(a) The *stt3a-2* mutant suppresses growth defects triggered by VIGS of *BAK1/SERK4* but not *MEKK1*. Bar = 1 cm (b) The *stt3a-2* mutant suppresses cell death (left panel) and H_2O_2 production (right panel) by VIGS of *BAK1/SERK4*. Bar = 2 mm. (c) The *stt3a-2* mutant suppresses *PR1* and *PR2* expression by VIGS of *BAK1/SERK4*. (d) The *stt3a-1* mutant suppresses growth defects by VIGS of *BAK1/SERK4*. Plant phenotypes are shown from WT (C24) and *stt3a-1* two weeks after VIGS. Bar = 1 cm. (e) Complementation of the *stt3a-2* mutant with *STT3a* restores growth defects by VIGS of *BAK1/SERK4*. CL#2-3 and CL#9-1 are two homozygous complementation lines. Bar = 1 cm. (f) The *stt3a-2* mutant rescues the seedling lethality of the *bak1-4/serk4-1* mutant. Seedlings were grown on ½MS plate and photographed at 16 days after germination. Bar = 1 cm. (g) The alleviated cell death and H_2O_2 accumulation in *bak1-4/serk4-1/stt3a-2*. Bar = 2 mm. (h) The reduced *PR1* and *PR2* expression in *bak1-4/serk4-1/stt3a-2*. The data in c & h are shown as mean ± SE from three independent repeats. The different letters denote statistically significant difference according to one-way ANOVA followed by Tukey test ($p<0.05$).

The above experiments were repeated three times with similar results.

Figure 4. The BIR1-regulated cell death is STT3a-dependent.

(a) Scheme of the *STT3a* gene and T-DNA insertion sites in *stt3a-1* (CS6388) and *stt3a-2* (CS800052). Solid bars indicate exons and lines indicate introns. Arrows indicate the T-DNA insertion sites. (b) The *stt3a-2* mutant did not affect the *BAK1/SERK4* VIGS efficiency. Expression of *BAK1* and *SERK4* in WT and *stt3a-2* plants two weeks after VIGS of a vector control or *BAK1/SERK4* was analyzed by RT-PCR. *UBQ1* was used as an internal control. (c) PCR confirmation of complementation lines. The DNA from WT, *stt3a-2* and complementation homozygous lines #2-3 and #9-1 was PCR amplified with the indicated primers to confirm the transformation of *STT3a* gene. The plasmid DNA from the binary vector *pCB301* containing the genomic DNA of *STT3a* was used as a positive control. *HPT*: Hygromycin phosphotransferase gene from the *pCB301* vector. The primer pair of LP and RP amplified the genomic DNA fragment of *STT3a* and the primer pair of LBb1 and RP amplified the T-DNA insertion from the *stt3a-2* mutant. (d) Fresh weight of 16-day-old seedlings of WT, *bak1-4/serk4-1*, *stt3a-2* and *bak1-4/serk4-1/stt3a-2* grown on ½MS plate. The data are shown as means ± SE (n = 15). The different letters denote statistically significant difference according to one-way ANOVA followed by Tukey test ($p<0.05$). (e) Plant phenotypes of WT and *stt3a-2* after VIGS with a vector control or *BIR1*. Bar = 1 cm. (f) Expression of *BIR1* in WT and *stt3a-2* plants after VIGS of a vector control or *BIR1*. (g) The *stt3a-2* mutant suppresses *PR1* and *PR2* expression triggered by VIGS of *BIR1*. The expression of *PR1* and *PR2* was normalized to the expression of *UBQ10*. The data are shown as mean ± SE from three independent repeats. The different letters denote statistically significant difference according to two-way ANOVA followed by Tukey test ($p<0.05$).

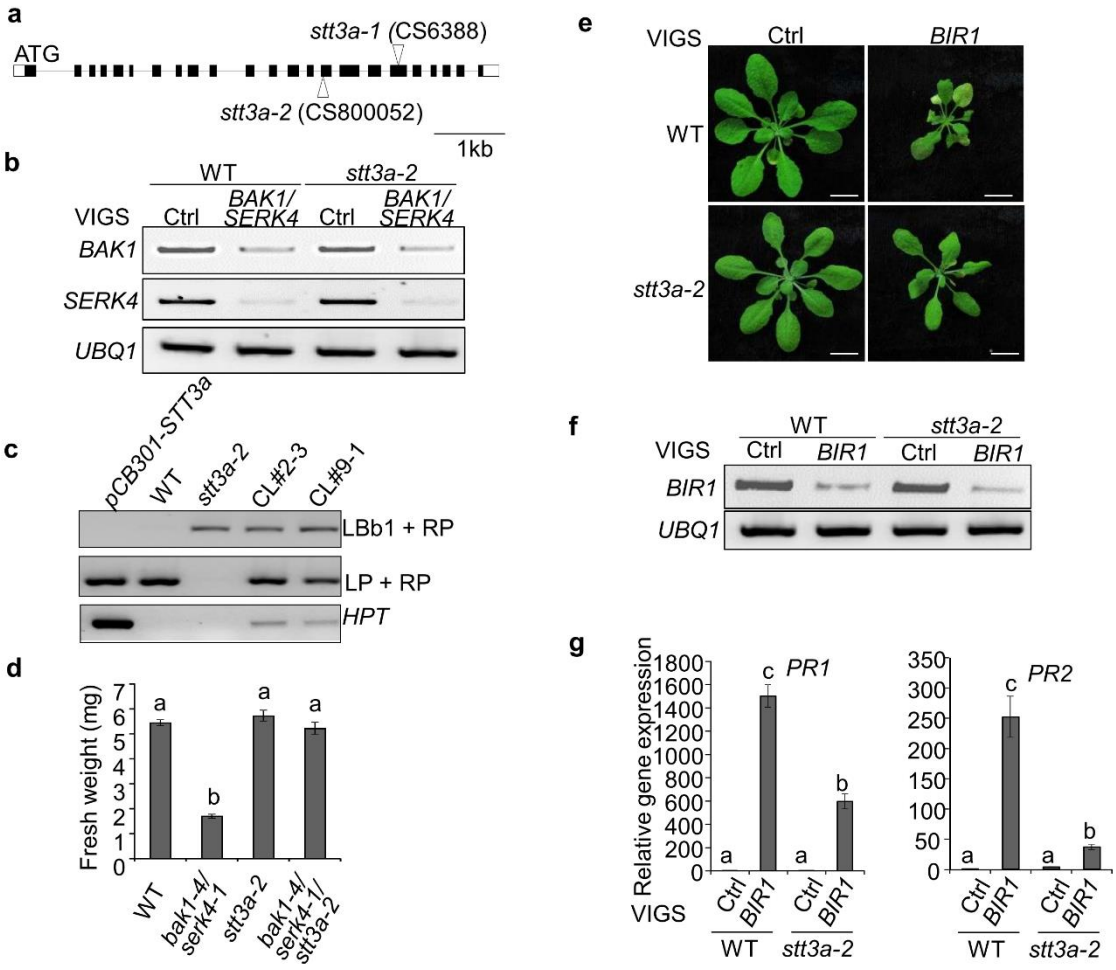
a
ATG
stt3a-1 (CS6388)
stt3a-2 (CS800052)
1kb
b
WT
stt3a-2
VIGS
Ctrl
BAK1/ SERK4
Ctrl
BAK1/ SERK4
BAK1
SERK4
UBQ1
c
pCB301-STT3a
WT
stt3a-2
CL#2-3
CL#9-1
LBb1 + RP
LP + RP
HPT
d
Fresh weight (mg)
WT
bak1-4/ serk4-1
stt3a-2
bak1-4/ serk4-1/ stt3a-2
e
VIGS
Ctrl
BIR1
WT
stt3a-2
f
WT
stt3a-2
VIGS
Ctrl
BIR1
Ctrl
BIR1
BIR1
UBQ1
g
Relative gene expression
PR1
PR2
VIGS
Ctrl
BIR1
WT
stt3a-2

Plant cell death and defense activation are often modulated by temperature and other environmental factors (Hua, 2013). When grown on ½MS medium plates, seedling lethality of *bak1-4*/*serk4-1* was largely ameliorated at 30ºC when compared with that at 23ºC (Fig. 5a & 5b). The elevated expression of *PR1* and *PR2* in *bak1-4*/*serk4-1* was also reduced when grown at 30ºC (Fig. 5c). The alleviation of seedling lethality and growth defects of *bak1-4*/*serk4-1* by the elevated temperature was a relatively subtle effect for plants grown on soil (Fig. 5d). However, the *bak1-4/serk4-1/stt3a-2* triple mutant grew significantly better on soil at 30ºC than that at 23ºC (Fig. 5d). The *bak1-4/serk4-1/stt3a-2* mutant could ultimately develop to maturity and occasionally produce some viable seeds when grown on soil at 30ºC.

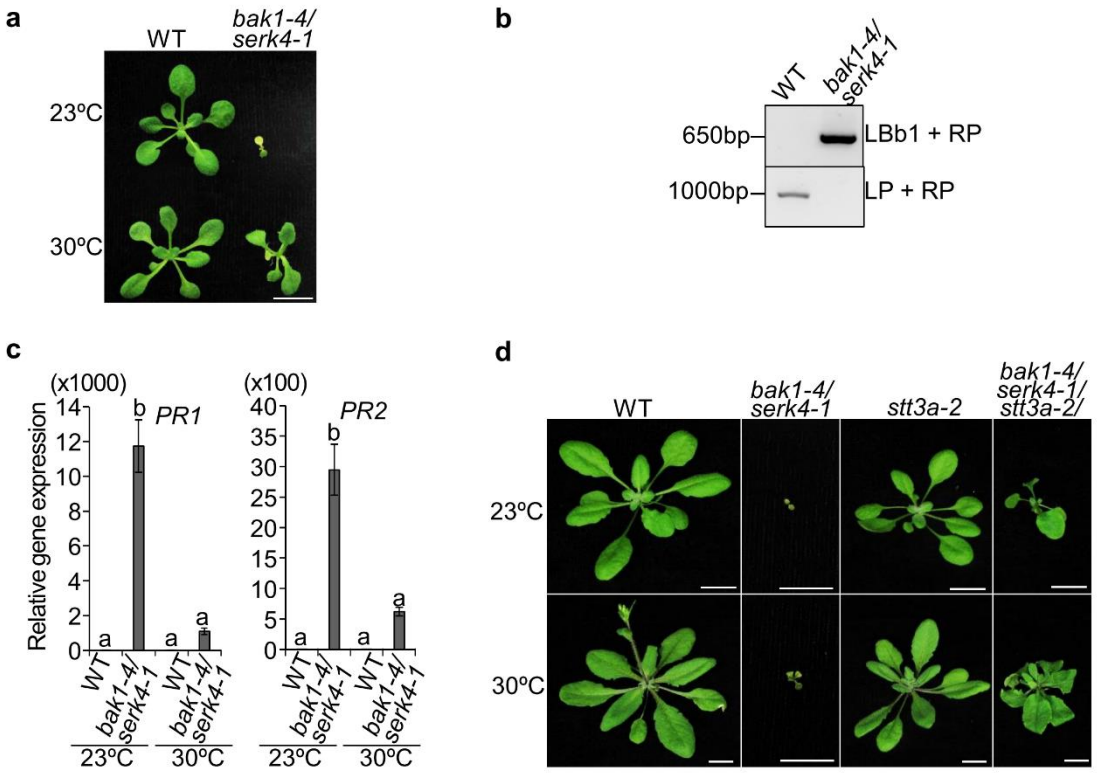

Figure 5. Temperature dependence of *bak1/serk4* cell death.

(a) Plant phenotype of WT and the *bak1-4/serk4-1* mutant at 23ºC and 30ºC. Seedlings were grown on ½MS plates with 12/12 hr light/dark in a growth chamber. The picture was taken 16 days after germination. Bar =1 cm. (b) The PCR confirmation of *bak1-4/serk4-1* mutant plants grown at 30ºC with the indicated primers. The primer pair of LP and RP amplified the genomic DNA fragment of *BAK1* and the primer pair of LBb1 and RP amplified the T-DNA insertion. (c) Relative *PR1* and *PR2* expression in WT and the *bak1-4/serk4-1* mutant at 23ºC and 30ºC. Seedlings grown on ½MS plates at different temperatures were harvested at 16 days after germination. The expression of *PR1* and *PR2* was normalized to the expression of *UBQ10*. The data are shown as mean ± SE from three independent repeats. The different letters denote statistically significant difference according to two-way ANOVA followed by Tukey test ($p<0.05$). (d) Plant phenotype of WT, *bak1-4/serk4-1, stt3a-2* and *bak1-4/serk4-1/stt3a-2* mutants at 23ºC and 30ºC on soil. Pictures of the *bak1-4/serk4-1* mutant were taken at 16 days after germination. Pictures for WT, *stt3a-2* and *bak1-4/serk4-1/stt3a-2* mutants were taken at 25 days after germination. Bar = 1 cm.

STT3 is the catalytic subunit of the oligosaccharyltransferase (OST) complex that is involved in protein *N*-glycosylation modifications (Fig. 6a) (Koiwa et al., 2003).

There are two family members of STT3, STT3a and STT3b, in *Arabidopsis*. The mutations in *STT3b* (*stt3b-2* and *stt3b-3*) did not affect the cell death by silencing of *BAK1/SERK4*, suggesting the specific function of *STT3a* in this process (Fig. 6b). This is consistent with the observation that STT3a, but not STT3b, is involved in *Arabidopsis* salt and osmotic stresses (Koiwa et al., 2003). In addition to the catalytic STT3 subunit, the OST complex also consists of several non-catalytic subunits that regulate substrate specificity, stability, or complex formation (Farid et al., 2013). The highly conserved subunit OST3/6 regulates overall protein glycosylation and is involved in plant immunity by controlling biogenesis of the EF-Tu receptor EFR (Farid et al., 2013). The *ost3/6* mutant also suppressed BAK1/SERK4-regulated cell death (Fig. 6b).

The OST complex transfers the lipid (dolichol)-linked *N*-glycan precursor $Glc_3Man_9GlcNAc_2$ (Glc: glucose; Man: mannose; GlcNAc: *N*-acetylglucosamine) to the acceptor proteins in the endoplasmic reticulum (ER) (Fig. 6a) (Liu and Li, 2014; Pattison and Amtmann, 2009). The *N*-glycan precursor is preassembled by a series of glucosyltransferases encoded by asparagine-linked glycosylation (ALG) proteins (Fig. 6a). Loss-of-function of some ALG proteins prevented assembly of the *N*-glycan precursor and reduced protein *N*-glycosylation effeciency in *Arabidopsis* (Farid et al., 2011; Hong et al., 2012). The *alg10*, but not *alg3* or *alg12* mutant, suppressed *BAK1/SERK4* silencing-mediated cell death (Fig. 6c), suggesting that proper assembly of *N*-glycan precursor is essential in *bak1/serk4* cell death. ALG10 catalyzes the last step of *N*-glycan precursor assembly by transferring the terminal glucose residue to the precursor, an essential step for the OST complex recognition. The *Arabidopsis alg10*

mutant had a severe defect in protein *N*-glycosylation and increased sensitivity to salt stress (Farid et al., 2011).

After transferring of *N*-glycan precursor to the acceptor proteins by the OST complex, the terminal two glucose residues of the oligosaccharides are subsequently removed by glucosidase I and glucosidase II (RSW3 in *Arabidopsis*), and then recognized by the ER chaperone-like lectins, calnexin (CNX) and calreticulin (CRT3) for proper protein folding and secretion (Fig. 6a) (Liu and Li, 2014; Pattison and Amtmann, 2009). The incompletely- or mis-folded proteins will be recognized by UDP-glucose:glycoprotein glucosyltransferase (UGGT) for additional CNX/CRT cycles and another round of folding (Fig. 6a) (Howell, 2013; Liu and Li, 2014; Pattison and Amtmann, 2009). ER-localized HSP70 proteins, BiPs, and their associated factors ERdj3 and SDF2 also play important roles to prevent export of misfolded proteins (Fig. 6a) (Howell, 2013). Some specific ERQC components, such as CRT3, UGGT, ERdj3b and SDF2, were genetically implicated in the protein folding and degradation of mutated bri1 receptor and immune receptor EFR and in BIR1-mediated cell death (Haweker et al., 2010; Jin et al., 2009; Jin et al., 2007; Li et al., 2009; Lu et al., 2009; Nekrasov et al., 2009; Saijo et al., 2009; Sun et al., 2014; von Numers et al., 2010; Zhang et al., 2015). We observed that *erdj3b-1* and *sdf2-2*, but not *crt3-1* or *rsw3-1*, partially suppressed *BAK1/SERK4* silencing-mediated cell death (Fig. 6d). RT-PCR analysis indicated a similar silencing efficiency of *BAK1/SERK4* by VIGS in WT and different mutants (Fig. 7a). As reported with genetic mutants (Sun et al., 2014), *crt3-1, erdj3b-1* and *sdf2-2* suppressed *BIR1* silencing-mediated cell death (Fig. 6d). We further generated genetic

mutants of *bak1-4/serk4-1/crt3-1*, *bak1-4/serk4-1/erdj3b-1* and *bak1-4/serk4-1/sdf2-2*. Similar to VIGS assays, *bak1-4/serk4-1/erdj3b-1* and *bak1-4/serk4-1/sdf2-2*, but not *bak1-4/serk4-1/crt3-1*, alleviated *bak1-4/serk4-1* seedling lethality and H_2O_2 production (Fig. 7b). The data further support that distinct mechanisms yet with certain overlapping features control BAK1/SERK4- and BIR1-regulated cell death.

Proteins with native conformation after ERQC will be exported to the Golgi apparatus for further modifications, such as formation of complex and hybrid *N*-glycans catalyzed by stepwise enzymatic reactions, including β1,2-*N*-acetylglucosaminyltransferase I (CGL1/GNTI), α-mannosidase II (HGL1/MANII), GNTII, β1,2-xylosyltransferase (XYLT), α1,3-fucosyltransferase (FUCTa and FUCTb), β1,3-galactosyltransferase (GALT) and α1,4-fucosyltransferase (FUCTc) (Fig. 6a) (Kang et al., 2008). To investigate if *N*-glycan maturation in the Golgi apparatus also plays a role in *bak1/serk4* cell death, we silenced *BAK1/SERK4* in the *cgl1-3* and *hgl1-1* single mutants and *fucTa/fucTb/xylT* triple mutant (Fig. 6e). All these mutants showed similar levels of cell death and growth retardation as WT plants after silencing of *BAK1/SERK4* by VIGS (Fig. 6e). Apparently, these mutants also did not affect the *BIR1* silencing-mediated cell death (Fig. 6e). These data suggest that protein glycosylation modification for proper folding in ER, but not *N*-glycan modification in Golgi, is essential for the initiation of *bak1/serk4* and *bir1* cell death. *N*-glycan modification in the Golgi apparatus is also not required for EFR maturation in plant immunity (Haweker et al., 2010).

Preventing protein *N*-glycosylation often leads to protein misfolding, a major contributor to ER stress, thereby resulting in unfolded protein response (UPR) (Howell, 2013). Defects in protein glycosylation and ERQC in the *sst3a*, *erdj3b* and *sdf2* mutants likely induce ER stress and UPR. *Arabidopsis* UPR signaling pathway is composed of two arms: one involving the bifunctional protein kinase/RNA ribonuclease IRE1 and its target RNA bZIP60, and another involving ER membrane-associated transcription factors, such as bZIP28 (Howell, 2013). To test if UPR may contribute to *bak1/serk4* cell death, we silenced *BAK1/SERK4* in the *ire1a/ire1b* and *bzip28/bzip60* double mutants, both of which are deficient in UPR induction (Deng et al., 2013). Neither *ire1a/ire1b* nor *bzip28/bzip60* affected cell death by VIGS of *BAK1/SERK4* (Fig. 7c), suggesting that UPR may not directly link to BAK1/SERK4-regulated cell death.

Figure 6. Control of BAK1/SERK4-regulated cell death by protein N-glycosylation and specific components of ERQC.

(a) A schematic overview of protein *N*-glycan assembly in ER and modification in Golgi apparatus and ERQC system. The OST complex transfers the dolichol-linked *N*-glycan precursor preassembled by different ALG glucosyltransferases to the acceptor proteins in the ER. The *N*-glycan precursor is then modified by ER glucosidase, and recognized by CNX and CRT3 for proper protein folding. The mis-folded proteins undergo additional CNX/CRT cycles by UGGT and glucosidase for another round of folding. The BiP/ERdj3/SDF2 complex also controls proper protein folding. The correctly folded proteins will be exported to the Golgi apparatus to form complex *N*-glycans catalyzed by different enzymes. (b) The *ost3/6*, but not *stt3b* mutants, suppresses cell death by VIGS of *BAK1/SERK4*. Phenotypes of different plants are shown two weeks after VIGS. Bar = 1 cm. (c) The *alg10*, but not *alg3* or *alg12* mutant, suppresses cell death by VIGS of *BAK1/SERK4*. Bar = 1 cm. (d) Differential ERQC components are required for BAK1/SERK4- and BIR1-regulated cell death. The *erdj3b-1* and *sdf2-2* mutants partially suppressed BAK1/SERK4- and BIR1-regulated cell death by VIGS. However, the *crt3-1* mutant, only suppressed BIR1-, but not BAK1/SERK4-regulated cell death by VIGS. Bar = 1 cm. (e) The *N*-glycan modification in the Golgi apparatus may not be required for BAK1/SERK4-regulated cell death. Various mutants impaired in *N*-glycan modification in the Golgi apparatus did not suppress cell death by VIGS of *BAK1/SERK4* or *BIR1*. Bar = 1 cm. The above experiments were repeated three times with similar results.

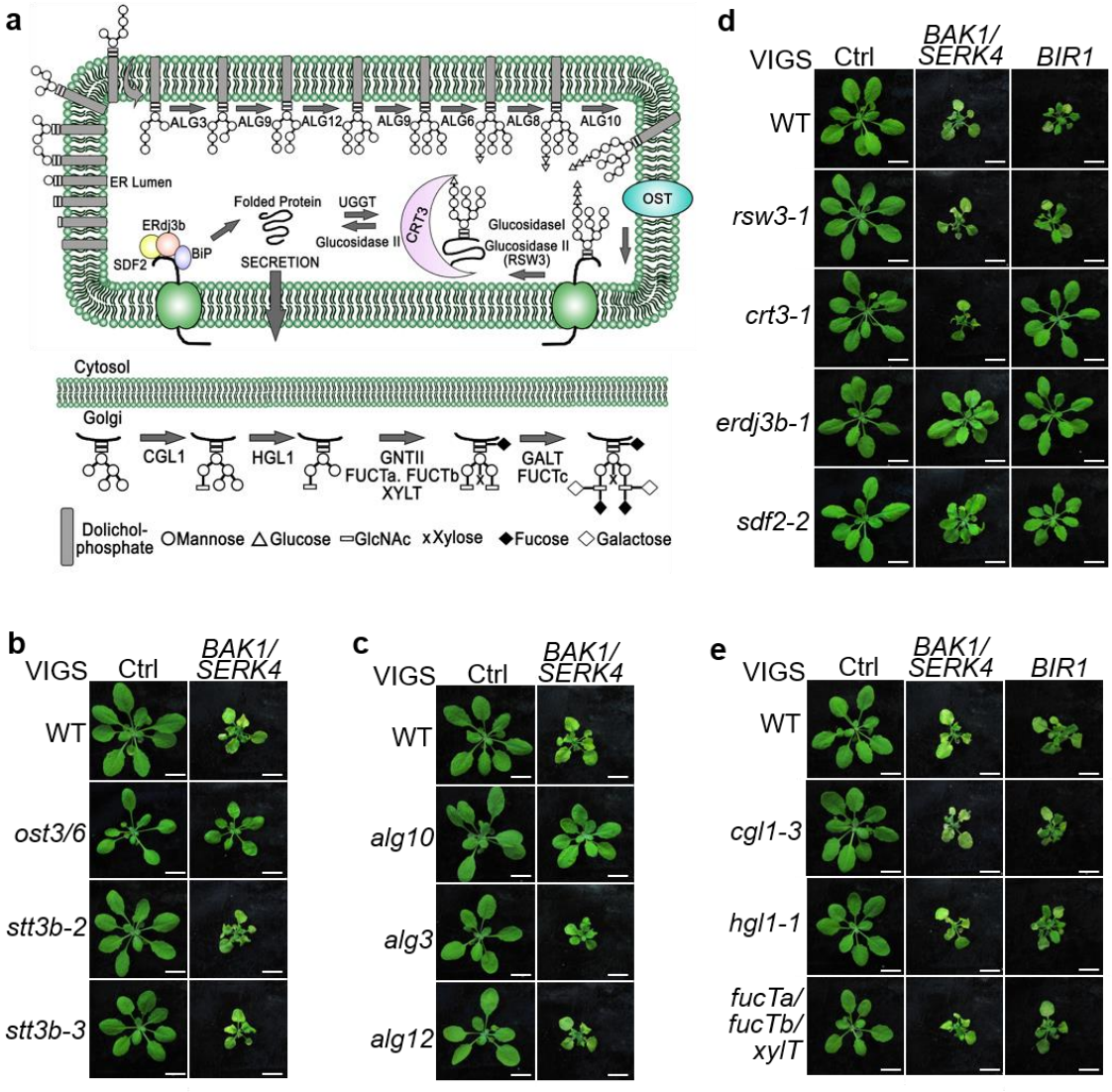
a
ALG3
ALG9
ALG12
ALG9
ALG6
ALG8
ALG10
ER Lumen
OST
ERdj3b
BiP
SDF2
Folded Protein
UGGT
Glucosidase II
SECRETION
CRT3
Glucosidase I
Glucosidase II
(RSW3)
Cytosol
Golgi
CGL1
HGL1
GNTII
FUCTa. FUCTb
XYLT
GALT
FUCTc
Dolichol-
phosphate
Mannose
Glucose
GlcNAc
Xylose
Fucose
Galactose
d
VIGS
Ctrl
BAK1/
SERK4
BIR1
WT
rsw3-1
crt3-1
erdj3b-1
sdf2-2
b
VIGS
Ctrl
BAK1/
SERK4
WT
ost3/6
stt3b-2
stt3b-3
c
VIGS
Ctrl
BAK1/
SERK4
WT
alg10
alg3
alg12
e
VIGS
Ctrl
BAK1/
SERK4
BIR1
WT
cgl1-3
hgl1-1
fucTa/
fucTb/
xylT

Figure 7. ERQC, but not UPR signaling components, are involved in bak1/serk4 cell death.

(a) The *ost3/6, alg10, erdj3b-1 and sdf2-2* mutants did not affect the *BAK1/SERK4* VIGS efficiency. Expression of *BAK1* and *SERK4* in WT and different mutant plants two weeks after VIGS of a vector control or *BAK1/SERK4* was analyzed by RT-PCR. *UBQ1* was used as an internal control. (b) Specific ERQC components contribute to *bak1/serk4* cell death. Col-0 WT, *bak-4/serk4-1*, *bak1-4/serk4-1/erdj3b-1*, *bak1-4/serk4-1/sdf2-2*, *bak1-4/serk4-1/crt3-1* and *bak1-4/serk4-1/stt3a-2* plants were grown on soil and photographed at 12 days after germination (top panel, Bar = 0.5 cm). Cotyledons were stained with trypan blue for cell death (middle panel) and DAB for H_2O_2 accumulation (bottom panel). Bar = 1 mm in middle and bottom panels. (c) The UPR mutants did not affect *BAK1/SERK4*-regulated cell death by VIGS. Plants silenced with *CLA1* showed albino phenotype as a visual marker of VIGS efficiency. Bar = 1 cm.

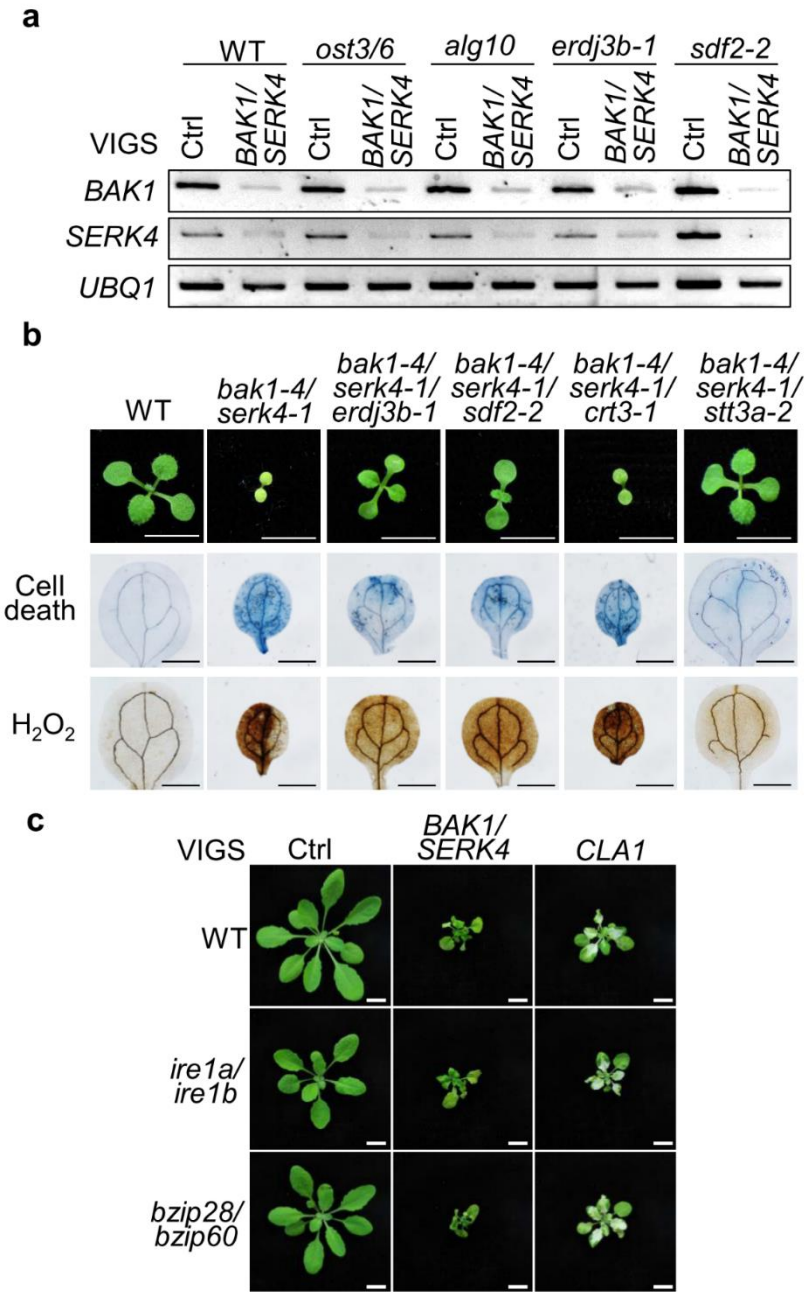
a
WT
ost3/6
alg10
erdj3b-1
sdf2-2
VIGS
Ctrl
BAK1/ SERK4
BAK1
SERK4
UBQ1
b
WT
bak1-4/ serk4-1
bak1-4/ serk4-1/ erdj3b-1
bak1-4/ serk4-1/ sdf2-2
bak1-4/ serk4-1/ crt3-1
bak1-4/ serk4-1/ stt3a-2
Cell death
H2O2
c
VIGS
Ctrl
BAK1/ SERK4
CLA1
WT
ire1a/ ire1b
bzip28/ bzip60

Figure 8. Uncoupled BAK1 functions in cell death control, immunity and BR signaling.

(a) The *stt3a-2* mutation did not interfere with the compromised flg22-induced MAPK activation in the *bak1-4* mutant. Ten-day-old seedlings were treated without or with 100 nM flg22 for 15 and 30 min. The MAPK activation was analyzed by immunoblot with α-pERK antibody (top panel), and the protein loading is shown by Ponceau S staining for RuBisCo (RBC) (bottom panel). (b) The *stt3a-2* mutation did not interfere with the compromised flg22-induced MAPK activation in the *bak1-4/serk4-1* mutant. (c) The *stt3a-2* mutation did not affect the compromised flg22-induced BIK1 phosphorylation in the *bak1-4* mutant. Protoplasts from different plants were transfected with HA-tagged BIK1 and treated with 100 nM flg22 for 10 min. BIK1-HA proteins were detected by immunoblot using α-HA antibody (top panel), and the protein loading is shown by Ponceau S staining for RBC (bottom panel). (d) The *stt3a-2* mutation did not affect the compromised flg22-induced marker gene expression in the *bak1-4/serk4-1* mutant. Ten-day-old seedlings were treated without or with 100 nM flg22 for 30 or 60 min for qRT-PCR analysis. The data are shown as mean ± SE from three independent repeats. Asterisks indicate statistically significant differences from WT within the same time point according to two-way ANOVA followed by Tukey test ($p<0.05$). (e, f) The *bak1- 4/ serk4-1* sensitivity to BRZ still occurs in the *bak1-4*/*serk4-1/stt3a-2* mutant. The seedlings of indicated genotypes were grown in the dark for five days on ½MS plates with or without 2 μM BRZ (e), and hypocotyl lengths were quantified (f). The data are shown as mean ± SE from 20 seedlings. Bar = 0.5 cm. The different letters denote statistically significant difference according to two-way ANOVA followed by Tukey test ($p<0.05$).
The experiments in a, b, c & d were repeated three times and e & f were repeated twice with similar results.

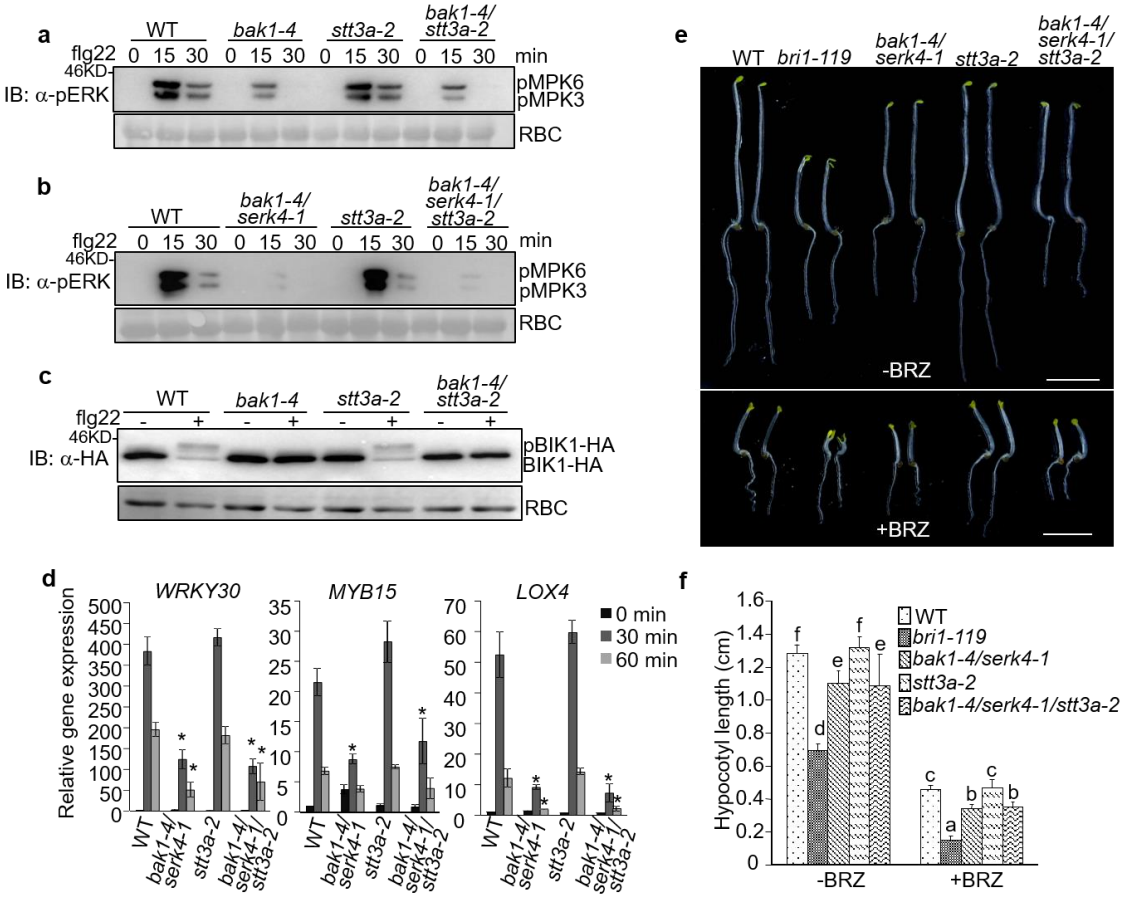
a
WT
bak1-4
stt3a-2
bak1-4/ stt3a-2
flg22
0 15 30 0 15 30 0 15 30 0 15 30 min
46KD
IB: α-pERK
pMPK6
pMPK3
RBC
b
WT
bak1-4/ serk4-1
stt3a-2
bak1-4/ serk4-1/ stt3a-2
flg22
0 15 30 0 15 30 0 15 30 0 15 30 min
46KD
IB: α-pERK
pMPK6
pMPK3
RBC
c
WT
bak1-4
stt3a-2
bak1-4/ stt3a-2
flg22
- + - + - + - +
46KD
IB: α-HA
pBIK1-HA
BIK1-HA
RBC
d
WRKY30
MYB15
LOX4
Relative gene expression
0 min
30 min
60 min
WT
bak1-4/ serk4-1
stt3a-2
bak1-4/ serk4-1/ stt3a-2
e
WT
bri1-119
bak1-4/ serk4-1
stt3a-2
bak1-4/ serk4-1/ stt3a-2
-BRZ
+BRZ
f
Hypocotyl length (cm)
WT
bri1-119
bak1-4/serk4-1
stt3a-2
bak1-4/serk4-1/stt3a-2
-BRZ
+BRZ

In contrast to the negative regulation in cell death, BAK1 and SERK4 positively regulate plant immunity and BR signaling (Chinchilla et al., 2007; Gou et al., 2012; Heese et al., 2007; Li et al., 2002; Nam and Li, 2002; Postel et al., 2010; Roux et al., 2011). We tested whether the mutation in *stt3a* also suppressed *bak1* or *bak1/serk4* deficiency in flagellin and BR signaling. Flg22 triggers rapid phosphorylation of MAPKs and receptor-like cytoplasmic kinase BIK1(Wu et al., 2014). The *bak1-4* and *bak1-4/serk4-1* mutants displayed a compromised flg22-induced MAPK activation (Fig. 8a & 8b), and BIK1 phosphorylation (Fig. 8c). The *stt3a* mutant did not affect flg22 signaling as previously reported (Fig. 8a) (Haweker et al., 2010). The compromised flg22-induced MAPK activation and BIK1 phosphorylation remained same in *bak1-4/stt3a-2* and *bak1-4/serk4-1/stt3a-2* as those in *bak1-4* or *bak1-4/serk4-1* (Fig. 8a, 8b & 8c). Similar with *bak1-4/serk4-1, bak1-4/serk4-1/stt3a-2* showed a compromised expression of flg22-induced genes, *WRKY30, MYB15* and *LOX4,* compared to WT or *stt3a-2* (Fig. 8d). Taken together, these results suggest that *stt3a-2* did not suppress *bak1-4 or bak1-4/serk4-1* deficiency in flagellin-mediated immune signaling. When grown in the dark, the hypocotyls of *bak1-4/serk4-1* mutant elongated slightly, but significantly shorter than those of WT plants (Fig. 8e & 8f). In the presence of brassinazole (BRZ), an inhibitor of BR biosynthesis, *bak1-4/serk4-1* displayed shorter hypocotyl elongation than WT. The *stt3a-2* mutant exhibited similar hypocotyl elongation as WT plants. The hypocotyl elongation of *bak1-4/serk4-1/stt3a-2* was similar to that of *bak1-4/serk4-1* in the absence or presence of BRZ (Fig. 8e & 8f),

suggesting that *stt3a-2* did not interfere with the responsiveness of *bak1-4/serk4-1* to BRZ.

As *PR* genes are highly upregulated in the *bak1/serk4* cell death process, we determined the genome-wide transcriptional changes in *bak1-4/serk4-1* by RNA-sequencing (RNA-seq) analysis. Among 24,572 detectable transcripts (Fig. 9a), we identified 3637 differentially expressed genes (fold change ≥ 2 and false discovery rate [FDR] < 0.1) in *bak1-4/serk4-1* compared to WT plants (Fig. 9b). Interestingly, Gene Ontology (GO) enrichment analysis indicated that genes encoding proteins associated with membrane, especially plasma membrane, were highly enriched among the up-regulated genes in *bak1-4/serk4-1* (Fig. 9c). Remarkably, among 44 *CRK* genes, the expression of 22 *CRKs* was up-regulated in *bak1-4/serk4-1* (Fig. 9d). The induction of *CRK4, CRK5, CRK7, CRK8, CRK19* and *CRK20* in *bak1-4/serk4-1* was confirmed by quantitative RT-PCR (qRT-PCR) (Fig. 9e).

Figure 9. Members of CRK genes are up-regulated in the *bak1/serk4* mutant.

(a) DESeq's *plotMA* displays differential expression (log_2 fold changes between *bak1- 4/ serk4-1* and WT in y-axis) versus expression strength (the mean of normalized counts in x-axis). Genes with significantly differential expression with FDR < 0.10 and fold change ≥ 2 are color-coded in red. (b) The Heatmaps of up-regulated and down-regulated genes in the *bak1/serk4* mutant compared to WT. The original means of read counts were subjected to data adjustment by log_2 transformation using MeV4.0 for the heatmaps. The genes are plotted in the order of fold changes. (c) Gene Ontology (GO) enrichment analysis based on the cellular component. The x-axis indicates the enrichment scores [$-log_{10}$ (p-value)] (p-value: the possibility of the significant enrichment) for each cellular component GO item in the y-axis. (d) Members of *CRKs* are induced in *bak1/serk4*. The upper panel indicates log_2 fold change of different *CRK* genes (*bak1-4/serk4-1* vs. WT) and the bottom panel shows normalized expression level from two independent repeats (#1 and #2). (e) Expression of some *CRKs* by qRT-PCR analysis. Ten-day-old seedlings grown on ½MS plates were subjected for qRT-PCR analysis. The data are shown as means ± SE from three biological replicates. * indicates a significant difference with $p<0.05$ when compared to WT with a Student's *t*-test.

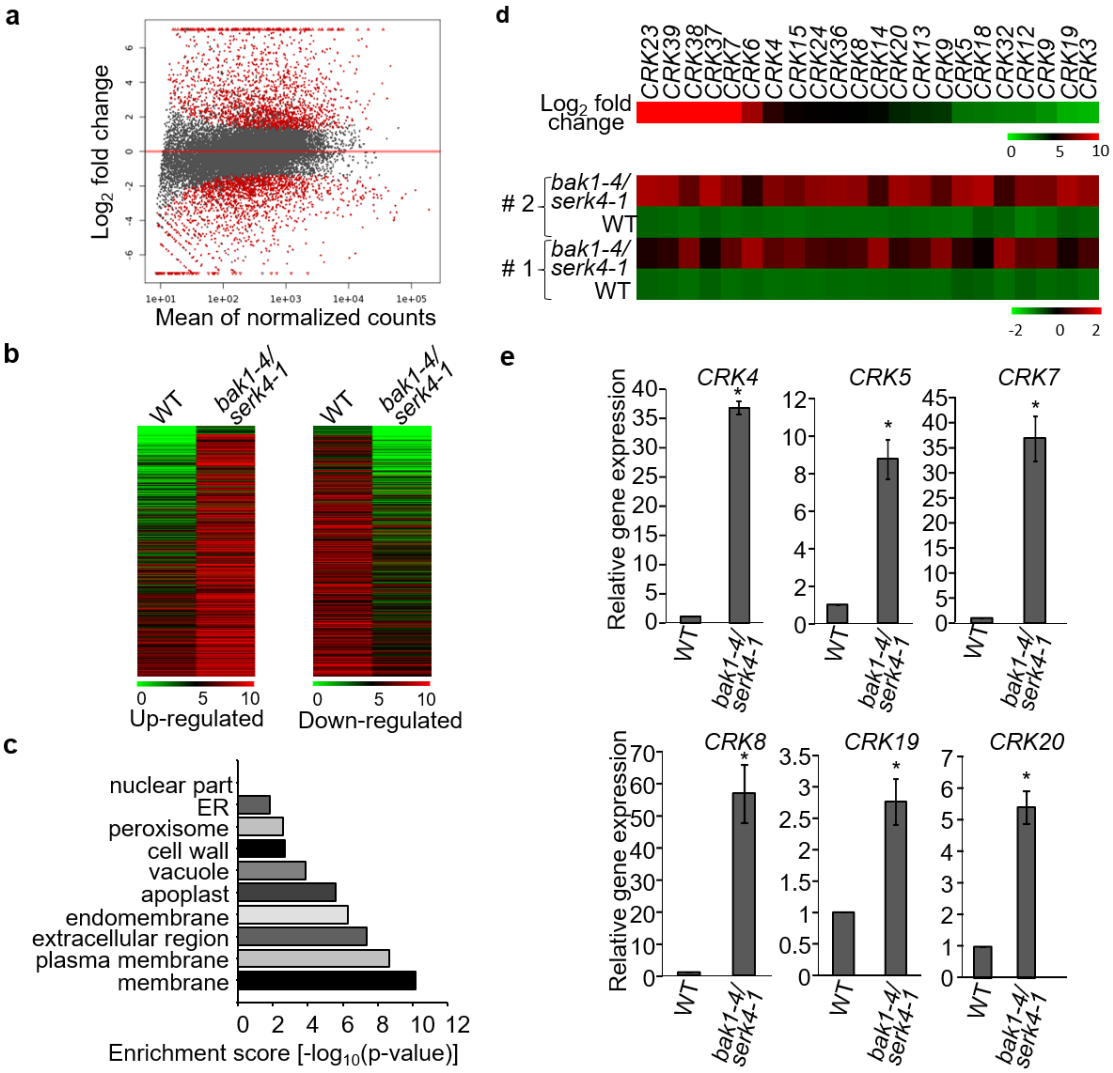
a
Log2 fold change
Mean of normalized counts
b
WT
bak1-4/ serk4-1
Up-regulated
Down-regulated
c
nuclear part
ER
peroxisome
cell wall
vacuole
apoplast
endomembrane
extracellular region
plasma membrane
membrane
Enrichment score [-log10(p-value)]
d
CRK23 CRK39 CRK38 CRK37 CRK7 CRK6 CRK4 CRK15 CRK24 CRK36 CRK8 CRK14 CRK20 CRK13 CRK9 CRK5 CRK18 CRK32 CRK12 CRK9 CRK19 CRK3
Log2 fold change
2
1
e
CRK4
CRK5
CRK7
CRK8
CRK19
CRK20
Relative gene expression

It has been reported that overexpression of certain *CRKs*, such as *CRK4*, *CRK5*, *CRK13*, *CRK19* and *CRK20*, was able to induce cell death in *Arabidopsis* transgenic plants (Acharya et al., 2007; Chen et al., 2003; Chen et al., 2004). When transiently expressed in *Nicotiana benthamiana*, *CRK4* and *CRK5* elicited water-soaking and subsequent cell death (Fig. 10a & 11a). We tested whether CRK proteins were glycosylated and whether STT3a-mediated protein glycosylation was required for CRK-mediated cell death. Glycosylated proteins often display a slower migration than nonglycosylated proteins in an immunoblot. When treated with tunicamycin, an inhibitor of protein *N*-glycosylation, both CRK4 and CRK5 proteins exhibited faster migration than proteins without treatment, suggesting that CRK4 and CRK5 proteins are likely *N*-glycosylated in *Arabidopsis* cells (Fig. 10b). Consistently, Endoglycosidase H treatment released CRK4 proteins with reduced molecular weight (Fig. 11b). CRK4 proteins when expressed in *stt3a-2* migrated faster than that in WT (Fig. 10c), indicating that STT3a is required for CRK4 glycosylation. Notably, we have consistently observed that the accumulation of CRK4 proteins after tunicamycin treatment or in *stt3a* appeared to be reduced when compared to proteins without treatment or in WT (Fig. 10b & 11c), suggesting that *N*-glycosylation may regulate CRK4 protein stability.

We further introduced *CRK4* under the control of an estrogen-inducible promoter into WT and *stt3a-2*. The cell death caused by ectopic expression of *CRK4* in WT plants was largely alleviated in *stt3a-2* upon estradiol application (Fig. 10d). Similar with the above transient assays, the CRK4 protein level was lower in *stt3a-2* than that in WT in multiple transgenic lines (Fig. 10e). We aligned the extracellular domain of CRK4 with

its closest homolog CRK5. Out of five potential *N*-glycosylation sites (Asn in Asn-X-Ser/Thr, where X is any amino acid except Pro), we identified two sites that are conserved among CRK4 and CRK5 (Fig. 11c). We mutated them in CRK4 to Gln ($CRK4^{N181Q}$ and $CRK4^{N286Q}$) and found that $CRK4^{N181Q}$ showed a faster migration than WT CRK4 when expressed in *Arabidopsis* protoplasts (Fig. 10f) or *N. benthamiana* (Fig. 11d), resembling the CRK4 expression in *stt3a* (Fig. 10c). The protein level of $CRK4^{N181Q}$ was comparable with that of WT CRK4, suggesting that mutation of one glycosylation site may not affect CRK4 protein stability. Significantly, $CRK4^{N181Q}$ mutant reduced cell death intensity and H_2O_2 accumulation compared to WT CRK4 when transiently expressed in *N. benthamiana* (Fig. 10g). Since $CRK4^{N181}$ is a conserved site between CRK4 and CRK5, it is likely that the corresponding site in CRK5 is required for its cell death-inducing ability. The results suggest that *N*-glycosylation is essential for CRK4-mediated cell death and CRK4 is one of the substrates of STT3a in *bak1/serk4* cell death. To test whether loss of *CRK4* suppresses *bak1/serk4* cell death, we silenced *BAK1/SERK4* in *crk4* mutant. However, the *crk4* mutant did not affect the cell death by VIGS of *BAK1/SERK4 (*Fig. 11e & 11f*)*, indicating that mutation of *CRK4* is not sufficient to suppress *bak1/serk4* cell death.

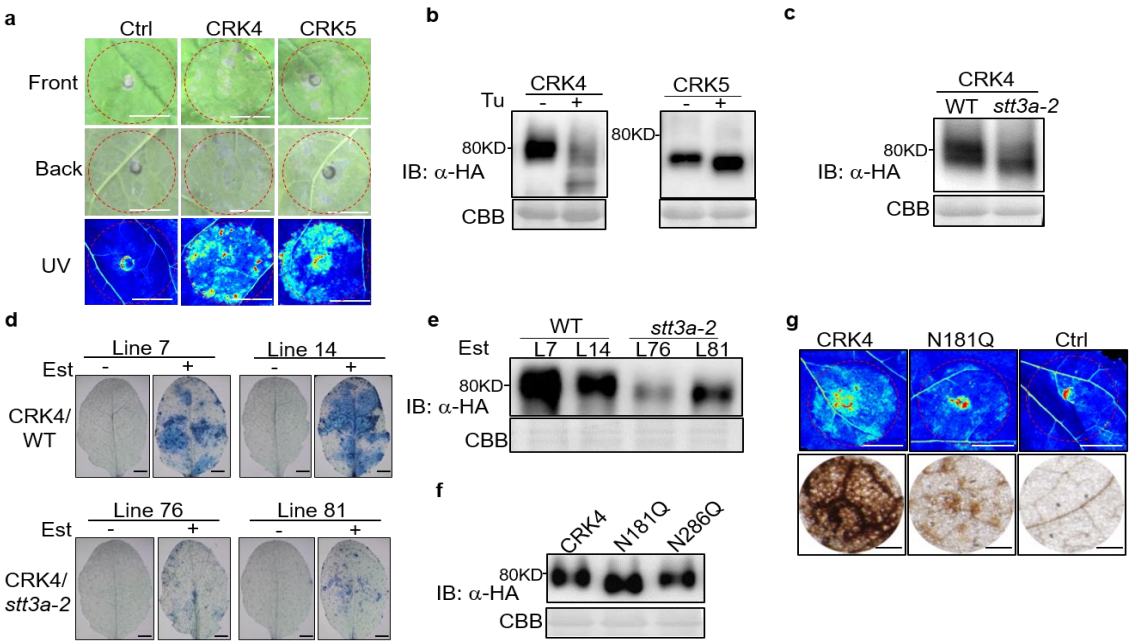

Figure 10. CRK4-induced cell death requires STT3a-mediated *N*-glycosylation.

(a) Expression of CRK4 or CRK5 in *N. benthamiana* induces cell death. The cell death was visualized on the front (top panel) and back (middle panel) sides of a leaf or under UV light with the ChemiDoc Imaging System (bottom panel) four days after infiltration. The infiltrated areas were labeled with red dashed circle. Bar = 1 cm. (b) Tunicamycin treatment modifies protein migration of CRK4 and CRK5. Protoplasts from Col-0 WT were transfected with *CRK4-HA* or *CRK5-HA* and treated without or with tunicamycin (1 μM). The proteins were detected by immunoblot with α-HA antibody (upper panel). Coomassie Brilliant Blue (CBB) staining is a loading control (lower panel). (c) CRK4 exhibits elevated protein migration rate in *stt3a-2*. Protoplasts from Col-0 WT or the *stt3a-2* mutant were transfected with *CRK4-HA*. (d) STT3a is required for CRK4-induced cell death in *Arabidopsis*. Leaves of four-week-old transgenic plants of estradiol-inducible *CRK4-HA* in WT and *stt3a* background were infiltrated with estradiol (10 μM) or Mock. Cell death staining was performed four days after infiltration. Two independent lines for each background are shown. Bar = 2mm. (e) CRK4 protein expression in transgenic plants. Detached leaves from four-week-old transgenic plants were soaked in estradiol solution (10 μM) for 24 hr. The HA-tagged CRK4 protein was detected by immunoblot with α-HA antibody. (f) Expression of CRK4 and its putative *N*-glycosylation mutants in *Arabidopsis* protoplasts. (g) CRK4-induced cell death is partially blocked by N181Q mutation in *N. benthamiana*. The cell death was documented four days after inoculation of *Agrobacterium* carrying different constructs in *N. benthamiana*. The upper panel: the cell death was visualized as autofluorescence under UV light with the ChemiDoc Imaging System, Bar = 1 cm; the bottom panel: H_2O_2 accumulation by DAB staining, Bar = 100 μm.

Figure 11. Protein glycosylation of CRKs.

(a) CRK4 and CRK5 protein expression in *N. benthamiana* transient assay. Agrobacteria containing a *pCB302* vector carrying different *CRK* genes driven by CaMV 35S promoter were infiltrated into *N. benthamiana* leaves. Leaf samples were collected 36 hr after infiltration for protein isolation and immunoblot with α-HA antibody. (b) Endo H treatment of CRK4 proteins. Protoplasts were transfected with CRK4-HA and incubated for 12 hr. Total protein was extracted, boiled with glycoprotein denaturing buffer, and then digested with Endo H at 37 ℃ for 3 hr. Red line indicates CRK4 proteins released by Endo H treatment. (c) Sequence alignment of CRK4 and CRK5 amino acid sequences. The sequences of extracellular domains were aligned by Clustal X 2.1 program and the putative *N*-glycosylation residues were predicted in PROSITE database (http://prosite.expasy.org/scanprosite/). The conserved putative *N*-glycosylation residues in CRK4 and CRK5 were indicated by a red triangle and the consensus motif N-X-S/T, where X is any amino acid except P, was boxed in red. * on the top of the amino acid indicates every 10 amino acids. (d) $CRK4^{N181Q}$ shows a slightly faster migration than CRK4 when expressed in *N. benthamiana*. Proteins were extracted 36 hr after inoculation of Agrobacterium carrying *35S::CRK4-HA* or *35S:*$CRK4^{N181Q}$*-HA*. (e) The *crk4* mutant does not affect the cell death by VIGS of *BAK1/SERK4*. Phenotypes of WT and *crk4* mutant plants are shown two weeks after VIGS of *BAK1/SERK4*. Bar = 1 cm. (f) RT-PCR analysis of *CRK4* expression in WT and *crk4* mutant. *UBQ1* was used as an internal control.

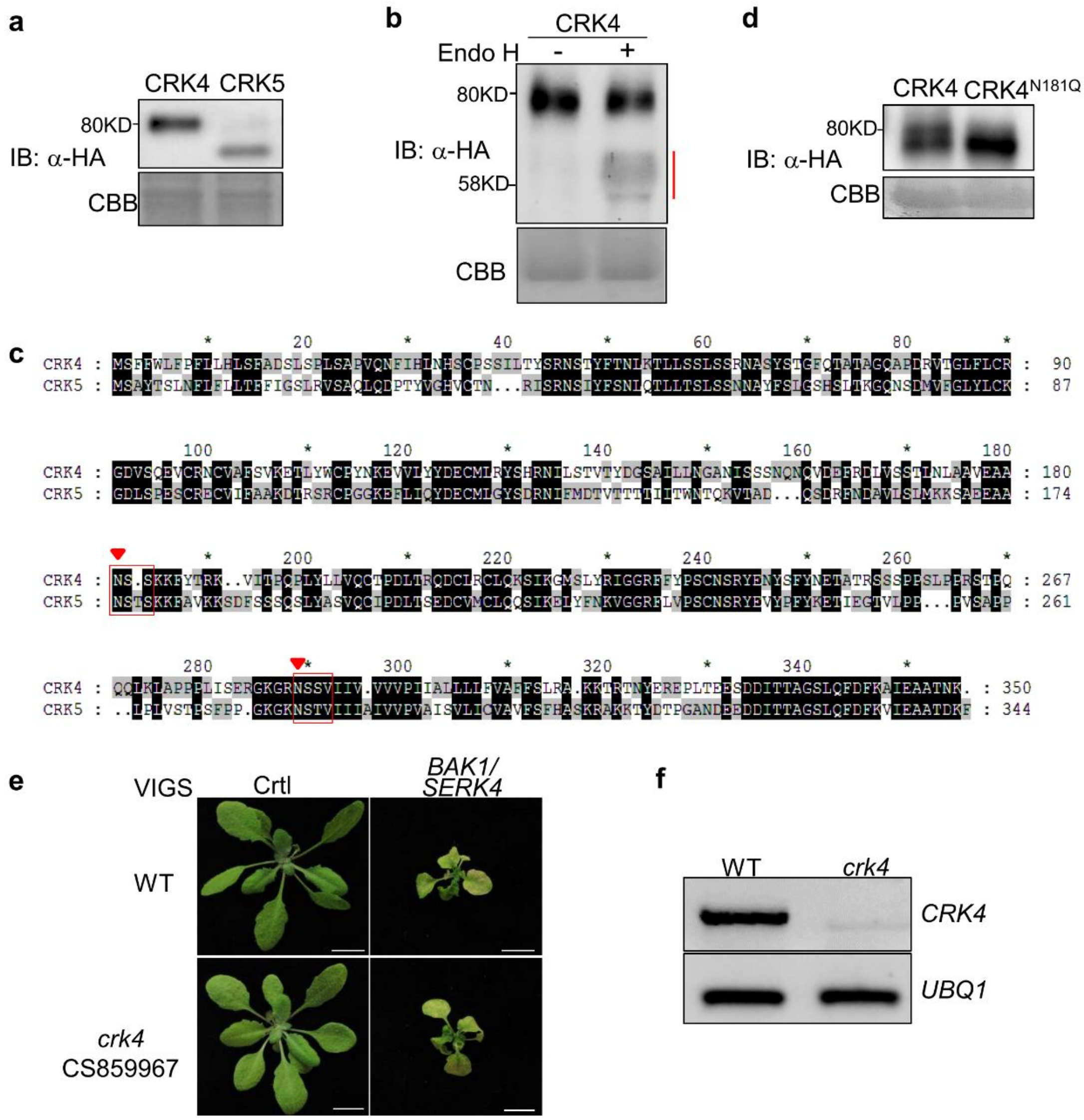
a
CRK4 CRK5
80KD
IB: α-HA
CBB
b
CRK4
Endo H - +
80KD
IB: α-HA
58KD
CBB
d
CRK4 CRK4N181Q
80KD
IB: α-HA
CBB
c
CRK4
CRK5
e
VIGS
Crtl
BAK1/SERK4
WT
crk4
CS859967
f
WT crk4
CRK4
UBQ1

2.5 Discussion

The mechanisms of cell death control are poorly understood in plants. To uncover the pathways and mechanisms regulating *bak1/serk4* cell death, we have developed an unbiased and highly efficient genetic screen which combines the features of both forward and reverse genetics. We have identified *stt3a* as a suppressor of *bak1/serk4* cell death. Systematic investigation of components in protein *N*-glycosylation pathways and ERQC indicates that *N*-glycan production in ER and specific ERQC components involved in protein folding are essential in the activation of *bak1/serk4* cell death. By combining RNA-seq, genetic and biochemical analyses, we provide evidence that CRK4 serves as one of client proteins for STT3a-mediated protein *N*-glycosylation and ERQC in *bak1/serk4* cell death.

Although BAK1 and BIR1 are in a complex, the mechanisms regulating their functions in cell death control are distinct. The *bir1*-mediated cell death depends on SOBIR1 and the R protein-mediated signaling (Gao et al., 2009). However, *sobir1* and the R protein signaling mutants did not affect *bak1/serk4* cell death (Fig. 1f, 1g & 1h). Both *bak1/serk4* and *bir1* cell death requires STT3a (Fig. 3) although SOBIR1 protein level was not affected in *stt3a* (Zhang et al., 2015). It has been shown that SOBIR1 protein accumulation was reduced in *erdj3b*, suggesting that ERQC is important for biogenesis of SOBIR1 (Sun et al., 2014). It is likely that activation of SOBIR1 also requires *N*-glycosylation modification in ER. Thus, protein glycosylation and ERQC are common features in BAK1/SERK4- and BIR1-regulated cell death, but different client proteins are likely deployed for *N*-glycosylation modification.

BAK1 family RLKs serve as a shared signaling node that modulates the interconnected architecture of the complex cellular signaling networks yet disseminate different biological outcomes (aan den Toorn et al., 2015; Liebrand et al., 2014). Mounting evidence suggests that BAK1 family RLKs function independently in different signaling pathways. For instance, the involvement of BAK1 and SERK4 in cell death control can be separated from their involvement in BR signaling (He et al., 2007; Kemmerling et al., 2007). Similarly, their function in stomatal patterning is uncoupled from function in BR signaling (Meng et al., 2015). The *bak1-5* mutant had severe defects in plant immunity, but did not affect BR signaling and cell death control (Schwessinger et al., 2011). These results are consistent with our observation that *stt3a* did not suppress *bak1* or *bak1/serk4* deficiency in flg22 and BR signaling, reinforcing that the signaling pathway of BAK1/SERK4-regualted cell death is uncoupled from their functions in flg22-triggered immunity and BR-mediated development.

Many *CRK* genes are induced by defense hormone SA treatment and bacterial pathogen infections (Chen et al., 2003; Chen et al., 2004). Constitutive expression of *CRK4* or *CRK5* at the modest level enhanced plant resistance to virulent bacteria *Pseudomonas syringae* (Chen et al., 2003; Yeh et al., 2015). In addition, chemical-induced expression of *CRK4* or *CRK5* triggered cell death in *Arabidopsis* (Chen et al., 2003; Chen et al., 2004). These observations point to the potential role of CRKs in plant defense responses. We observed an enrichment of *CRK* genes among upregulated genes in *bak1/serk4* (Fig. 5d & 5e). In addition, CRK4-induced cell death depends on STT3a-mediated protein *N*-glycosylation (Fig. 6d). The CRK4 *N*-glycosylation mutant reduced

the ability to trigger cell death (Fig. 6g). It is likely that the non-glycosylated or under-glycosylated CRK4 protein is misfolded in ER and finally removed by ER-associated degradation, thereby resulting in the reduced protein level in *stt3a* (Fig. 6e). However, *crk4* did not suppress *bak1/serk4* cell death (Fig. 11e & 11f). This may be due to the redundant function of several *CRKs*, which are able to induce cell death. We also could not exclude the possible contribution of other genes. Notably, *SOBIR1* is also moderately induced in *bak1/serk4*. Thus, CRK4 is one of client proteins of *N*-glycosylation and ERQC involved in BAK1/SERK4-regualted cell death.

3 BAK1/SERK4 NEGATIVELY CONTROL CELL DEATH BY REGULATING CYCLIC NUCLEOTIDE GATED CHANNEL 20

3.1 Summary

Plant LRR-RLKs play essential roles in perception of external and intrinsic signal, and initiation of signaling transduction. BAK1, a shared and essential LRR-RLK in different signaling, and SERK4 redundantly and negatively regulate cell death with largely unknown mechanism. By deploying a high-efficient genetic screen for suppressors of cell death triggered by virus-induced gene silencing of *BAK1/SERK4* on *Arabidopsis* knockout mutant collections, we revealed that cyclic nucleotide-gated channel 20 (CNGC20) plays an important role in *bak1/serk4* cell death. Systemic investigation of CNGC family members in *Arabidopsis* showed that only CNGC20 is required for *bak1/serk4* cell death. Interestingly, *in vivo* and *in vitro* assays indicated that BAK1 directly interacts with and phosphorylates membrane-resident CNGC20. Mass spectrometry and mutagenesis analysis revealed that specific phosphorylation sites of CNGC by BAK1 are indispensable for its function in cell death control.

3.2 Introduction

In addition to the preformed and dynamic barrier presented by the plant cell wall, sessile plants appear to have evolved largely expanded numbers of plasma membrane-resident receptor-like kinases (RLKs) and receptor-like proteins (RLPs) to cope with invading microbes (Liebrand et al., 2014). Intriguingly, plant growth and development are intimately intertwined with plant innate immunity and symbiosis process via actions of members of RLKs (Belkhadir et al., 2014; Shiu and Bleecker, 2003). BRI1

(BRASSINOSTEROID INSENSITIVE 1) and FLS2 (FLAGELLIN-SENSITIVE 2), two well-studied leucine-rich repeat-RLKs (LRR-RLKs), are involved in brassinosteroid (BR) hormone-mediated plant growth and development, and bacterial flagellin or flg22 (a 22-amino-acid peptide corresponding to the amino (N)-terminus of flagellin)-triggered plant defense response, respectively (Gómez-Gómez and Boller, 2000; Li and Chory, 1997). Both BRI1 and FLS2 heterodimerize with a subgroup of LRR-RLKs, named somatic embryogenesis receptor kinases (SERKs), which comprise of five members in *Arabidopsis*. SERK5, probably a nonfunctional kinase in *Arabidopsis* Columbia-0 (Col-0) ecotype, plays important roles regulating BR signaling and cell death control in Landsberg erecta (Ler) ecotype (Wu et al., 2015). SERK1, SERK2, SERK3 and SERK4 participate in a wide range of physiological response (aan den Toorn et al., 2015). SERK1 and SERK2 play a crucial and redundant role in male gametophyte development (Albrecht et al., 2005; Colcombet et al., 2005). SERK3, also known as BAK1 (BRI1 associated receptor kinase 1), and SERK4 function in plant immunity by association with FLS2 and other immune receptors (Chinchilla et al., 2007; Heese et al., 2007; Postel et al., 2010; Roux et al., 2011). Receptor like protein 23 (RLP23) forms complex with another LRR-RLK SOBIR1 (suppressor of BIR1-1), and recruits BAK1 upon ligand nlp20 binding (Albert et al., 2015). SERK1, BAK1 and SERK4 function in BR signaling by association with BRI1 (Gou et al., 2012; Li et al., 2002; Nam and Li, 2002). SERK1, SERK2, BAK1 and SERK4 regulate stomatal patterning via EPF (EPIDERMAL PATTERNING FACTORS) peptide ligand-induced association with ERECTA (ER) family LRR-RLKs (Meng et al., 2015). SERK1, SERK2, BAK1 and

SERK4 also mediate floral organ abscission signaling through IDA (INFLORESCENCE DEFICIENT IN ABSCISSION) ligand-stimulated heterodimerization with two closely related LRR-RLKs HAESA (HAE) and HAESA-LIKE2 (HSL2) (Meng et al., 2015; Meng et al., 2016). In addition, SERK1, SERK2 and BAK1 regulate PSK (Phytosulfokine) peptide hormone-mediated root growth via association with its receptor LRR-RLK PSKR (Ladwig et al., 2015; Wang et al., 2015a).

BAK1 and SERK4 redundantly and negatively regulate BR-independent cell death pathway with enigmatic mechanism (He et al., 2007; Kemmerling et al., 2007). The *bak1-4/serk4-1* null mutant is postembryonic seedling lethal associated with spontaneous cell death and constitutive H_2O_2 production (He et al., 2007). Recent studies start to uncover the veil underlying BAK1/SERK4-mediated cell death. Components involved in nucleocytoplasmic trafficking, especially molecules directly or indirectly involved in endogenous salicylic acid accumulation, is critical in BAK1/SERK4-mediated cell death control (Du et al., 2016). Furthermore, BAK1/SERK4-mediated cell death is partially salicylic acid (SA) dependent. In addition, *N*-glycosylation of cysteine-rich receptor-like kinase 4 (CRK4) mediated by STT3a and specific endoplasmic reticulum (ER) quality control (ERQC) components are essential to activate *bak1/serk4* cell death (de Oliveira et al., 2016). BIR1, a BAK1-interacting RLK, also exhibited autonomous cell death which could be suppressed by another RLK SOBIR1 (suppressor of BIR1-1). Moreover, overexpression of SOBIR1 leads to activate defense response and cell death. Systemic investigation of *N*-glycosylation and specific ERQC components revealed distinct and overlapping mechanism underlying BAK1/SERK- and BIR1-

mediated cell death. Despite of these advances, the pathway underlying BAK1 and SERK4-mediated cell death control remains largely fragmented.

Intracellular signaling molecules, including cyclic nucleotide monophosphates (cNMPs) and Ca^{2+} often released by the cell, have long been known to trigger series of physiological changes and relay signal transduction from external cues. Cyclic nucleotide-gated channel (CNGC) proteins, which could bind cNMP and uptake Ca^{2+}, function as non-selective ligand-gated channels in both animals and plants. CNGCs comprise of 6 transmembrane segments (S1-S6) with a pore region (P loop) between S5 and S6, one cyclic nucleotide-binding domain (CNBD) and one calmodulin-binding domain (CaMBD) (Bouche et al., 2005). It has been proposed that CNGC forms hetero-tetramer composed of different subunits to be functional in animals. The *Arabidopsis* genome encodes 20 *CNGCs* which have been implicated in diverse physiological responses, including development and defense. CNGC2 and CNGC4 are involved in plant defense response. Furthermore, moss CNGCb and *Arabidopsis* CNGC2 act as thermosensors and regulate Ca^{2+} influx triggered by heat shock response (HSR) (Clough et al., 2000; Finka et al., 2012; Jurkowski et al., 2004). The *cpr22* mutant, which fuses 5' portion of CNGC11 and 3' portion of CNGC12 and produces a novel but functional chimeric CNGC11/12, exhibits increased resistance to pathogen (Yoshioka et al., 2006). Recent study indicates that CNGC14 is required for root gravitropism. In addition, CNGC17 participates in PSK-mediated signaling via association with PSKR, BAK1 and H^+-ATPase (Ladwig et al., 2015; Shih et al., 2015). CNGC18 functions as an essential Ca^{2+} channel required for pollen tube guidance to ovules in *Arabidopsis* (Gao et al.,

2016). Although the essential roles of CNGCs in diverse cellular responses are emerging, the regulatory mechanisms of CNGCs in plants remain obscure.

In the present study, we identified a suppressor of *bak1/serk4* cell death via virus-induced gene silencing, an unbiased and efficient genetic screening on *Arabidopsis* T-DNA mutant collections. One suppressor carries a mutation in *CNGC20* responsible for the suppression of *bak1/serk4* cell death. Interestingly, *in vivo* and *in vitro* assays indicated that BAK1 directly interacts with and phosphorylates membrane-resident CNGC20. Mass spectrometry and mutagenesis analysis revealed that specific phosphorylation sites of CNGC20 by BAK1 are indispensable for its function in cell death control. In conclusion, our findings unravel novel components and provide mechanistic insights in plant cell death regulation.

3.3 Materials and methods

3.3.1 Plant and pathogen materials and growth conditions

Arabidopsis accessions Col-0 (WT), various mutants and transgenic plants used in this study were grown in soil (Metro Mix 366) in a growth room at 23°C, 45% relative humidity, 70 μE $m^{-2}s^{-1}$ light with a 12-hr light/12-hr dark photoperiod for two-weeks before VIGS assays or 30 days for protoplast isolation and pathogen assays. The *bak1-4* and *bak1-4/serk4-1* mutants were reported previously (de Oliveira et al., 2016). All the *Arabidopsis* T-DNA insertion lines (SALK_013823C, SALK_087793C, SALK_042821C, SALK_037558C, SAIL_302_A04, SALK_007105) were obtained from the *Arabidopsis* Biological Resource Center (ABRC) and confirmed by PCR and RT-PCR using primers listed in Supplementary Table S4. Seedlings were grown on agar

plates containing ½ Murashige and Skoog medium (½MS) with 0.5% sucrose, 0.8% agar and 2.5 mM MES at pH 5.7, in a growth room at 23°C or 30°C, 45% humidity, 70 μE $m^{-2}s^{-1}$ light with a 12-hr light/12-hr dark photoperiod.

P. syringae pv. *maculicola* ES4326 (*Psm*), *Pseudomonas syringae* pv. *tomato* (*Pst*) DC3000 (avrRpt2), *Pst* DC3000 (avrRpm1) and *Pst* DC3000 (avrRps4) were cultured for overnight at 28ºC in the King's B medium with the appropriate antibiotics (50 ug/ml streptomycin, rifampicin or kanamycin). Bacteria were harvested by centrifugation at 3500 rpm, washed with ddH_20, and adjusted to the desired density with 10 mM $MgCl_2$. Leaves of 4-week-old plants were hand-infiltrated with bacterial suspension using a 1-ml needleless syringe and collected at the indicated time for HR or bacterial growth assays. To measure bacterial growth, two leaf discs were ground in 100μl H_2O and serial dilutions were plated on TSA medium (1% Bacto tryptone, 1% sucrose, 0.1% glutamic acid, 1.5% agar) with appropriate antibiotics. Bacterial colony forming units (cfu) were counted 2 days and 4 days after incubation at 28°C. Each data point is shown as triplicates.

3.3.2 Plasmid construction and generation of transgenic plants

The VIGS of *BAK1*/*SERK4*, *MEKK1* and *BIR1* constructs and the *pHBT-BIK1-HA* construct were reported previously (de Oliveira et al., 2016). The *CNGC20* gene was amplified from Col-0 genomic DNA with primers containing NcoI at N terminus and StuI at C terminus (Table S4), and ligated into a plant protoplast expression vector *pHBT* with a *CaMV 35S* promoter at N-terminus and an HA epitope-tag at C-terminus. The point mutations of $CNGC20^{N430Q}$ and $CNGC20^{N452/455/Q}$ were generated by site-directed

mutagenesis with primers listed in Table S4. To construct the *pCABIA1300* binary vector containing the native promoter driven *CNGC20* for *Agrobacterium*-mediated transformation, the *CNGC20* promoter was amplified with primers containing XhoI at N terminus and NcoI at C terminus (Table S4), and ligated into *pHBT* containing the CNGC20 genomic DNA fragment. The native promoter driven *CNGC20* genomic fragment together with the HA epitope and the NOS terminator were released from the *pHBT* vector via digestion with XhoI and EcoRI, and ligated into the *pCABIA1300* binary vector pre-cut with EcoRI and SalI. The sequence of all the genes or promoters were verified by the targeted Sanger-sequencing. *Arabidopsis* transgenic plants were generated using *Agrobacterium*-mediated transformation by the floral-dip method.

3.4 Results

To identify components involved in BAK1/SERK4-regulated cell death, we carried out a VIGS-based genetic screen of a sequence-indexed library of *Arabidopsis* T-DNA insertion lines. After screening ~6000 homozygous lines, a series of mutants were isolated based on the suppression of cell death upon VIGS of *BAK1/SERK4*. One mutant *btl1* (*b*ak *t*o *l*ife) is SALK_013823C. The *btl1* mutant largely suppressed the dwarfism and leaf chlorosis triggered by VIGS of *BAK1/SERK4* compared to wild-type (WT) plants (Fig. 12A). Trypan blue staining indicated that cell death triggered by silencing of *BAK1/SERK4* was significantly reduced in the *btl1* mutant. The 3,3'-diaminobenzidine (DAB) staining indicated that the elevated H_2O_2 accumulation caused by VIGS of *BAK1/SERK4* was almost completely abolished in *btl1* (Fig. 12B & 12C). In addition, compared to WT, *btl1* showed much reduced accumulation of *PR1* and *PR2* genes upon

VIGS of *BAK1*/*SERK4* (Fig. 12D). MEKK1, a MAP kinase (MAPK) kinase kinase downstream of BAK1/SERK4 in flagellin-mediated signaling, and BIR1, a BAK1-interacting receptor-like kinase, are also involved in cell death regulation. Silencing of *MEKK1* and *BIR1* by VIGS in WT plants resulted in severe dwarfism and cell death (Fig. 12E). However, the *btl1* mutant did not suppress MEKK1- and BIR1-regulated cell death (Fig. 12E), suggesting different mechanisms underlying BAK1/SERK4-, MEKK1- and BIR1-regulated cell death. The data also suggest that *btl1* did not affect the gene silencing machinery.

The *btl1* mutant (*SALK_013823C*) was annotated to bear a T-DNA fragment inserted at the 8th intron of a gene (*AT1G60995*) encoding an uncharacterized protein containing the membralin domain. To verify whether the annotated T-DNA in *AT1G60995* is the cause for suppression of BAK1/SERK4-mediated cell death in the *btl1* mutant, we isolated and characterized two additional alleles of T-DNA mutants of *AT1G60995* (Fig. 13A). Geno-typing and RT-PCR analysis showed that these mutants showed reduced *AT1G60995* transcripts (Fig. 13B). However, unlike *btl1*, neither of mutants could suppress VIGS of BAK1/SERK4-mediated cell death (Fig. 13C). Furthermore, transformation of either the *35S* promoter or the native promoter driven *AT1G60995* into the *btl1* mutant did not restore growth defects triggered by VIGS of BAK1/SERK4 (Fig. 13D). Next we tested the possibility whether the N-terminal part of *AT1G60995* in *btl1* is functional and functions dominantly to suppress VIGS of BAK1/SERK4-mediated cell death. We transformed *N-AT1G60995* into WT plants. Silencing *BAK1/SERK4* in these transgenic plants still resulted in severe dwarfism and

cell death as that in WT plants (Fig. 13E). All the above data indicate that the T-DNA insertion in *AT1G60995* may not be the cause for the suppression of *BAK1/SERK4*-mediated cell death.

Figure 12. The *btl1* mutant specifically suppresses BAK1/SERK4-mediated cell death.

(A) The *btl1* mutant suppresses growth defects triggered by VIGS of *BAK1/SERK4*. Plant phenotypes are shown two weeks after VIGS of *BAK1/SERK4 or* a vector control (Ctrl.). Bar = 5 mm. (B) The *btl1* mutant suppresses cell death by VIGS of *BAK1/SERK4*. True leaves of WT (Col-0) and *btl1* after VIGS of *BAK1/SERK4* or a vector control were stained with trypan blue for cell death. Bar = 2 mm. (C) The *btl1* mutant suppresses H_2O_2 production by VIGS of *BAK1/SERK4*. True leaves of WT and *btl1* after VIGS of *BAK1/SERK4* or a vector control were stained with DAB for H_2O_2 accumulation. Bar = 2mm. (D) The *btl1* mutant suppresses *PR1* and *PR2* expression by VIGS of *BAK1/SERK4*. The expression of *PR1* and *PR2* was normalized to the expression of *UBQ10*. The data are shown as mean ± SE from three independent repeats. The different letters denote statistically significant difference according to one-way ANOVA followed by Tukey test ($p<0.05$). (E) The *btl1* mutant suppresses *BAK1*/*SERK4*-mediated cell death but not *MEKK1*- and *BIR1*-mediated cell death.
The above experiments were repeated at least three times with similar results.

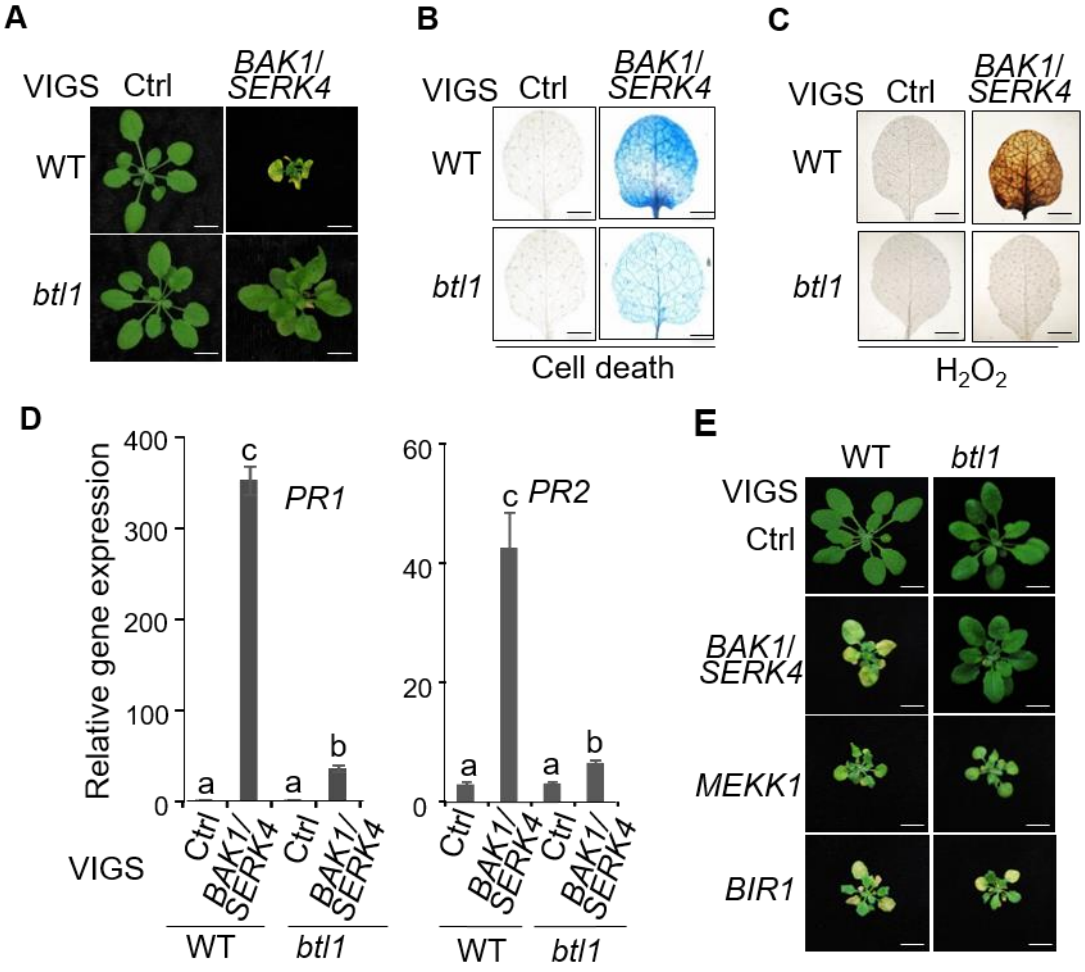
A
VIGS Ctrl
BAK1/ SERK4
WT
btl1
B
VIGS Ctrl
BAK1/ SERK4
WT
btl1
Cell death
C
VIGS Ctrl
BAK1/ SERK4
WT
btl1
H2O2
D
Relative gene expression
PR1
PR2
VIGS
Ctrl
BAK1/ SERK4
WT
btl1
E
WT
btl1
VIGS
Ctrl
BAK1/ SERK4
MEKK1
BIR1

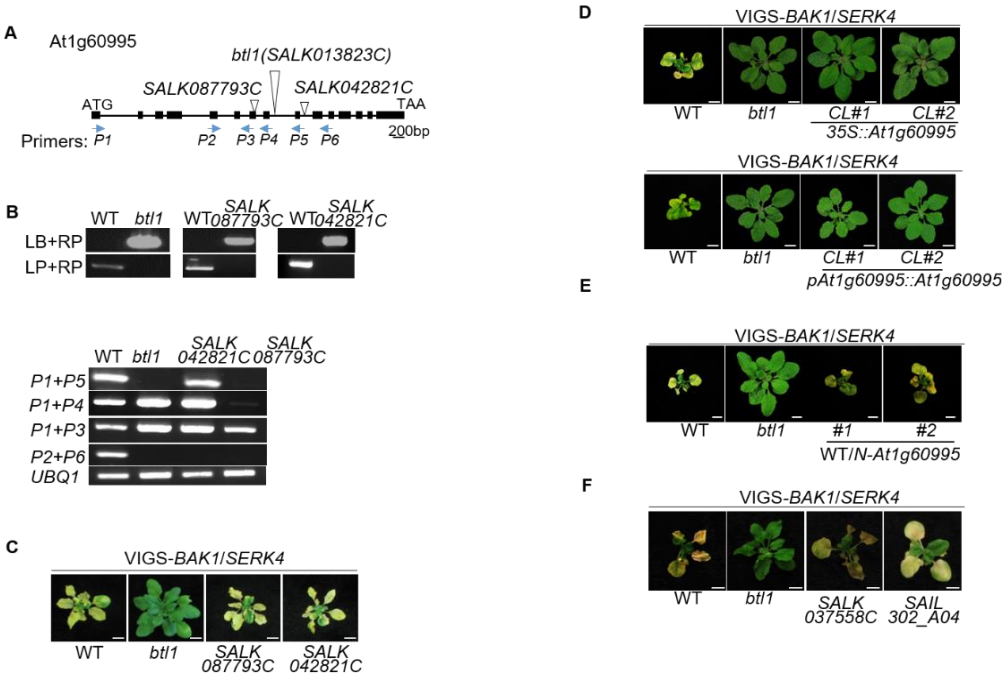

Figure 13. The T-DNA insertions in *At1g60995* and *At1g11020* are not causative for the suppression of *bak1/serk4* cell death.

A. Scheme of the *At1g60995* gene and T-DNA insertional sites in *btl1*/SALK013823C, SALK087793C and SALK042821C. Solid bars indicate exons and lines indicate introns. Arrows indicate the primers used for genotyping and RT-PCR analysis. Bar=200bp
B. PCR and RT-PCR confirmation of three T-DNA insertional lines of *At1g60995*. The DNA from WT, *btl1* and SALK087793C and SALK042821C was PCR-amplified with the primers indicated in Fig. S1A to confirm all the three lines are homozygous. The primer pair of LP and RP amplified the genomic DNA fragment of *At1g60995* and the primer pair of LB and RP amplified the T-DNA insertion from the *At1g60995* mutant. The cDNA from WT, *btl1* and SALK087793C and SALK042821C was PCR-amplified with indicated primers. *UBQ1* was used as an internal control. C. Unlike *btl1*, two independent alleles of T-DNA insertional mutants of *At1g60995* do not suppress growth defects by VIGS of *BAK1/SERK4*. Plant phenotypes are shown from WT, *btl1*, SALK087793C and SALK042821C two weeks after VIGS of *BAK1/SERK4*. Bar=5 mm.
D. Complementation of the *btl1* mutant with *At1g60995* driven by the *35S* promoter (top panel) or the native promoter (bottom panel) does not restore growth defects by VIGS of *BAK1/SERK4*. Bar = 5 mm. E. Transformation of the WT with *btl1* mutant form does not restores growth defects by VIGS of *BAK1/SERK4*. Bar = 5 mm. F. Unlike *btl1*, two independent T-DNA insertional alleles of *At1g11020* do not suppress growth defects by VIGS of *BAK1/SERK4*. Plant phenotypes are shown from WT, *btl1*, SALK037558C and SAIL302_A04 two weeks after VIGS of *BAK1/SERK4*. Bar = 5 mm.

To examine the possibility that additional mutations in *btl1* contribute the suppression of *BAK1/SERK4*-mediated cell death, we performed the whole genome-sequencing analysis of *btl1* and revealed that the *btl1* mutant may carry additional two T-DNA fragments inserted at *AT1G11020* and *CNGC20* (Table 1). Likely due to the high sequence similarity between *CNGC20* and *CNGC19*, CNGC19 is predicted to carry a T-DNA insertion. We performed the targeted Sanger-sequencing and confirmed the presence of T-DNA fragments in *AT1G11020* and *CNGC20* but not *CNGC19* in the *btl1* mutant (Fig 14A & Table 2). In addition, geno-typing and RT-PCR analyses indicate that *btl1* carries a T-DNA insert in *CNGC20* but not *CNGC19*, and shows reduced transcripts of *CNGC20* but not *CNGC19* (Fig 14B & 14D). We further isolated and characterized additional alleles of T-DNA insertion mutants for each gene (Fig. 14A, 14C & 14D). Neither T-DNA insertion homozygous alleles of *AT1G11020* suppressed *BAK1/SERK4*-mediated cell death (Fig. 14F), indicating that *AT1G11020* may not be the causal gene responsible for the cell death suppression phenotype triggered by VIGS-*BAK1/SERK4* in *btl1*.

Table 1. T-DNA insertions identified from the whole genome-sequence analysis of the *btl1 (SALK _013823C)* mutant.

Gene Locus	Gene Identity	T-DNA Insertion Position in *ncd2*	Confirmation of T-DNA insertion in *ncd2*	Additional independent T-DNA lines analyzed
At1g60995	Unknown protein, containing membralin domain	*8th* intron	confirmed by targeted sequencing	SALK_087793C (T-DNA in *7th* exon)
				SALK_042821C (T-DNA in *9th* intron)
At1g11020	RING/FYVE/PHD zinc finger superfamily protein	*1st* intron	confirmed by targeted sequencing	SALK_037558C (T-DNA in *1st* intron)
				SAIL_302_A04 (T-DNA in *1st* intron)
At3g17690	Cyclic nucleotide gated channel 19	*10th* exon	Not confirmed by genotyping	SALK_007105 (T-DNA) in *2nd* intron

Table 1. Continued

Gene Locus	Gene Identity	T-DNA Insertion Position in *ncd2*	Confirmation of T-DNA insertion in *ncd2*	Additional independent T-DNA lines analyzed
At3g17700	Cyclic nucleotide gated channel 20	*11th* exon	confirmed by targeted sequencing	SALK_129133 C (T-DNA in *4th*
				SALK_074919 C (T-DNA in *10th* exon)

Table 2. Sequence of *CNGC20* with the T-DNA insertion site underlined in the *btl1 (cngc20-3)* mutant.

ATGGCTTCCCACAACGAAAACGATGATATTCCCATGCTTCCGATTTCAGACC

CATCATCTCGTACTAGAGCCAGAGCTTTCACTTCCAGGAGTCGTAGCGTTTCT

CTCTCAAACCCTACTTCCTCCATTGAAGGATTTGACACTTCCACTGTGGTTTT

AGGCTACACGGGTCCTCTTCGAACTCAGAGACGTCCTCCTTTAGTTCAAATG

AGTGGTCCTCTTACCTCTACTCGCAAGCATGAACCTCTCTTTCTTCCTCATCC

TTCTTCTGATTCCGTTGGTGTCTCTTCTCAGCCTGAGAGGTATCCTTCTTTTGC

TGCTCTTGAACATAAAAACTCCTCAGAGGATGAGTTCGTTTTGAAACACGCA

AATCTCTTGAGGTCTGGACAATTGGGAATGTGTAATGATCCTTACTGTACTA

CTTGCCCTTCTTACTACAACCGTAAGGCTGCTCAAATCCCTACTTCTAGAGTT

TCTGCCCTTTTTGATTCCACGgtaaagttttgatttttgttactttacattcacaaatatagcttcaggatcaagta

aatgtcgttgaaacagagtcttttgttttcttgctagTTCCATAACGCTCTGTATGATGATGCTAAAG

GTTGGGCAAGGAGATTTGCTTCCTCTGTTAATAGATACTTACCTGGAATCAT

Table 2. Continued

GAATCCTCATGCCAAAGAGGTTCAAACCTGGACTAAATTCTTCGCCCTTTCA

TGCTTGTTAGCTATTTTTATAGATCCCCTCTTCTTCTTCCTCATAAAAGTCCAA

GAGgtatgtttttccttcagagatatctttgcttttccaagtgtttttatcttgcctttacaccacctttttgaccatctttatttttctcact

gtagCAAAACAAATGTATTATGATTGATTGGCCGATGACTAAAGCATTTGTAG

CTGTAAGAAGTGTAACAGATGTTATATTCACTATGAACATTCTACTTCAGgtgc

ttttcttttgcttacatttttccatctctttataaacaaaatatgttggctttagtgctcacgtttgccatattggttgcagTTCCGAT

TGGCCTATGTAGCTCGTGAGTCTACGGTAGTTGGAGCTGGCCAGTTAGTTAG

TCATCCCAAAAAAAATTGCCCTTCATTACCTCAAAGGAAAGTTTTTCCTTGACT

TGTTCATAGTGATGCCACTTCCACAGgtattgttacgttagagctcctactggttttaagtaatggtaatca

gaagatgttcatttatgttttcttttgtttacagATATTGATACTATGGATAATACCAGCACATTTGG

GTGCATCCGGGGCAAACTATGCGAAAAACCTTCTACGAGCTGCAGTTCTTTT

CCAATACATTCCAAAGTTATATAGACTTCTACCGTTTCTTGCTGGACAAACA

CCTACCGGATTCATATTTGAGTCAGCTTGGGCTAATTTTGTTATTAATCTTCT

CACTTTCATGCTTGCTGGACATGTTGTTGGTTCTTGCTGGTATCTATTTGGTCT

GCAGgtatgacaaactctcaaaatgtctttcatttttatcttgtcctgatcagcagaagatgcataaagtgatttatattgtttcccg

ttttctgttggttctttcagAGAGTTAATCAGTGCCTTCGAAATGCTTGCGGTAATTTTGGG

CGTGAATGTCAAGATCTTATAGATTGTGGTAATGGAAATAGCAGTGTATTAG

TACGAGCTACCTGGAAAGATAATGCGAGTGCCAATGCTTGTTTCCAAGAAGA

TGGTTTTCCTTATGGAATCTATTTAAAAGCAGTCAATCTTACCAATCATTCTA

ATCTCTTCACAAGATACAGTTACTCTCTCTTCTGGGGCTTCCAGgtaactgtttttttttt

ctctctttcagtttttagtaggaaactaagaacaactactcaactactttgcattgattggcatacttggaactcttcattaagatcatt

Table 2. Continued

aattttataattctcatagCAAATCAGCACTCTTGCTGGCAACCAAGTCCCAAGCTACTTT

CTAGGGGAGGTCTTCTTTACTATGGGTATCATTGGACTAGGGCTTTTACTTTT

TGCGCTTCTTATTGGTAATATGCAAAATTTCCTTCAAGCTCTTGGTAAAAGgta

aacaattccatcattgtactaaaatagatatttcaagacataatggttggttctataaacactaactactcaggtgattgtgttttgtcc

atattagGAATTTGGAAATGACGCTGAGACGGCGTGATGTGGAGCAATGGATGA

GCCATAGACGGTTGCCAGATGGTATAAGAAGgtatgtggactttgcctataaaactttgttttatcctt

tgaatattctttttcttaaagagttacattggtctcagtttcagtagtttcactattaaactaactgaataatggttcgacattatcagG

AGGGTGCGAGAGGCTGAGCGGTTTAACTGGGCTGCTACTAGAGGCGTTAAC

GAAGAATTGCTTTTTGAGAATATGCCTGATGATCTTCAAAGAGATATAAGAC

GACACCTCTTCAAATTTCTCAAGAAGgtaaacatatgtgaaacttctgtatgcatagatcccaattccata

tagtgttgcaaagagctagttctagaagctgtaactgcaagtaatagttagagaccacagattaaaccattgctgagaaatagtatt

gaaatttgaatgggtttgcagGTGAGAATATTTTCGTTGATGGATGAACCAATCTTAGATG

CAATCCGTGAGAGGCTGAAACAGAGGACATACATAGGGAGTAGCACAGTGT

TGCACCGTGGAGGACTAGTTGAGAAAATGGTATTCATAGTGAGAGGTGAGA

TGGAGAGCATTGGAGAAGATGGTTCTGTTCTTCCATTATATGAAGGCGATGT

TTGTGGTGAAGAACTCCTCACTTGGTGCCTCGAACGCTCTTCTGTAAACCCC

Ggtaccatccctttgactctatctctatgtgttcataaatcccaaaaagtttggttccttagatgacacttcgttaagaaaaagcttg

gaactgagtatgttctgaaaccttcagATGGGACGAGGATAAGGATGCCATCAAAGGGATTG

CTTAGTAGCAGAAATGTAAGGTGTGTGACAAATGTGGAGGCGTTTTCGCTGA

GTGTAGCCGATCTGGAAGACGTAACGAGCTTGTTTTCGAGATTCTTGAG**GAG**

TCATAGAGTCCAAGGAGCCATAAGGTACGACTCTCCATATTGGAGGCTACG

Table 2. Continued

AGCGGCTAGGCAGATTCAAGTGGCGTGGAGATACCGTAGGAGACGGCTTCA

TAGATTATGCACTCCTCAGTCTAGTTATAGCCTT**TAG**

Note: The start codon (ATG) and stop codon (TAG) are in bold. The capital letters denote exons while the small letters indicate introns. GAGT, which are in bold and underlined, bears an T-DNA insert based on the whole genome-sequence analysis of *btl1*, which was further confirmed by targeted sequence analysis of this region.

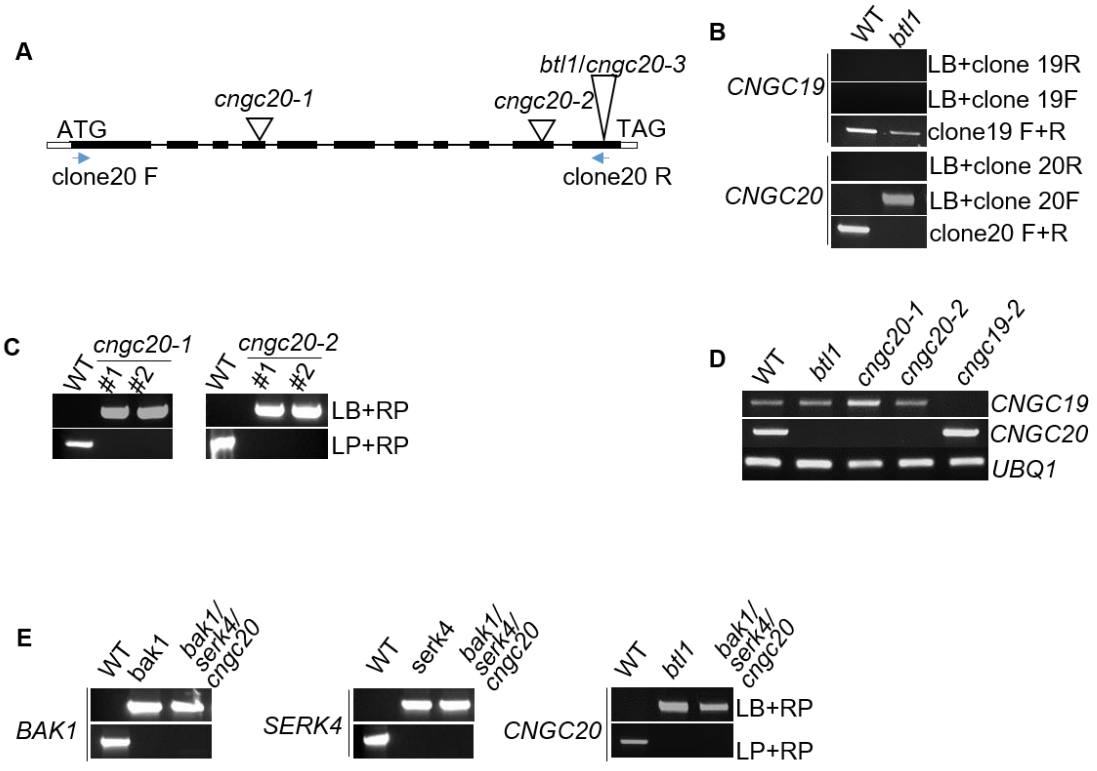

Figure 14. Characterization of the T-DNA insertions in *cngc20* mutants.

A. Scheme of the *CNGC20* gene and T-DNA insertion sites in *cngc20-1* (SALK129133C), *cngc20-2* (SALK074919C) and *ncd2* (*cngc20-3)*. Solid bars indicate exons and lines indicate introns. Arrows indicate the T-DNA insertion sites.
B. Geno-typing PCR analysis to confirm that the *btl1* mutant carries a T-DNA insertion in *CNGC20* but not *CNGC19*. The DNA from WT and *btl1* was PCR amplified with the indicated primers to confirm T-DNA insertion happens in *CNGC20* but not *CNGC19*.
C. Geno-typing PCR analysis of the T-DNA insertions in *cngc20-1*, *cngc20-2*. The DNA from WT, *cngc20-1*, and *cngc20-2* was PCR-amplified with the indicated primers to confirm all the three lines used are homozygous. The primer pair of LP and RP is to amplify the genomic DNA fragment of *CNGC20,* and the primer pair of LB and RP is to amplify the T-DNA insertions.
D. RT-PCR analysis of *CNGC20* and *CNGC19* expression in *btl1*, *cngc20-1*, *cngc20-2* and *cngc19-2*. The cDNA of *CNGC20* or *CNGC19* from WT, *btl1*, *cngc20-1*, *cngc20-2* and *cngc19-2* was PCR-amplified. *UBQ1* was used as an internal control.
E. Geno-typing PCR analysis of the *bak1/serk4/cngc20-3* triple mutant. The DNA from WT, *bak1*, *serk4*, *btl1* and *bak1/serk4/cngc20-3* was PCR-amplified with the indicated primers to confirm that *bak1/serk4/cngc20* is a triple homozygous mutant.

Importantly, two alleles of *cngc20* mutants, *cngc20-1* and *cngc20-2*, suppressed VIGS-*BAK1/SERK4*-mediated cell death similar as *btl1* (Fig. 15A). The cell death and elevated H_2O_2 accumulation caused by VIGS of *BAK1/SERK4* were almost completely abolished in *cngc20* mutants (Fig. 15B). Compared to WT, *cngc20* mutants showed much reduced accumulation of *PR1* and *PR2* genes upon VIGS of *BAK1*/*SERK4* (Fig. 15C). Furthermore, transformation of a genomic fragment containing the *CNGC20* gene into *btl1* restored VIGS-*BAK1/SERK4*-mediated cell death (Fig. 15D). To investigate if the *cngc20* mutation could genetically suppress *bak1-4/serk4-1* seedling lethality, we generated the *bak1-4/serk4-1/btl1* triple mutant. The *bak1-4/serk4-1/btl1* triple mutant overcame seedling lethality of *bak1-4/serk4-1* and resembled WT plants at two-week-old stage when grown on ½MS medium plates (Fig. 15E). When grown in soil, the *bak1-4/serk4-1/btl1* triple mutant developed true leaves. However, three weeks later, the *bak1-4/serk4-1/btl1* triple mutant showed a delayed growth rate compared to WT, became severely dwarfed and occasionally settle seeds at 30ºC. In addition, cell death, H_2O_2 accumulation, and *PR1* and *PR2* expression were significantly ameliorated in *bak1-4/serk4-1/btl1* compared to those in *bak1-4/serk4-1* (Fig. 15F & 15G). Taken together, these results suggest that *cngc20* mutation leads to the suppression of BAK1/SERK4-mediated cell death.

Figure 15. The *cngc20* mutant suppresses BAK1/SERK4-mediated cell death.

(A) Different alleles of *cngc20* mutants suppress growth defects by VIGS of *BAK1/SERK4*. Plant phenotypes are shown from WT, *btl1*, *cngc20-1* and *cngc20-2* two weeks after VIGS of *BAK1/SERK4*. Bar = 5 mm. (B) The *cngc20* mutants suppress cell death and H_2O_2 production by VIGS of *BAK1/SERK4*. True leaves of WT, *btl1*, *cngc20-1* and *cngc20-2* after VIGS of *BAK1/SERK4* were stained with trypan blue for cell death (upper panel) and DAB for H_2O_2 accumulation (lower panel). Bar = 2 mm. (C) The *cngc20* mutants suppress *PR1* and *PR2* expression by VIGS of *BAK1/SERK4*. The expression of *PR1* and *PR2* was normalized to the expression of *UBQ10*. The data are shown as mean ± SE from three independent repeats. The different letters denote statistically significant difference according to one-way ANOVA followed by Tukey test ($p<0.05$). (D) Complementation of the *btl1* mutant with the *CNGC20* genomic fragment with an HA epitope tag at its C-terminus under the control of its native promoter restores growth defects by VIGS of *BAK1/SERK4*. CL#4 and CL#18 are two representative lines. Bar=5 mm. The CNGC20 proteins in transgenic plants were shown with a western blotting using an HA-HRP antibody (right panel). The protein loading is shown by Ponceau S staining for RuBisCo (RBC). (E) The *cngc20-3* mutant rescues the seedling lethality of the *bak1-4/serk4-1* mutant (top panel). Seedlings were grown on ½MS plate and photographed at 14 days after germination. Bar = 2 mm. The *bak1-4/serk4-1/cngc20-3* does not fully restore the growth of the *bak1-4/serk4-1* mutant to the wild type level. The plants were germinated in soil and photographed at 21 days after germination. Bar = 5 mm. (F) The alleviated cell death and H_2O_2 accumulation in *bak1-4/serk4-1/cngc20-3* compared to the *bak1-4/serk4-1* mutant. Bar = 1 mm. (G) The reduced *PR1* and *PR2* expression in *bak1-4/serk4-1/cngc20-3* compared to the *bak1-4/serk4-1* mutant. The different letters denote statistically significant difference according to one-way ANOVA followed by Tukey test ($p<0.05$).
The above experiments were repeated three times with similar results.

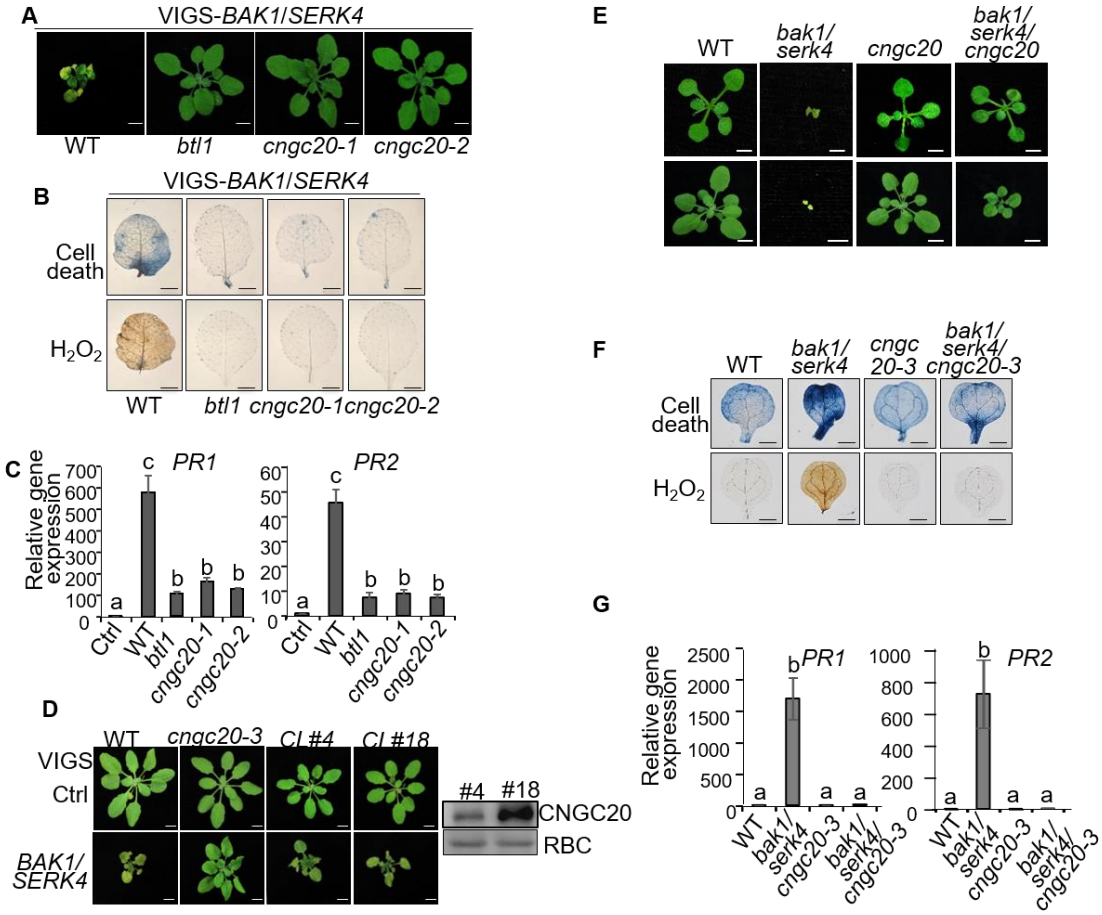
A
VIGS-BAK1/SERK4
WT
btl1
cngc20-1
cngc20-2
B
VIGS-BAK1/SERK4
Cell death
H2O2
WT
btl1
cngc20-1
cngc20-2
C
Relative gene expression
PR1
PR2
Ctrl
WT
btl1
cngc20-1
cngc20-2
D
WT
cngc20-3
CI #4
CI #18
VIGS Ctrl
BAK1/SERK4
#4
#18
CNGC20
RBC
E
WT
bak1/serk4
cngc20
bak1/serk4/cngc20
F
WT
bak1/serk4
cngc 20-3
bak1/serk4/cngc20-3
Cell death
H2O2
G
Relative gene expression
PR1
PR2
WT
bak1/serk4
cngc20-3
bak1/serk4/cngc20-3

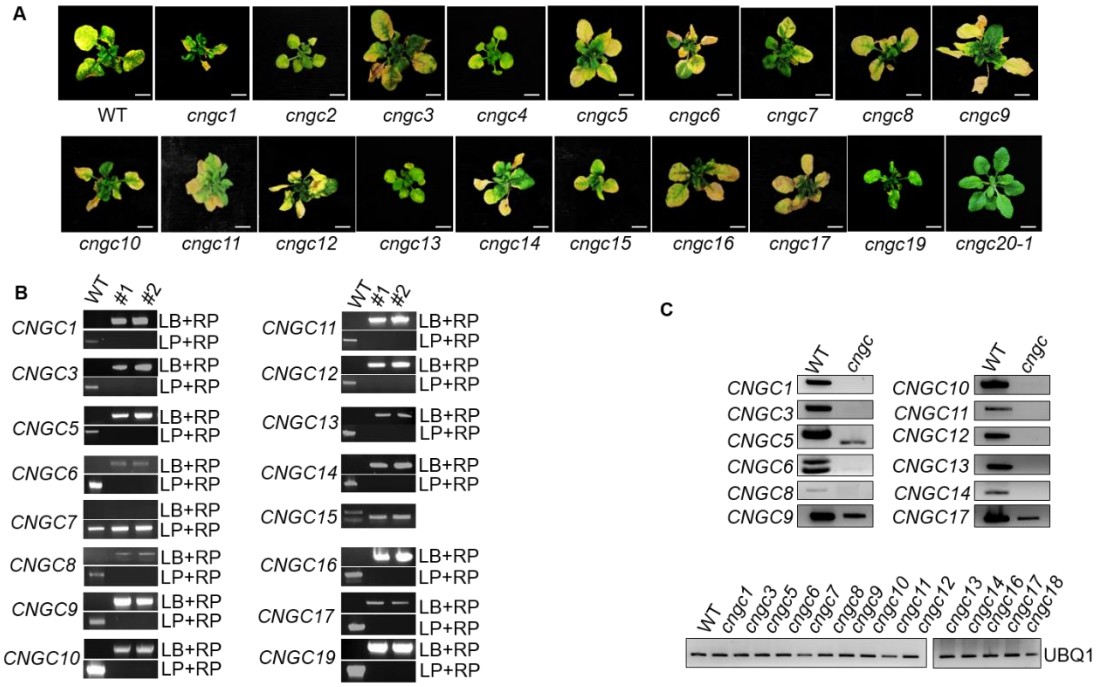

Figure 16. VIGS of *BAK1/SERK4* in various *cngc* mutants.

A. Unlike *cngc20-1*, mutants of other *CNGC* members do not appear to suppress growth defects by VIGS of *BAK1/SERK4*. Plant phenotypes are shown two weeks after VIGS of *BAK1/SERK4*. B. Geno-typing PCR analysis of *cngc* mutants. The DNA from WT and *cngc* mutants was PCR-amplified with the indicated primers to confirm that the lines used are homozygous except *cngc7*, which is WT. The primer pair of LP and RP is to amplify the genomic DNA fragment of *CNGCs* and the primer pair of LB and RP is to amplify the T-DNA insertions from the *cngc* mutants. C. RT-PCR analysis of *CNGC* expression in *cngc* mutants. The cDNA of *CNGCs* from WT and *cngc* mutants was PCR-amplified. *UBQ1* was used as an internal control.

The *Arabidopsis* genome encodes 20 *CNGC*s which mediates various abiotic and biotic stresses and developmental processes. To examine whether other CNGCs play a role in BAK1/SERK4-meidated cell death, we obtained all the other *cngc* mutants and performed comprehensive VIGS of BAK1/SERK4. The *cngc18* mutant is male sterile and could not set homozygous seeds. The *cngc2* and *cngc4* mutants, also known as *dnd1* (*d*efense, *n*o *d*eath 1) and *dnd2* respectively, showed compromised cell death triggered by different avirulent pathogens. Geno-typing and RT-PCR analysis confirmed that all

the mutants, except *cngc7* which is WT, are homozygous for the T-DNA insertion and showed reduced *CNGC* transcripts (Fig. 16B & 16C). Interestingly, all the other *cngc* out mutants could not suppress VIGS of BAK1/SERK4-mediated cell death (Fig. 16A).

Table 3. T-DNA insertional mutants of CNGC family members.

CNGCs	Gene Locus	Salk Line Number	T-DNA Insertion Position	Confirmation of T-DNA Insertion
CNGC1	At5g53130	SAIL_443_B11	*4th* exon	Ture knock out
CNGC2	At5g15410	*dnd1-1*	Trp_{290}→stop codon	Truncated protein
CNGC3	At2g46430	SALK_056832C	*3rd* exon	Ture knock out
CNGC4	At5g54250	*dnd2-1*	Trp_{89}→stop codon	Truncated protein
CNGC5	At5g57940	SALK_149893C	*5th* exon	Ture knock out
CNGC6	At2g23980	SALK_042207	*2nd* intron	Ture knock out
CNGC7	At1g15990	SALK_060871C	*1st* exon	Wild type
CNGC8	At1g19780	GABI_101C03	*4th* intron	Ture knock out

Table 3. Continued

CNGCs	Gene Locus	Salk Line Number	Insertion Position	Confirmation of T-DNA Insertion
CNGC9	At4g30560	SALK_026086	*5th* intron	Homozygous
CNGC10	At1g01340	SALK_015952C	*7th* exon	Ture knock out
CNGC11	At2g46440	SALK_026568C	*7th* intron	Ture knock out
CNGC12	At2g46450	SALK_092657	*5th* exon	Ture knock out
CNGC13	At4g01010	SALK_060826	*3rd* exon	Ture knock out
CNGC14	At2g24610	WiscDsLox437E09	2nd exon	Ture knock out
CNGC15	At2g28260	CS93507	point mutation	Homozygous
CNGC16	At3g48010	SAIL_726_B04	*3rd* exon	Homozygous
CNGC17	At4g30360	SALK_041923	*5th* exon	Homozygous
CNGC19	At3g17690	SALK_007105	*2nd* intron	Ture knock out
CNGC20	At3g17700	SALK_074919C	*10th* exon	Ture knock out

In addition to the negative role in regulating cell death, BAK1 and SERK4 positively regulate plant immunity and BR signaling. We tested whether the mutation in *cngc20* exerts any effects on the *bak1* deficiency in flagellin signaling and BR signaling. Flg22 triggers rapid phosphorylation of MAPKs and receptor-like cytoplasmic kinase BIK1. The *bak1-4* mutant displayed a compromised flg22-induced MAPK activation (Fig. 17A), and BIK1 phosphorylation (Fig. 17B). The compromised flg22-induced MAPK activation and BIK1 phosphorylation remained similar in *bak1-4/cngc20-1* as those in *bak1-4* (Fig. 17A & 17B). We also detected ROS production, another early event triggered by flg22. Similar with *bak1-4, bak1-4/cngc20-1* exhibited much less ROS production compared to WT or *cngc20-1* (Fig. 17C). Similar with *bak1-4, bak1-4/cngc20-1* showed compromised expression of flg22-induced genes, *WRKY30* and *MYB15,* compared to WT or *cngc20-1* (Fig. 17D). In addition, the *cngc20* mutation did not affect plant resistance to *Pseudomonas syringae* pv *maculicola* (*Psm*) ES4326. Bacterial growth was comparable in *cngc20* mutants with that in WT and the disease symptom of *cngc20* mutants is similar with WT (Fig. 17E). Furthermore, we examined whether effector-triggered immunity (ETI) response is affected in *cngc20* mutants. The *cngc20* mutants showed similar resistance with WT, as shown in bacterial growth and symptom development to *Pst* DC3000 carrying *avrRpt2* or *avrRps4* (Fig. 17F & 17G). ETI is often associated with localized cell death, referred as the hypersensitive response (HR). The progression of *Pst avrRpt2* and *avrRpm1*-triggered HR was similar in the *cngc20* mutants as that in WT plants (Fig. 17H). Taken together, the data suggest that

CNGC20 may not play a vital role in flagellin-mediated immune signaling and ETI response.

Figure 17. Unaltered flg22-mediated signaling and ETI responses in the *cngc20* mutant.

(A) The *cngc20-1* mutant did not affect the compromised flg22-induced BIK1 phosphorylation in the *bak1-4* mutant. Protoplasts from different plants were transfected with HA-tagged BIK1 and treated with 100 nM flg22 for 10 min. BIK1-HA proteins were detected by immunoblot using α-HA antibody (top panel), and the protein loading is shown by Ponceau S staining for RuBisCo (RBC) (bottom panel). (B) The *cngc20-1* mutant did not interfere with the compromised flg22-induced MAPK activation in the *bak1-4* mutant. Ten-day-old seedlings were treated without or with 100 nM flg22 for 15 and 30 min. The MAPK activation was analyzed by immunoblot with α-pERK antibody (top panel), and the protein loading is shown by Ponceau S staining for RBC (bottom panel). (C) The *cngc20-1* mutant did not impact the compromised flg22-induced ROS production in the *bak1-4* mutant. Leave discs from 4-week-old plants were treated with 100 nM flg22 for 30 min. The data are shown as means ± se from 24 leaf discs. (D) The *cngc20-1* mutant did not affect the compromised flg22-induced marker gene expression in the *bak1-4* mutant. Ten-day-old seedlings were treated without or with 100 nM flg22 for 30 or 60 min for qRT-PCR analysis. The data are shown as mean ± SE from three independent repeats. The different lettersindicate statistically significant differences from WT within the same time point according to two-way ANOVA followed by Tukey test ($p<0.05$). (E, F and G) The *cngc20* mutants exhibited similar resistance to *Psm* (E), *Pst* DC3000*avrRpt2* (F) and *Pst* DC3000*avrRps4* (G) infection. WT and *btl12*, *cngc20-1* and *cngc20-2* were hand-inoculated with bacteria at OD_{600} $=5\times10^{-4}$, and the bacterial counting was performed 2 and 4 days post-inoculation (dpi). The data are shown as mean ± se from three independent repeats. The disease symptom is shown at 4 dpi (bottom panel). (H and I) Comparable HR triggered by *Pst* DC3000*avrRpt2* (H) and *Pst* DC3000*avrRpm1* (I) in *cngc20* mutant plants and WT. Four-week-old WT and mutant plants were hand-inoculated with bacteria at OD=0.1. HR was examined by counting the percentage of wilting leaves of total inoculated leaves (18) at different time points after inoculation.
The experiments in B, C, D were repeated three times and A, E, F, G, H, I were repeated twice with similar results.

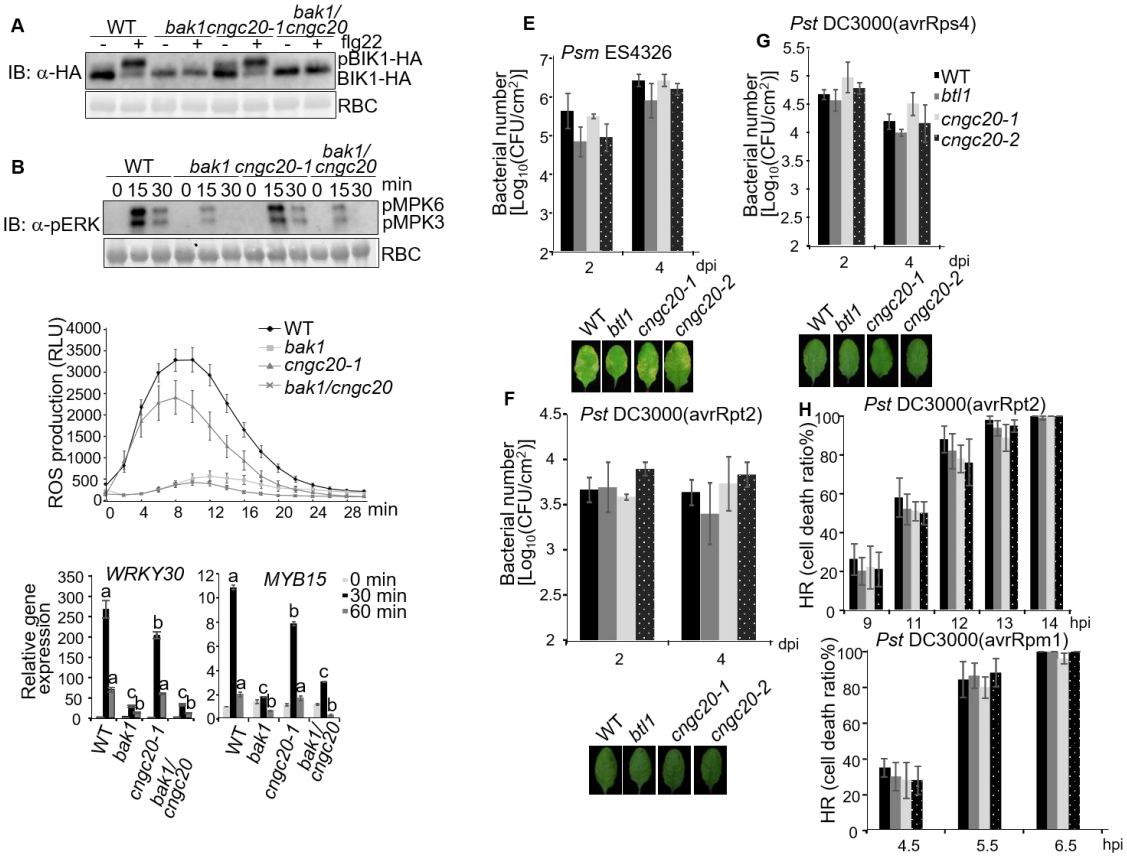
A
WT
bak1
cngc20-1
bak1/cngc20
flg22
IB: α-HA
pBIK1-HA
BIK1-HA
RBC
B
min
IB: α-pERK
pMPK6
pMPK3
RBC
ROS production (RLU)
WT
bak1
cngc20-1
bak1/cngc20
WRKY30
MYB15
0 min
30 min
60 min
Relative gene expression
E
Psm ES4326
Bacterial number [Log10(CFU/cm2)]
dpi
F
Pst DC3000(avrRpt2)
G
Pst DC3000(avrRps4)
WT
btl1
cngc20-1
cngc20-2
H
Pst DC3000(avrRpt2)
Pst DC3000(avrRpm1)
HR (cell death ratio%)
hpi

We next tested whether CNGC20 associates with BAK1 to regulate cell death. The coimmunoprecipitation (CoIP) assay using co-expressing FLAG-tagged CNGC20 and HA-tagged BAK1 in *Arabidopsis* protoplasts indicated that BAK1 was able to coimmunoprecipitate CNGC20 (Fig. 18A). In addition, when transiently expressed in *Nicotiana benthamiana*, BAK1-FLAG could immunoprecipitate CNGC20-HA (Fig. 18B). We further transformed *pCNGC20::CNGC20-HA* into *pBAK1::BAK1-FLAG* transgenic plants for CoIP assay. BAK1 could immunoprecipitate CNGC20 when expressed under the control of their native promoters, indicating BAK1 associates with CNGC20 in vivo (Fig. 18C). The association between BAK1 and CNGC20 was further confirmed by bimolecular fluorescence complementation (BiFC) assay (Fig. 18D). BAK1 was fused to the N-terminal fragment of YFP (BAK1-nYFP), whereas CNGC20 was fused to the C-terminal fragment of YFP (CNGC20-cYFP). The YFP signals were observed on the cell plasma membrane when co-expressing BAK1-nYFP and CNGC20-cYFP in *Arabidopsis* protoplasts (Fig. 18D). CNGC20 is a transmembrane protein consisting of N-terminal and C-terminal cytosolic domains (CNGC20N and CNGC20C) (Fig 18E). To further examine which cytosolic domain associates with BAK1, the CoIP assay using co-expressing FLAG-tagged CNGC20N or CNGC20C and HA-tagged full length BAK1 in *Arabidopsis* protoplasts indicated full length BAK1 associates with CNGC20N but not CNGC20C (Fig. 19A). Interestingly, the juxtamembrane and cytosolic kinase domains of BAK1 (BAK1JK) could immunoprecipitate both CNGC20N and CNGC20C (Fig. 18F). Next we test whether CNGC20N or CNGC20C directly interacts with BAK1. The maltose-binding protein (MBP)-tagged BAK1JK (MBP-

BAK1JK) could be pulled down by the glutathione S-transferase (GST)-tagged CNGC20N or CNGC20C but not by GST itself (Figure. 18G & 18H). Interestingly, BAK1 kinase mutant could not interact with CNGC20C, suggesting that kinase activity of BAK1 is required for the interaction with CNGC20C (Fig. 19B). Moreover, the interaction between BAK1 and CNGC20N was confirmed by yeast two-hybrid assay (Fig 18I). All the data above indicate that CNGC20 interacts with BAK1 via its N- and C-terminus.

Figure 18. The interaction between CNGC20 and BAK1.

(A) CNGC20 associates with BAK1 in *Arabidopsis* protoplast. CNGC20-FLAG and BAK1-HA proteins were transiently co-expressed in *Arabidopsis* protoplasts. Protein extracts were immunoprecipitated with α-FLAG agarose beads (IP: α-FLAG) and immunoblotted with α-HA antibody (IB: a-HA) (upper panel). The protein inputs are shown with immunoblotting before immunoprecipitation (lower two panels). (B) CNGC20 associates with BAK1 in *N. benthamiana*. CNGC20-HA and BAK1-FLAG proteins were transiently co-expressed in *N. benthamiana*. Protein extracts were immunoprecipitated with α-FLAG agarose beads (IP: a-FLAG) and immunoblotted with α-HA antibody (IB: a-HA) (upper panel). The protein inputs are shown with immunoblotting before immunoprecipitation (lower two panels). (C) CNGC20 associates with BAK1 in transgenic plants. Protein extracts from transgenic plants containing *pBAK1::BAK1-FLAG* and *pCNGC20::CNGC20-HA* were immunoprecipitated with α-FLAG agarose beads (IP: a-FLAG) and immunoblotted with a-HA (IB: a-HA) or a-FLAG (IB: a-FLAG) (upper two panels). The protein inputs are shown with immunoblotting before immunoprecipitation (lower two panels). (D) Interaction between CNGC20 and BAK1 by BiFC assay in *Arabidopsis* protoplast. BAK1-nYFP and CNGC20-cYFP proteins were transiently co-expressed in protoplast. YFP signals were observed using a confocal microscopy. EV indicates the empty vector used as control. Bar=10μm. (E) Protein structure of CNGC20 to indicate CNGC20 N-terminus and C-terminus. (F) Both N-terminus and C-terminus of CNGC20 (hereafter, CNGC20N and CNGC20C) interact with the juxtamembrane and cytosolic kinase domains of BAK1 (hereafter, BAK1JK) in *Arabidopsis* protoplast. BAK1JK-FLAG and CNGC20N-HA or CNGC20C-HA proteins were transiently co-expressed in *Arabidopsis* protoplasts. Protein extracts were immunoprecipitated with α-FLAG agarose beads (IP: a-FLAG) and immunoblotted with a-HA antibody (IB: a-HA) (upper panel). The protein inputs are shown with immunoblotting before immunoprecipitation (lower two panels). (G) CNGC20N interacts with BAK1JK *in vitro* pull-down (PD) assay. GST or GST-CNGC20N immobilized on glutathione Sepharose beads was incubated with MBP or MBP-BAK1JK-HA proteins. The beads were washed and pelleted for immunoblotting analysis with a-HA antibody (PD: GST; IB: a-HA) (upper panel). CBB staining of input proteins is shown on the bottom. (H) CNGC20C interacts with BAK1JK *in vitro* pull-down (PD) assay. GST or GST-CNGC20N immobilized on glutathione Sepharose beads was incubated with MBP or MBP-BAK1JK-HA proteins. The beads were washed and pelleted for immunoblotting analysis with a-HA antibody (PD: GST; IB: a-HA) (upper panel). CBB staining of input proteins is shown on the bottom. (I) BAK1 interacts with CNGC20N in yeast two hybrid assay. The interaction between pAD-BAK1K and pBK-CNGC20N was tested on SD-H-L-T supplemented with 1 mM 3-amino-1,2,4-triazole (3AT). Serial dilutions of the yeast colonies were plated.

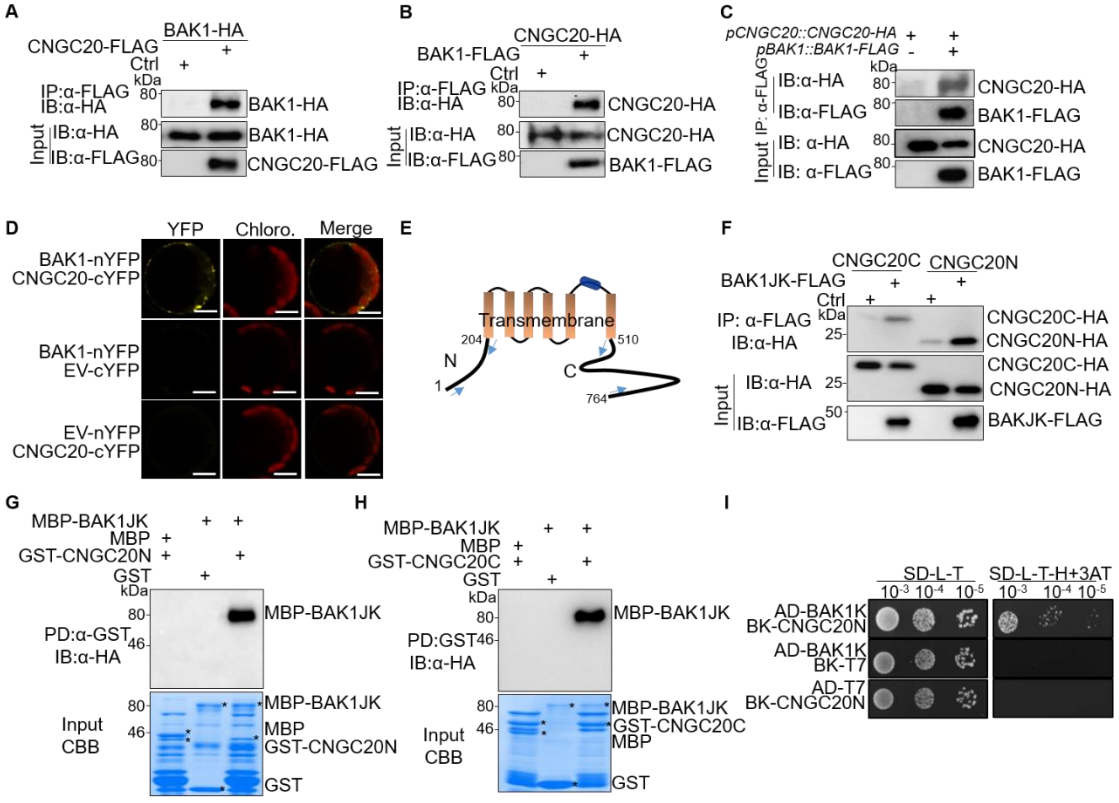
A
BAK1-HA
CNGC20-FLAG
Ctrl
kDa
IP:α-FLAG
IB:α-HA
80
BAK1-HA
Input
IB:α-HA
80
BAK1-HA
IB:α-FLAG
80
CNGC20-FLAG
B
CNGC20-HA
BAK1-FLAG
Ctrl
kDa
IP:α-FLAG
IB:α-HA
80
CNGC20-HA
Input
IB:α-HA
80
CNGC20-HA
IB:α-FLAG
80
BAK1-FLAG
C
pCNGC20::CNGC20-HA
pBAK1::BAK1-FLAG
kDa
IP: α-FLAG
IB:α-HA
80
CNGC20-HA
IB:α-FLAG
80
BAK1-FLAG
Input
IB: α-HA
80
CNGC20-HA
IB: α-FLAG
80
BAK1-FLAG
D
YFP
Chloro.
Merge
BAK1-nYFP
CNGC20-cYFP
BAK1-nYFP
EV-cYFP
EV-nYFP
CNGC20-cYFP
E
Transmembrane
204
510
N
C
1
764
F
CNGC20C
CNGC20N
BAK1JK-FLAG
Ctrl
kDa
IP: α-FLAG
IB:α-HA
25
CNGC20C-HA
CNGC20N-HA
Input
IB:α-HA
25
CNGC20C-HA
CNGC20N-HA
IB:α-FLAG
50
BAKJK-FLAG
G
MBP-BAK1JK
MBP
GST-CNGC20N
GST
kDa
80
PD:α-GST
IB:α-HA
46
MBP-BAK1JK
Input
CBB
80
46
MBP-BAK1JK
MBP
GST-CNGC20N
GST
H
MBP-BAK1JK
MBP
GST-CNGC20C
GST
kDa
80
PD:GST
IB:α-HA
46
MBP-BAK1JK
Input
CBB
80
46
MBP-BAK1JK
GST-CNGC20C
MBP
GST
I
SD-L-T
SD-L-T-H+3AT
10-3 10-4 10-5
10-3 10-4 10-5
AD-BAK1K
BK-CNGC20N
AD-BAK1K
BK-T7
AD-T7
BK-CNGC20N

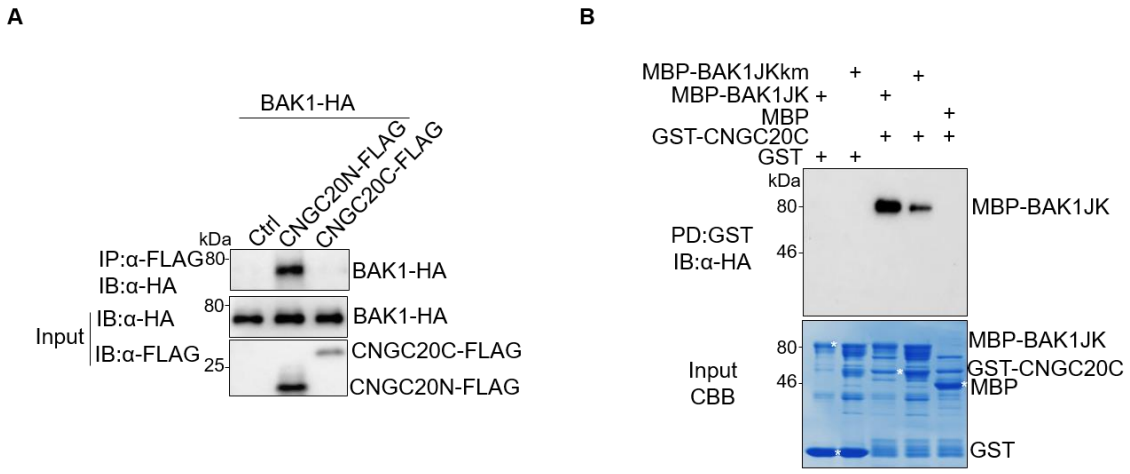

Figure 19. The interaction between CNGC20 and BAK1.

(A) Full length BAK1 interacts with CNGC20N but not CNGC20C. The CNGC20N-FLAG or CNGC20C-FLAG and BAK1-HA proteins were transiently co-expressed in *Arabidopsis* protoplast. Protein extracts were immunoprecipitated with a-FLAG antibody (IP: a-FLAG) and immunoblotted with a-HA antibody (IB: a-HA) (top panel). The protein inputs are shown with immunoblotting before immunoprecipitation (bottom two panels). (B) BAK1 kinase activity is required for the interaction with CNGC20C. GST or GST-CNGC20C immobilized on glutathione Sepharose beads was incubated with MBP, MBP-BAK1JK-HA or MBP-BAK1JKKM-HA proteins. The beads were washed and pelleted for immunoblotting analysis with a-HA antibody (PD: GST; IB: a-HA) (top panel). CBB staining of input proteins is shown on the bottom.

As BAK1 possesses strong kinase activity, it is reasonable to test phosphorylation event between BAK1 and CNGC20. In vitro kinase assay indicated that BAK1 directly phosphorylates both CNGC20N and CNGC20C (Fig. 20A& 20B), BAK1 kinase mutant lost the capacity to phosphorylate CNGC20C (Fig. 20B), which is consistent with previous pull down assay (Fig. 19B). The phosphorylated CNGC20N and CNGC20C were further subjected for liquid chromatography-tandem mass spectrometry (LC-MS/MS) analysis. We identified Ser156 and Ser184 as the phosphorylation sites by BAK1 at CNGC20N, while Thr560 and Ser618 were major phosphorylation sites by BAK1 at CNGC20C (Fig. 20C). The T560A did not affect the

phosphorylation by BAK1. Surprisingly, the T155/S156/S184/S185/A quadruple mutant of CNGC20N did not change the phosphorylation status by BAK1, while the T560/S617/S618/T619A quadruple mutant of CNGC20C significantly compromised phosphorylation by BAK1 (Fig. 20D & 20E). We hypothesize that CNGC20 activity may be negatively regulated by BAK1 via phosphorylation. To test the hypothesis, we transformed the phosphor-mimetic form of CNGC20 (T560/S617/S618/T619D), which resembles loss-of-function of CNGC20, into *cngc20* mutant. The phosphor- mimetic form of CNGC20 did not restore the cell death as wild type CNGC20 did (Fig. 20F), suggesting that specific phosphorylation sites of CNGC20 by BAK1 are indispensable for its function in cell death control.

Figure 20. Phosphorylation of CNGC20C by BAK1 is essential for CNGC20's function in *bak1/serk4* cell death.

(A) BAK1 phosphorylates CNGC20N. The *in vitro* kinase assay was performed by incubating MBP or MBP-BAK1JK as kinase with GST or GST-CNGC20N as substrate. The phosphorylation of CNGC20N by BAK1JK with autoradiography (upper panel). And the protein loading control was shown by Coomassie blue staining (lower panel). (B) BAK1 phosphorylates CNGC20C. The *in vitro* kinase assay was performed by incubating MBP, MBP-BAK1JK or MBP-BAK1JKkm as kinase with GST or GST-CNGC20N as substrate. The phosphorylation of CNGC20C by BAK1JK with autoradiography (upper panel). And the protein loading control was shown by Coomassie blue staining (lower panel). (C) LC-MS/MS analysis reveals that Thr560 and Ser618 of CNGC20C are phosphorylated by BAK1JK. (D) The T155A/S156A/S183A/S184A quadruple mutant of CNGC20N couldn't block the phosphorylation by BAK1. The *in vitro* kinase assay was performed by incubating MBP-BAK1JK as kinase with GST, GST-CNGC20N or GST-CNGC20N^{QA} as substrate. The phosphorylation was analyzed by autoradiography (upper panel). And the protein loading control was shown by Coomassie blue staining (lower panel). (E) The T560A/S617A/S618A/T619A quadruple mutant of CNGC20C significantly compromised phosphorylation by BAK1JK. The *in vitro* kinase assay was performed by incubating MBP-BAK1JK as kinase with GST, GST-CNGC20C or GST-CNGC20C^{QA} as substrate. The phosphorylation was analyzed by autoradiography (upper panel). And the protein loading control was shown by Coomassie blue staining (lower panel). (F) Complementation of the *btl1* mutant with the *CNGC20*^{QD} genomic fragment with an HA epitope tag at its C-terminus under the control of its native promoter restores growth defects by VIGS of *BAK1/SERK4.* CL#3 and CL#5 are two representative lines. Bar=5 mm.

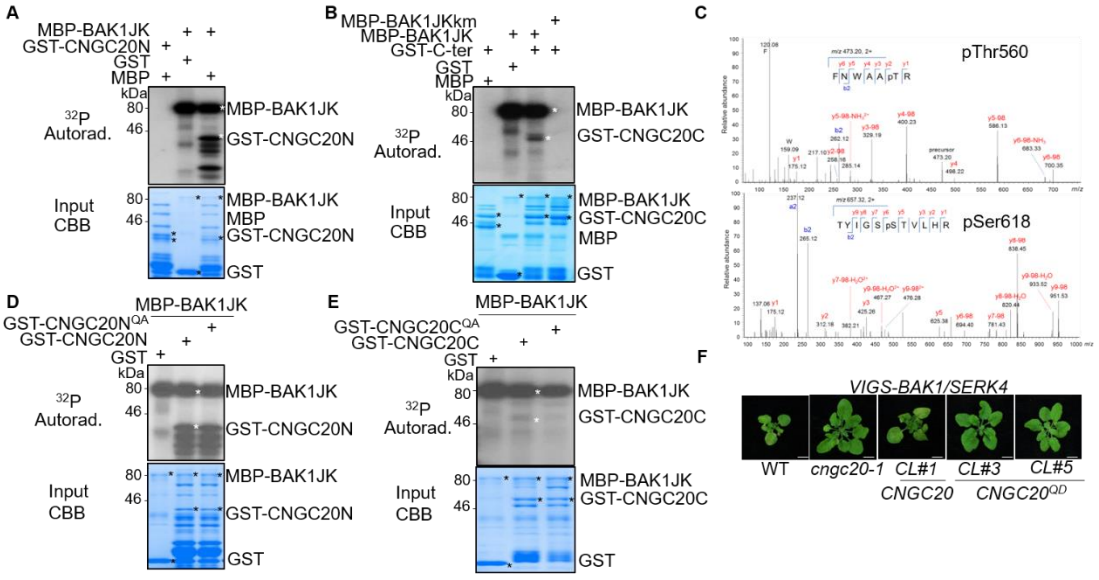
A
MBP-BAK1JK
GST-CNGC20N
GST
MBP
kDa
80
46
32P Autorad.
MBP-BAK1JK
GST-CNGC20N
Input CBB
MBP-BAK1JK
MBP
GST-CNGC20N
GST
B
MBP-BAK1JKkm
MBP-BAK1JK
GST-C-ter
GST
MBP
MBP-BAK1JK
GST-CNGC20C
MBP-BAK1JK
GST-CNGC20C
MBP
GST
C
pThr560
F N W A A pT R
pSer618
T Y I G S pS T V L H R
D
GST-CNGC20NQA
GST-CNGC20N
MBP-BAK1JK
E
GST-CNGC20CQA
GST-CNGC20C
F
VIGS-BAK1/SERK4
WT
cngc20-1
CL#1
CL#3
CL#5
CNGC20
CNGC20QD

The working model for CNGC in animals has been well established. Classical CNGC channels in animals exist as heterotetramers that are composed of A and B subunits. Several residues in human CNGC HCN have been shown to be important for inter-subunit interaction (Fig. 21B). The identified phosphorylation sites locate in C-linker and CNBD, respectively (Fig. 21A & 21B). This is consistent with that C-terminus of CNGC is important for its regulation and function. To test whether CNGC20 functions similarly in animals, first we performed CoIP assay to determine whether CNGC20 forms dimer, FLAG-tagged CNGC20 could associate with HA-tagged CNGC20 in *Arabidopsis* protoplasts (Fig. 21C), indicating that CNGC20 could form dimer. Next we sought to address which domain of CNGC20 mediates dimerization by coIP assay in *Arabidopsis* protoplast, CNGC20C could associate with itself (Fig. 21D), suggesting that CNGC20 forms dimerization via its C terminus. This is consistent with crystal structure of human CNGC HCN which showed that tetrameric assemble is mediated by its soluble C-terminal domains (Cukkemane et al., 2011). Furthermore, we tested if phosphorylation mutant of CNGC20 affect CNGC20 dimerization, the coIP assay showed that T560/S617/S618/T619D mutant interfered with CNGC20 dimerization (Fig. 21E). Consistently, the BiFC assay revealed that T560/S617/S618/T619D mutant exhibited weaker YFP signal compared with wild type CNGC20 (Fig. 21F), Taken together, CNGC20 homodimerizes through C-terminus and the phosphorylation by BAK1 affect the CNGC20 dimerization.

Figure 21. Phosphorylation of CNGC20 by BAK1 affects CNGC20 dimerization.

(A) Linear protein scheme of CNGC20 to indicate the phosphorylation residues location. (CNGC20 N terminus: (1-205)aa; CNGC20 transmembrane domain: (206-516)aa; C-linker region: (517-592)aa; CNBD: (593-712)aa; CaMBD: (713-732)aa. The phosphorylation sites of CNG20 by BAK1 were shown as red arrows. (B) Amino acid alignment of partial C-linker region and CNBD domain among human CNGC protein HCN, *Arabidopsis* CNGC19 and CNGC20. The secondary structure for α-helix and β-sheet are labled with letters. Red stars under the sequence indicate phosphorylation residues and the critical residues for interaction were indicated by a red rectangle. (C) Dimerization of CNGC20 in *Arabidopsis* protoplasts. CNGC20-FLAG and CNGC20-HA proteins were transiently co-expressed in protoplasts. Protein extracts were immunoprecipitated with α-FLAG agarose beads (IP: a-FLAG) and immunoblotted with a-HA antibody (IB: a-HA) (upper panel). The protein inputs are shown with immunoblotting before immunoprecipitation (lower two panels). (D) Dimerization of CNGC20 is mediated by CNGC20C. CNGC20C-FLAG and CNGC20C-HA proteins were transiently co-expressed in *Arabidopsis* protoplasts. Protein extracts were immunoprecipitated with α-FLAG agarose beads (IP: a-FLAG) and immunoblotted with a-HA antibody (IB: a-HA) (upper panel). The protein inputs are shown with immunoblotting before immunoprecipitation (lower two panels). (E) The T560D/S617D/S618D/T619D quadruple phosphor-mimetic mutant displays weaker dimerization. CNGC20-FLAG, phosphor-mimetic from CNGC20^{QD}-FLAG or phosphor-inactive form CNGC20^{QA}-FLAG and CNGC20-HA, CNGC20^{QD}-HA or CNGC20^{QA}-HA proteins were transiently co-expressed in *Arabidopsis* protoplasts, respectively. Protein extracts were immunoprecipitated with α-FLAG agarose beads (IP: a-FLAG) and immunoblotted with a-HA antibody (IB: a-HA) (upper panel). The protein inputs are shown with immunoblotting before immunoprecipitation (lower two panels). (F) Phosphor-inactive form of CNGC20 show weaker dimerization by BiFC assay. CNGC20-nYFP co-expressed with CNGC20-cYFP, CNGC20^{QD}-cYFP or EV-cYFP proteins in *Arabidopsis* protoplast. YFP signals were observed using a confocal microscopy. EV indicates the empty vector used as control. Bar=10μm.

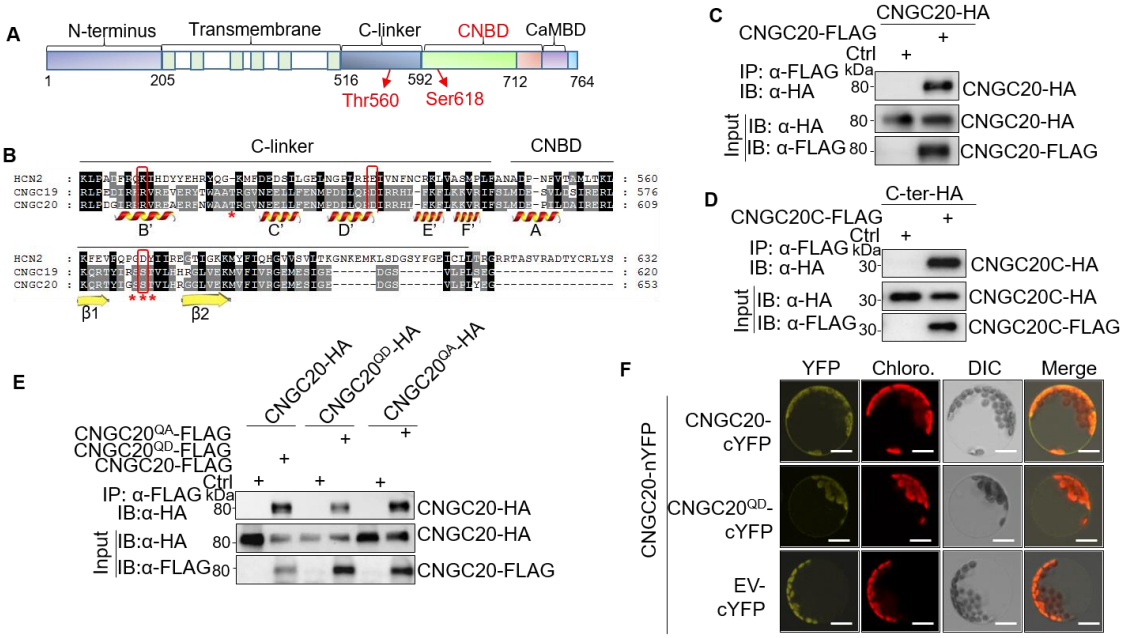
A
N-terminus
Transmembrane
C-linker
CNBD
CaMBD
1
205
516
592
712
764
Thr560
Ser618
B
C-linker
CNBD
HCN2
CNGC19
CNGC20
B'
C'
D'
E'
F'
A
β1
β2
C
CNGC20-HA
CNGC20-FLAG
Ctrl
IP: α-FLAG
IB: α-HA
kDa
80
CNGC20-HA
Input
IB: α-HA
IB: α-FLAG
CNGC20-FLAG
D
C-ter-HA
CNGC20C-FLAG
30
CNGC20C-HA
CNGC20C-FLAG
E
CNGC20-HA
CNGC20QD-HA
CNGC20QA-HA
CNGC20QA-FLAG
CNGC20QD-FLAG
CNGC20-FLAG
IP: α-FLAG
IB:α-HA
IB:α-FLAG
F
YFP
Chloro.
DIC
Merge
CNGC20-nYFP
CNGC20-cYFP
CNGC20QD-cYFP
EV-cYFP

We have identified *stt3a* as a suppressor of BAK1/SERK4-mediated cell death and CNGC20 is a membrane-resident protein. We hypothesize that CNGC20 may have *N*-glycosylation modification dependent on STT3a. First CNGC20 proteins when expressed in *stt3a-2* migrated faster than that in WT (Fig. 22A), indicating that STT3a is required for CNGC20 glycosylation. Out of five potential *N*-glycosylation sites (Asn in Asn-X-Ser/Thr, where X is any amino acid except Pro), we mutate three sites to Gln (CNGC20 (N430/452/N455Q) and found that CNGC20 (N430/452/N455Q) showed a faster migration than WT CNGC20 when expressed in *Arabidopsis* protoplasts (Fig. 22B), resembling the CNGC expression in *stt3a* (Fig. 22A). Next we test the localization of CNGC20 and CNGC20 (N430/452/N455Q) in WT or CNGC20 in *stt3a-2* mutant. Interestingly, the CNGC20 (N430/452/455Q) protein exhibited similar accumulation in the endomembrane in WT compared with CNGC20 in *stt3a-2* mutant, indicating that glycosylation modification of CNGC20 depends on STT3a is required for targeting to plasma membrane. To test whether CNGC20 glycosylation is required for cell death control, we transformed CNGC20 (N430/452/N455Q) under its native promoter into *cngc20-1* mutant. Surprisingly, the CNGC20 (N430/452/N455Q) restores the cell death triggered by VIGS BAK1/SERK4, suggesting that the glycosylation modification of CNGC20 may not be required for its function in *bak1/serk4* cell death control (Fig. 22C).

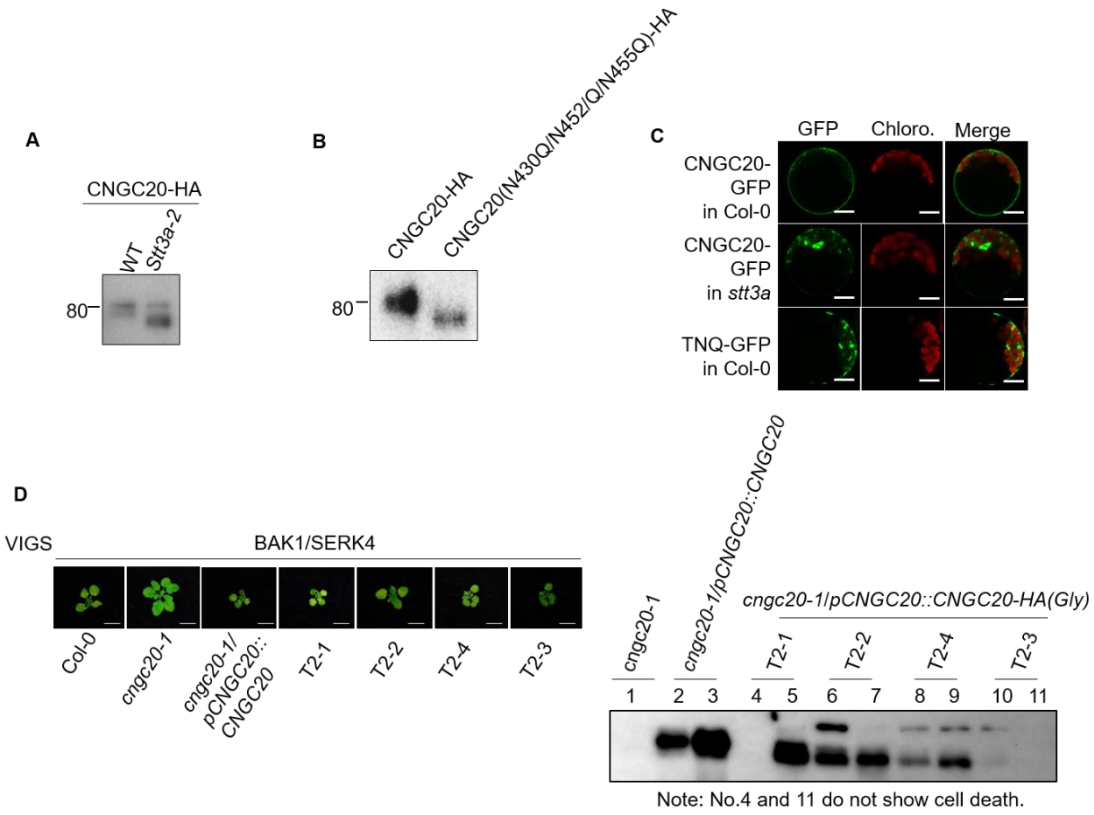

Figure 22. Glycosylation of CNGC20 by STT3a may not be required for CNGC20's function in *bak1/serk4* cell death.

(A) The CNGC20 protein migrates faster in *stt3a-2* mutant compared with in WT. Protoplasts from WT and *stt3a-2* mutant were transfected with *CNGC20-HA*. The proteins were detected by immunoblot with α-HA antibody. (B) The glycosylation mutant protein CNGC20 (N430/452/N455Q) migrates faster than WT CNGC20 protein. Protoplasts from WT were transfected with *CNGC20-HA* and CNGC20 (N430/452/N455Q)-HA. The proteins were detected by immunoblot with α-HA antibody. (C) The mutant CNGC20 (N430/452/455Q) protein exhibited similar accumulation in the endomembrane in WT compared with CNGC20 in *stt3a-2* mutant. Protoplasts from WT or *stt3a-2* were transfected with *CNGC20-GFP* or *CNGC20 (N430/452/455Q)-GFP*. YFP signals were observed using a confocal microscopy. Bar=10uM (D) Complementation of the *cngc20-1* mutant with glycosylation mutation form CNGC20 (N430/452/N455Q) with an HA epitope tag at its C-terminus under the control of its native promoter restores growth defects by VIGS of *BAK1/SERK4.* Bar=5 mm. The CNGC20 proteins in transgenic plants were shown with a western blotting using an HA-HRP antibody (right panel).

Table 4. Primers used in this study.

Cloning primers for VIGS analysis.

Gene	Forward Primer	Reverse Primer
BAK1	5'-CATGCCATGGGTATGGAGTCATGCTTCTTG-3'	5'-GGGGTACCCTTGTCTGAACATTTCCTCC-3'
SERK4	GGAATTCACAAAGATCACTCCTTTGCT	GGGGTACCATGCCATGGGTTATTGCTATAAAGCTCCA
BIR1	TTGGAATTCGCGGATCAGGCCAACATAG	TTGGGTACCGGGATAGGACCAACGAGACG
MEKK1	CGGAATTCTCAGGGAAGTCAGGCACAAG	GGGGTACCGGCTTGAACGGGTTCGAGAT

Note: The restriction enzyme sites are underlined.

Genotyping primers

Mutant	Left Primer (LP)	Right Primer (RP)
cngc1	CAGCTCTGCAAGGATCAAAC	TAGAAATGAACACCGCGAAAC
cngc3	AAATCAGAACCTTTAAGCGGC	TACCAAAGTTGAAAACCGTCG
cngc5	GAGCTTTCTGGTTAAGCCGTC	CACGCTCCCTAAGATCTTGTG
cngc6	TCCAGGATATGTGCTGGTTTC	TCCGTTGATCCTCTCTTCTTG
cngc7	ACATGTACCAAAACGCTCCAG	AAATCCCAATACATAAGCGGC
cngc8	AAGTTTGAGCCTGCTTTAGGG	ACTGGAGCGTTCTGGTACATG

Table 4. Continued

Mutant	Left Primer (LP)	Right Primer (RP)
cngc9	ATTTGCAGCAAACTTTGAAGC	TGTTTATGGTGGGGACTTTAG
cngc10	CCTGTGCTCTACACCGAGAAC	AGCATTCTCCCTCAGGTTTTC
cngc11	TTTACAGTGGTTGAGGTGGTG	TTTACAGTGGTTGAGGTGGTG
cngc12	ATTGTTCCCTTCGTTTGTGTG	AAAGGGAGCTAGCTTACACGC
cngc13	TGGATTTCAGAGGGAACAGAG	AGCCATCAAGTGTGTCACATG
cngc14	TAAGAATCCAAGTGGCCACAC	TGTTTCACGTAAAGTCAAACCC
cngc15	CAGTCAACAACAATGAGACTTG	AAGTAGGTATATCAAGAATTG
cngc16	TCAAATTCAAAACCGCTTTTG	CGTCTAACCTAGCAGTCGTCG
cngc17	CAGCAGCTTAGGTAATGGCAG	ATTGATTCAATCGCAGTGAGG
cngc19	ATGCATAACTTCCACGAGCAC	CGCAAATCTCTTGAGATCTGG

Table 4. Continued

Mutant	Left Primer (LP)	Right Primer (RP)
cngc20-1	AAAACAGTTACCTGGAAGCCC	TGCCTTTACACCACCTTTTTG
cngc20-2	GAATTTGGAAATGACGCTGAG	TATCTCCACGCCACTTGAATC
SALK_013823C	TTCAACATGCGAGTTTGTGTC	AAAATCACGGCATAACATTCG
SALK_087793C	CAACATATCTATATACCATGG	GACAAGCGATTCGATCACGTG
SALK_042821C	GACAAGCGATTCGATCACGTG	AAAATCACGGCATAACATTCG
bak1-4	CAGGGGCTATATGACCAATTG	TCCTATCTCTCCTACACCGCC
serk4-1	TGGCTCAGAAGAAAACCACAG	CTGCTCCACTTCTGTTTCCAC

Note: The T-DNA left and right border primers were selected accordingly to each mutant. For SALK lines, LBb1.3 (ATTTTGCCGATTTCGGAAC); for SAIL lines, LB (GCCTTTTCAGAAATGGATAAATAGCCTTGCTTCC); for GABI line, LB (TAATAACGCTGCGGACATCTACA); and for WiscDsLox lines, LB (CGTCCGCAATGTGTTATTAAGTTG) was used respectively.

Table 4. Continued

qRT-PCR primers

Gene	Forward Primer	Reverse Primer
PR1	GGTTAGCGAGAAGGCTAACTAC	CATCCGAGTCTCACTGACTTTC
PR2	GCATTCGCTGGATGTTTTG	CTTCAACCACACCAGCTTGGAC
WRKY30	GCAGCTTGAGAGCAAGAATG	AGCCAAATTTCCAAGAGGAT
MYB15	CTTGGCAATAGATGGTCAGC	TGAGTGTGCCATACGTTCTTG
LOX4	GTACAACAAGCGTTAGAGAC	TCGGGTCAAGAACAATATGG
UBQ10	AGATCCAGGACAAGGAAGGTATTC	CGCAGGACCAAGTGAAGAGTAG

RT-PCR primers

Gene	Forward Primer	Reverse Primer
UBQ1	ACCGGCAAGACCATCACTCT	AGGCCTCAACTGGTTGCTGT
CNGC19	CATGCCATGGCTCACACTAGGACTTTCACTTCC	CCCAAGCTGACTCAAATATG
CNGC20	CATGCCATGGCTTCCCACAACGAAAAC	GAAGGCCTAAGGCTATAACTAGA CTGAGG

Table 4. Continued

Gene	Forward Primer	Reverse Primer
At1g60995	P1 primer GCTCTAGACCATGGATCCGGAGCAGACG	
At1g60995	P2 primer CAACATATCTATATACCATGG	
At1g60995		P3 primer GAAGGCCTGTTGCCAAAGCAGGGATGCCG
At1g60995		P4 primer GAAGGCCTACCTTGACCAGCAGAGTTCTG
At1g60995		P5 primer GAAGGCCTTCCGAAATGCGCAGAACC
At1g60995		P6 primer GACAAGCGATTCGATCACGTG
CNGC1	CAGCTCTGCAAGGATCAAAC	TAGAAATGAACACCGCGAAAC

Table 4. Continued

Gene	Forward Primer	Reverse Primer
CNGC3	AAATCAGAACCTTTAAGCGGC	TACCAAAGTTGAAAACCGTCG
CNGC5	GATCGGACGTTCACTTGGTT	CACGCTCCCTAAGATCTTGTG
CNGC6	TCCAGGATATGTGCTGGTTTC	TCCGTTGATCCTCTCTTCTTG
CNGC8	CGGGATCCATGTCATCTAATGCTACGGGAATG	GAAGGCCTGTTCAAGTCATCTGTATCAAG
CNGC9	ATTTGCAGCAAACTTTGAAGC	TGTTTATGGTGGGGACTTTAG
CNGC10	CCTGTGCTCTACACCGAGAAC	CTAAGGGTCAGTTGTATGATTG
CNGC11	CGGGATCCATGAATCTTCAGAGGAGAAAATTTG	GAAGGCCTCGCATAAATCGCAGCACCTAAG
CNGC12	GCTCCTCGTTCTCAAGCATC	TCCTACCTCAACCAGAACCG
CNGC13	TGGATTTCAGAGGGAACAGAG	CCCCAACGAATTTGCTTGTA
CNGC14	ATGGAGTTCAAGAGAGACAATAC	GCTTCTGATTGATGGCAAGA

Table 4. Continued

Gene	Forward Primer	Reverse Primer
CNGC15	CAGTCAACAACAATGAGACTTG	AAGTAGGTATATCAAGAATTG
CNGC17	TATGGGATCTTTGGGAATGC	ATTGATTCAATCGCAGTGAGG

Cloning and point-mutation primers

Gene	Forward Primer	Reverse Primer
CNGC19	CATGCCATGGCTCACACTAGGACTTTCACTTCC	GAAGGCCTACGGTTGGAATTGGAGTGAGCAGT
CNGC20	CATGCCATGGCTTCCCACAACGAAAAC	GAAGGCCTAAGGCTATAACTAGA CTGAGG
Promoter CNGC20	CCGCTCGAGGTAAGTTCATTTCAGGTTTGGTTG	CATGCCATGGTTCTTGACCAAAATCACGGTTTC
CNGC20^{N430Q}	CCTGGAAAGAT**CAA**GCGAGTGCCAATGCTTGTTTC	GAAACAAGCATTGGCACTCGC**TTG**ATCTTTCCAGG
CNGC20 N452/455/Q	CTATTTAAAAGCAGTC**CAA**CTTACC**CAA**CATTCTAATCTCTTCAC	GTGAAGAGATTAGAATG**TTG**GGTAAG**TTG**GACTGCTTTTAAATAG
CNGC20-Nter	CGGGATCCATGGCTTCCCACAACG	GAAGGCCTAACCTCTTTGGCATGAGG

Table 4. Continued

Gene	Forward Primer	Reverse Primer
CNGC20-Cter	CGGGATCCATGGCTCTTGGTAAAAGG	GAAGGCCTAAGGCTATAACTAGA CTGAGG
At1g60995	GCTCTAGACCATGGATCCGGAGCAGACG	GAAGGCCTATCAACTGAAAGAGGATCATG
Promoter At1g60995	CGGAGCTCAGGACAAGGAAGGTCTGATTC	GCTCTAGAATTTCGGATCTCCGATGC
At1g60995-Nter	GCTCTAGACCATGGATCCGGAGCAGACG	GAAGGCCTACCTTGACCAGCAGAGTTCTG

Note: The restriction enzyme sites are underlined and the point mutation sites are underlined and in bold

3.5 Discussion

In the present study, we identified a suppressor of *bak1/serk4* cell death via virus-induced gene silencing, an unbiased and efficient genetic screening on *Arabidopsis* T-DNA mutant collections. The suppressor carries a mutation in *CNGC20* responsible for the suppression of *bak1/serk4* cell death. Systematic examination of VIGS of BAK1/SERK4 in all the mutants of CNGC members indicates that only CNGC20 plays an important role in the regulation of *bak1/serk4* cell death. Interestingly, BAK1 directly interacts with and phosphorylates membrane-resident CNGC20. Mass spectrometry and mutagenesis analysis revealed that specific phosphorylation sites of CNGC20 by BAK1 are indispensable for its function in cell death control.

CNGCs have emerged to play roles in a wide range of physiological processes, especially in programmed cell death processes. The mutant of CNGC2 or CNGC4 did

not display HR in response to different avirulent pathogens (Balague et al., 2003; Clough et al., 2000). The chimeric protein CNGC11/12 induces spontaneous cell death (Yoshioka et al., 2006). Our screen integrates CNGC20 to be a novel component of *bak1/serk4* cell death signaling. All these findings implies that activation of CNGCs may be indispensable for the cell death signal transduction.

CoIP, BIFC and yeast two-hybrid assay all suggest BAK1 interacts with CNGC20. In addition, BAK1 phosphorylates CNGC20 in vitro. These data suggest that CNGC20 is a direct substrate of BAK1 and BAK1 suppresses cell death through inactivating CNGC20 activity by phosphorylation. The phosphorylation occurred at C terminus of CNGC20 was substantiated by Mass spectrometry and mutagenesis analysis. Consistent with our data, the free C terminus of CNGCs consists of C-linker, CNBD and CaMBD domains which are essential for the channel regulation and function. A genetic screen for *cpr22* identified many important residues residing in the C terminus of CNGC11/12 which is identical with C-terminus of CNGC12 (Abdel-Hamid et al., 2013). In addition, CNGC20 possesses the longest N-terminus among all the CNGC members in *Arabidopsis*. The N-terminus of CNGC20 can also interact with BAK1 and can be phosphorylated by BAK1 in vitro, indicating it may have regulatory function.

It has been well established that CNGCs forms heterotetromer to be fully functional in animal system. It is tempting to speculate that plant CNGCs apply similar mechanism to fulfill its biological function. In line with this hypothesis, we showed that CNGC20 associated with itself. Additionally, CNG17 also forms oligomers involving in PSKR-mediated signaling (Ladwig et al., 2015). More interestingly, the

T560/S617/S618/T619D quadruple phosphor-mimetic mutant displays weaker oligomerization, suggesting that BAK1 inhibits CNGC20 activity probably by affecting its oligomerization via phosphorylation (data not shown here).

It is striking that CNGC20 is essential in the *bak1/serk4* cell death control whereas the other CNGCs have negligible role, including CNGC19, the closest homolog of CNGC20. This suggests that CNGC20 may form homotetramer to be functional in cell death control, which is different with animal CNGC. However, we cannot rule out the possibility that CNGC20 function in other signaling pathways in CNGC20-CNGC19 heterotetramer manner. It has been reported that both CNGC19 and CNGC20 are induced by salt stress (Kugler et al., 2009). In addition, in silicon analysis of CNGC20 showed that CNGC20 exhibited highest expression at senescence stage which indicates that CNGC20 is indeed involved in cell death control (http://bbc.botany.utoronto.ca/efp/cgi-bin/efpWeb.cgi).

Mounting studies showed that BAK1/SERK family are involved in multiple signaling networks, such as cell death control, plant innate immunity, BR-, PSKR- and EPF-triggered plant growth and development. How do the cell determine specificity of BAK1/SERK4? The discovery of *bak1-5* mutant, which carries a mutation in the subdomain preceding the catalytic loop and has weak kinase activity, specially compromised plant innate immunity without affecting plant growth and cell death (Schwessinger et al., 2011). This suggests that phosphorylation events among receptor complex is one of mechanisms determining signaling specificity. In addition, the extensive genetic analysis of higher-order mutants of *serks* suggest that different SERK

member has unequal genetic contributions to different biological processes (Meng et al., 2015; Meng et al., 2016). It is possible that different combinatorial codes of individual SERK members determine functional specificity in different signaling pathways. Another hypothesis we would like to propose is that CNGCs may contribute to determine the signaling specificity. It is tempting to speculate that CNGCs may participate in diverse signaling by association with BAK1. The diversity of CNGCs in plants and the functional characterization of CNGCs provide another level of regulation of signaling specificity. For example, CNGC17 functions together with BAK1 regulating PSKR signaling (Ladwig et al., 2015). Pep1 induced Ca^{2+} elevation via CNGC2 and PEPR1 recruited BAK1 to initiate the DAMP-triggered immunity signaling (Qi et al., 2010). Consistent with this hypothesis, our data showed that BAK1 function together with CNGC20 to regulate *bak1/serk4* cell death. More importantly, *cngc20* did not suppress *bak1* deficiency in flg22 and BR signaling, reinforcing that the signaling pathway of BAK1/SERK4-regualted cell death is uncoupled from their functions in flg22-triggered immunity and BR-mediated development. Future studies will be focused on to determine channel specificity for CNGC20 and which type of ions contributes to *bak1/serk4* cell death. More importantly, structure of CNGC20-BAK1 will provide insights for the mechanism how BAK1 regulates CNGC20 activity.

The activation of CNGC channel is initiated by binding cyclic nucleotide, including cAMP or cGMP. Further research will be needed to address whether cAMP or cGMP is elevated in the *bak1/serk4* mutant and further activates CNGC20 channel to induce cell death.

4 CONCLUSION

We identified two suppressors of *bak1/serk4* cell death on the basis of virus-induced gene silencing (VIGS) screen of *Arabidopsis* T-DNA insertion mutant collections. The successful application of VIGS of *BAK1*/*SERK4* phenocopies *bak1/serk4* cell death, providing an alternative way to study the *bak1/serk4* cell death. This method is helpful for the genetic lethal mutant examination. Compared with conventional genetic screening, such as EMS screening, T-DNA activation-tagging screening, VIGS is more efficient. We can get suppressors in one generation. Furthermore, the T-DNA library is sequence-indexed, we can easily know the gene identity once we get the suppressor, although the phenotype may not be linked with the annotated gene sometimes, like in the CNGC20 case. Continuing screening will uncover more novel components involved in *bak1/serk4* cell death pathway.

STT3a-mediated *N*-glycosylation and specific endoplasmic reticulum (ER) quality control (ERQC) components are essential to activate *bak1serk4* cell death. Genome-wide transcriptional analysis revealed the activation of members of cysteine-rich receptor-like kinase (*CRK*) genes in the *bak1serk4* mutant. Furthermore, the CRK4-induced cell death depends on STT3a-mediated protein *N*-glycosylation, suggesting that CRK4 as one of STT3a client proteins activates cell death in the *bak1serk4* mutant. However, the *crk4* mutant did not suppress *bak1/serk4* cell death. This may be due to functional redundancy among CRKs. Silencing of BAK1/SERK4 in higher-order of *crk* mutants may provide insights for CRKs involvement in *bak1/serk4* cell death.

In addition, our genetic screen revealed that CNGC20 plays an important role in *bak1/serk4* cell death. Interestingly, *in vivo* and *in vitro* assays indicated that BAK1 directly interacts with and phosphorylates membrane-resident CNGCs. Mass spectrometry and mutagenesis analysis revealed that specific phosphorylation sites of CNGC by BAK1 are indispensable for its function in cell death control.

As an important regulator involved in various processes in plant growth and development, the shoot apical meristem (SAM) growth of *bak1serk4* almost completely ceased one-week after germination (He et al., 2007). It is tempting to speculate that the seedling lethality in *bak1/serk4* might be caused by growth and development defects at the early stage of growth. Future detailed examination of the potential role of BAK1 and SREK4 in the SAM development may provide novel insights on the mechanism of plant cell death control. It is also possible that *bak1serk4* may activate cell death signaling governed by a novel RLK which may directly sense death signature. Identification of death signature and corresponding RLK will broaden our understanding of plant cell death signaling.

In conclusion, our findings unravel novel components and provide mechanistic insights in plant cell death regulation.

REFERENCES

aan den Toorn, M., Albrecht, C., and de Vries, S. (2015). On the Origin of SERKs: Bioinformatics Analysis of the Somatic Embryogenesis Receptor Kinases. Molecular Plant *8*, 762-782.

Abdel-Hamid, H., Chin, K., Moeder, W., Shahinas, D., Gupta, D., and Yoshioka, K. (2013). A Suppressor Screen of the Chimeric AtCNGC11/12 Reveals Residues Important for Intersubunit Interactions of Cyclic Nucleotide-Gated Ion Channels. Plant Physiology *162*, 1681-1693.

Acharya, B.R., Raina, S., Maqbool, S.B., Jagadeeswaran, G., Mosher, S.L., Appel, H.M., Schultz, J.C., Klessig, D.F., and Raina, R. (2007). Overexpression of CRK13, an Arabidopsis cysteine-rich receptor-like kinase, results in enhanced resistance to Pseudomonas syringae. The Plant journal : for cell and molecular biology *50*, 488-499.

Albert, I., Bohm, H., Albert, M., Feiler, C.E., Imkampe, J., Wallmeroth, N., Brancato, C., Raaymakers, T.M., Oome, S., Zhang, H.Q., *et al.* (2015). An RLP23-SOBIR1-BAK1 complex mediates NLP-triggered immunity. Nature Plants *1*, 9.

Albrecht, C., Russinova, E., Hecht, V., Baaijens, E., and de Vries, S. (2005). The Arabidopsis thaliana SOMATIC EMBRYOGENESIS RECEPTOR-LIKE KINASES1 and 2 control male sporogenesis. Plant Cell *17*, 3337-3349.

Balague, C., Lin, B.Q., Alcon, C., Flottes, G., Malmstrom, S., Kohler, C., Neuhaus, G., Pelletier, G., Gaymard, F., and Roby, D. (2003). HLM1, an essential signaling component in the hypersensitive response, is a member of the cyclic nucleotide-gated channel ion channel family. Plant Cell *15*, 365-379.

Belkhadir, Y., Yang, L., Hetzel, J., Dangl, J.L., and Chory, J. (2014). The growth-defense pivot: crisis management in plants mediated by LRR-RK surface receptors. Trends Biochem Sci *39*, 447-456.

Boller, T., and Felix, G. (2009). A Renaissance of Elicitors: Perception of Microbe-Associated Molecular Patterns and Danger Signals by Pattern-Recognition Receptors. In Annual Review of Plant Biology (Palo Alto: Annual Reviews), pp. 379-406.

Bonardi, V., Tang, S.J., Stallmann, A., Roberts, M., Cherkis, K., and Dangl, J.L. (2011). Expanded functions for a family of plant intracellular immune receptors beyond specific recognition of pathogen effectors. Proceedings of the National Academy of Sciences of the United States of America *108*, 16463-16468.

Bouche, N., Yellin, A., Snedden, W.A., and Fromm, H. (2005). Plant-specific calmodulin-binding proteins. In Annual Review of Plant Biology (Palo Alto: Annual Reviews), pp. 435-466.

Bruggeman, Q., Raynaud, C., Benhamed, M., and Delarue, M. (2015). To die or not to die? Lessons from lesion mimic mutants. Frontiers in Plant Science *6*, 22.

Burch-Smith, T.M., Schiff, M., Liu, Y., and Dinesh-Kumar, S.P. (2006). Efficient virus-induced gene silencing in Arabidopsis. Plant Physiol *142*, 21-27.

Chan, C.W.M., Schorrak, L.M., Smith, R.K., Bent, A.F., and Sussman, M.R. (2003). A cyclic nucleotide-gated ion channel, CNGC2, is crucial for plant development and adaptation to calcium stress. Plant Physiology *132*, 728-731.

Chen, K., Du, L., and Chen, Z. (2003). Sensitization of defense responses and activation of programmed cell death by a pathogen-induced receptor-like protein kinase in Arabidopsis. Plant molecular biology *53*, 61-74.

Chen, K., Fan, B., Du, L., and Chen, Z. (2004). Activation of hypersensitive cell death by pathogen-induced receptor-like protein kinases from Arabidopsis. Plant molecular biology *56*, 271-283.

Chinchilla, D., Bauer, Z., Regenass, M., Boller, T., and Felix, G. (2006). The Arabidopsis receptor kinase FLS2 binds flg22 and determines the specificity of flagellin perception. Plant Cell *18*, 465-476.

Chinchilla, D., Shan, L., He, P., de Vries, S., and Kemmerling, B. (2009). One for all: the receptor-associated kinase BAK1. Trends in Plant Science *14*, 535-541.

Chinchilla, D., Zipfel, C., Robatzek, S., Kemmerling, B., Nurnberger, T., Jones, J.D.G., Felix, G., and Boller, T. (2007). A flagellin-induced complex of the receptor FLS2 and BAK1 initiates plant defence. Nature *448*, 497-U412.

Chisholm, S.T., Coaker, G., Day, B., and Staskawicz, B.J. (2006). Host-microbe interactions: Shaping the evolution of the plant immune response. Cell *124*, 803-814.

Clark, S.E., Williams, R.W., and Meyerowitz, E.M. (1997). The CLAVATA1 gene encodes a putative receptor kinase that controls shoot and floral meristem size in Arabidopsis. Cell *89*, 575-585.

Clough, S.J., Fengler, K.A., Yu, I.C., Lippok, B., Smith, R.K., Jr., and Bent, A.F. (2000). The Arabidopsis dnd1 "defense, no death" gene encodes a mutated cyclic nucleotide-gated ion channel. Proc Natl Acad Sci U S A *97*, 9323-9328.

Colcombet, J., Boisson-Dernier, A., Ros-Palau, R., Vera, C.E., and Schroeder, J.I. (2005). Arabidopsis SOMATIC EMBRYOGENESIS RECEPTOR KINASES1 and 2 are essential for tapetum development and microspore maturation. Plant Cell *17*, 3350-3361.

Coll, N.S., Epple, P., and Dangl, J.L. (2011). Programmed cell death in the plant immune system. Cell Death and Differentiation *18*, 1247-1256.

Coll, N.S., Vercammen, D., Smidler, A., Clover, C., Van Breusegem, F., Dangl, J.L., and Epple, P. (2010). Arabidopsis Type I Metacaspases Control Cell Death. Science *330*, 1393-1397.

Cukkemane, A., Seifert, R., and Kaupp, U.B. (2011). Cooperative and uncooperative cyclic-nucleotide-gated ion channels. Trends in Biochemical Sciences *36*, 55-64.

de Oliveira, M.V.V., Xu, G., Li, B., de Souza Vespoli, L., Meng, X., Chen, X., Yu, X., de Souza, S.A., Intorne, A.C., de A. Manhães, A.M.E., *et al.* (2016). Specific control of Arabidopsis BAK1/SERK4-regulated cell death by protein glycosylation. Nature Plants *2*, 15218.

Deng, Y., Srivastava, R., and Howell, S.H. (2013). Protein kinase and ribonuclease domains of IRE1 confer stress tolerance, vegetative growth, and reproductive development in Arabidopsis. Proceedings of the National Academy of Sciences of the United States of America *110*, 19633-19638.

DeYoung, B.J., Bickle, K.L., Schrage, K.J., Muskett, P., Patel, K., and Clark, S.E. (2006). The CLAVATA1-related BAM1, BAM2 and BAM3 receptor kinase-like proteins are required for meristem function in Arabidopsis. Plant Journal *45*, 1-16.

Du, J., Gao, Y., Zhan, Y., Zhang, S., Wu, Y., Xiao, Y., Zou, B., He, K., Gou, X., Li, G., *et al.* (2016). Nucleocytoplasmic trafficking is essential for BAK1- and BKK1-mediated cell-death control. The Plant Journal *85*, 520-531.

Du, J., Verzaux, E., Chaparro-Garcia, A., Bijsterbosch, G., Keizer, L.C.P., Zhou, J., Liebrand, T.W.H., Xie, C.H., Govers, F., Robatzek, S., *et al.* (2015). Elicitin recognition confers enhanced resistance to Phytophthora infestans in potato. Nature Plants *1*, 5.

Farid, A., Malinovsky, F.G., Veit, C., Schoberer, J., Zipfel, C., and Strasser, R. (2013). Specialized roles of the conserved subunit OST3/6 of the oligosaccharyltransferase complex in innate immunity and tolerance to abiotic stresses. Plant physiology *162*, 24-38.

Farid, A., Pabst, M., Schoberer, J., Altmann, F., Glossl, J., and Strasser, R. (2011). Arabidopsis thaliana alpha1,2-glucosyltransferase (ALG10) is required for efficient N-glycosylation and leaf growth. Plant Journal *68*, 314-325.

Finka, A., Cuendet, A.F., Maathuis, F.J., Saidi, Y., and Goloubinoff, P. (2012). Plasma membrane cyclic nucleotide gated calcium channels control land plant thermal sensing and acquired thermotolerance. Plant Cell *24*, 3333-3348.

Fischer, C., Kugler, A., Hoth, S., and Dietrich, P. (2013). An IQ Domain Mediates the Interaction with Calmodulin in a Plant Cyclic Nucleotide-Gated Channel. Plant and Cell Physiology *54*, 573-584.

Frietsch, S., Wang, Y.F., Sladek, C., Poulsen, L.R., Romanowsky, S.M., Schroeder, J.I., and Harper, J.F. (2007). A cyclic nucleotide-gated channel is essential for polarized tip growth of pollen. Proceedings of the National Academy of Sciences of the United States of America *104*, 14531-14536.

Gao, M.H., Liu, J.M., Bi, D.L., Zhang, Z.B., Cheng, F., Chen, S.F., and Zhang, Y.L. (2008). MEKK1, MKK1/MKK2 and MPK4 function together in a mitogen-activated protein kinase cascade to regulate innate immunity in plants. Cell Research *18*, 1190-1198.

Gao, M.H., Wang, X., Wang, D.M., Xu, F., Ding, X.J., Zhang, Z.B., Bi, D.L., Cheng, Y.T., Chen, S., Li, X., *et al.* (2009). Regulation of Cell Death and Innate Immunity by Two Receptor-like Kinases in Arabidopsis. Cell Host & Microbe *6*, 34-44.

Gao, Q.F., Gu, L.L., Wang, H.Q., Fei, C.F., Fang, X., Hussain, J., Sun, S.J., Dong, J.Y., Liu, H., and Wang, Y.F. (2016). Cyclic nucleotide-gated channel 18 is an essential Ca2+ channel in pollen tube tips for pollen tube guidance to ovules in Arabidopsis. Proc Natl Acad Sci U S A.

Gao, X.Q., Chen, X., Lin, W.W., Chen, S.X., Lu, D.P., Niu, Y.J., Li, L., Cheng, C., McCormack, M., Sheen, J., *et al.* (2013). Bifurcation of Arabidopsis NLR Immune Signaling via Ca2+-Dependent Protein Kinases. Plos Pathogens *9*, 14.

Gómez-Gómez, L., and Boller, T. (2000). FLS2: An LRR Receptor–like Kinase Involved in the Perception of the Bacterial Elicitor Flagellin in Arabidopsis. Molecular Cell *5*, 1003-1011.

Gou, X.P., Yin, H.J., He, K., Du, J.B., Yi, J., Xu, S.B., Lin, H.H., Clouse, S.D., and Li, J. (2012). Genetic Evidence for an Indispensable Role of Somatic Embryogenesis Receptor Kinases in Brassinosteroid Signaling. Plos Genetics *8*, 12.

Harding, H.P., Zhang, Y.H., and Ron, D. (1999). Protein translation and folding are coupled by an endoplasmic-reticulum-resident kinase (vol 397, pg 271, 1999). Nature *398*, 90-90.

Haweker, H., Rips, S., Koiwa, H., Salomon, S., Saijo, Y., Chinchilla, D., Robatzek, S., and von Schaewen, A. (2010). Pattern Recognition Receptors Require N-Glycosylation to Mediate Plant Immunity. J Biol Chem *285*, 4629-4636.

He, K., Gou, X.P., Yuan, T., Lin, H.H., Asami, T., Yoshida, S., Russell, S.D., and Li, J. (2007). BAK1 and BKK1 regulate Brassinosteroid-dependent growth and BrassinosteroidIndependent cell-death pathways. Current Biology *17*, 1109-1115.

Heese, A., Hann, D.R., Gimenez-Ibanez, S., Jones, A.M.E., He, K., Li, J., Schroeder, J.I., Peck, S.C., and Rathjen, J.P. (2007). The receptor-like kinase SERK3/BAK1 is a central regulator of innate immunity in plants. Proceedings of the National Academy of Sciences of the United States of America *104*, 12217-12222.

Hong, Z., Kajiura, H., Su, W., Jin, H., Kimura, A., Fujiyama, K., and Li, J.M. (2012). Evolutionarily conserved glycan signal to degrade aberrant brassinosteroid receptors in Arabidopsis. Proceedings of the National Academy of Sciences of the United States of America *109*, 11437-11442.

Howell, S.H. (2013). Endoplasmic reticulum stress responses in plants. Annual review of plant biology *64*, 477-499.

Hua, B.G., Mercier, R.W., Zielinski, R.E., and Berkowitz, G.A. (2003). Functional interaction of calmodulin with a plant cyclic nucleotide gated cation channel. Plant Physiology and Biochemistry *41*, 945-954.

Hua, J. (2013). Modulation of plant immunity by light, circadian rhythm, and temperature. Current opinion in plant biology *16*, 406-413.

Huffaker, A., Pearce, G., and Ryan, C.A. (2006). An endogenous peptide signal in Arabidopsis activates components of the innate immune response. Proceedings of the National Academy of Sciences of the United States of America *103*, 10098-10103.

Huffaker, A., and Ryan, C.A. (2007). Endogenous peptide defense signals in Arabidopsis differentially amplify signaling for the innate immune response. Proc Natl Acad Sci U S A *104*, 10732-10736.

Jehle, A.K., Lipschis, M., Albert, M., Fallahzadeh-Mamaghani, V., Furst, U., Mueller, K., and Felix, G. (2013). The Receptor-Like Protein ReMAX of Arabidopsis Detects the Microbe-Associated Molecular Pattern eMax from Xanthomonas. Plant Cell *25*, 2330-2340.

Jeong, Y.J., Shang, Y., Kim, B.H., Kim, S.Y., Song, J.H., Lee, J.S., Lee, M.M., Li, J.M., and Nam, K.H. (2010). BAK7 displays unequal genetic redundancy with BAK1 in brassinosteroid signaling and early senescence in arabidopsis. Molecules and Cells *29*, 259-266.

Jin, H., Hong, Z., Su, W., and Li, J.M. (2009). A plant-specific calreticulin is a key retention factor for a defective brassinosteroid receptor in the endoplasmic reticulum. Proceedings of the National Academy of Sciences of the United States of America *106*, 13612-13617.

Jin, H., Yan, Z., Nam, K.H., and Li, J.M. (2007). Allele-specific suppression of a defective brassinosteroid receptor reveals a physiological role of UGGT in ER quality control. Molecular Cell *26*, 821-830.

Jinn, T.L., Stone, J.M., and Walker, J.C. (2000). HAESA, an Arabidopsis leucine-rich repeat receptor kinase, controls floral organ abscission. Genes & Development *14*, 108-117.

Jones, D.A., and Jones, J.D.G. (1997). The role of leucine-rich repeat proteins in plant defences. In Advances in Botanical Research Incorporating Advances in Plant Pathology, Vol 24, J.H. Andrews, and I.C. Tommerup, eds. (San Diego: Elsevier Academic Press Inc), pp. 89-167.

Jones, J.D.G., and Dangl, J.L. (2006). The plant immune system. Nature *444*, 323-329.

Jurkowski, G.I., Smith, R.K., Jr., Yu, I.C., Ham, J.H., Sharma, S.B., Klessig, D.F., Fengler, K.A., and Bent, A.F. (2004). Arabidopsis DND2, a second cyclic nucleotide-gated ion channel gene for which mutation causes the "defense, no death" phenotype. Mol Plant Microbe Interact *17*, 511-520.

Kang, J.S., Frank, J., Kang, C.H., Kajiura, H., Vikram, M., Ueda, A., Kim, S., Bahk, J.D., Triplett, B., Fujiyama, K., *et al.* (2008). Salt tolerance of Arabidopsis thaliana requires maturation of N-glycosylated proteins in the Golgi apparatus. Proceedings of the National Academy of Sciences of the United States of America *105*, 5933-5938.

Karlova, R., Boeren, S., Russinova, E., Aker, J., Vervoort, J., and de Vries, S. (2006). The Arabidopsis SOMATIC EMBRYOGENESIS RECEPTOR-LIKE KINASE1 protein complex includes BRASSINOSTEROID-INSENSITIVE1. Plant Cell *18*, 626-638.

Kemmerling, B., Schwedt, A., Rodriguez, P., Mazzotta, S., Frank, M., Abu Qamar, S., Mengiste, T., Betsuyaku, S., Parker, J.E., Mussig, C., *et al.* (2007). The BRI1-associated kinase 1, BAK1, has a Brassinoli-independent role in plant cell-death control. Current Biology *17*, 1116-1122.

Kim, T.W., Guan, S.H., Sun, Y., Deng, Z.P., Tang, W.Q., Shang, J.X., Sun, Y., Burlingame, A.L., and Wang, Z.Y. (2009). Brassinosteroid signal transduction from cell-surface receptor kinases to nuclear transcription factors. Nature Cell Biology *11*, 1254-U1233.

Kinoshita, T., Cano-Delgado, A.C., Seto, H., Hiranuma, S., Fujioka, S., Yoshida, S., and Chory, J. (2005). Binding of brassinosteroids to the extracellular domain of plant receptor kinase BRI1. Nature *433*, 167-171.

Koiwa, H., Li, F., McCully, M.G., Mendoza, I., Koizumi, N., Manabe, Y., Nakagawa, Y., Zhu, J.H., Rus, A., Pardo, J.M., *et al.* (2003). The STT3a subunit lsoform of the arabidopsis oligosaccharyltransferase controls adaptive responses to salt/osmotic stress. Plant Cell *15*, 2273-2284.

Kong, Q., Qu, N., Gao, M.H., Zhang, Z.B., Ding, X.J., Yang, F., Li, Y.Z., Dong, O.X., Chen, S., Li, X., *et al.* (2012). The MEKK1-MKK1/MKK2-MPK4 Kinase Cascade Negatively Regulates Immunity Mediated by a Mitogen-Activated Protein Kinase Kinase Kinase in Arabidopsis. Plant Cell *24*, 2225-2236.

Kugler, A., Kohler, B., Palme, K., Wolff, P., and Dietrich, P. (2009). Salt-dependent regulation of a CNG channel subfamily in Arabidopsis. Bmc Plant Biology *9*, 11.

Ladwig, F., Dahlke, R.I., Stuhrwohldt, N., Hartmann, J., Harter, K., and Sauter, M. (2015). Phytosulfokine Regulates Growth in Arabidopsis through a Response Module at the Plasma Membrane That Includes CYCLIC NUCLEOTIDE-GATED CHANNEL17, H+-ATPase, and BAK1. Plant Cell *27*, 1718-1729.

Lee, J.S., Kuroha, T., Hnilova, M., Khatayevich, D., Kanaoka, M.M., McAbee, J.M., Sarikaya, M., Tamerler, C., and Torii, K.U. (2012). Direct interaction of ligand-receptor pairs specifying stomatal patterning. Genes & Development *26*, 126-136.

Li, J., and Tax, F.E. (2013). Receptor-Like Kinases: Key Regulators of Plant Development and Defense. Journal of Integrative Plant Biology *55*, 1184-1187.

Li, J., Wen, J.Q., Lease, K.A., Doke, J.T., Tax, F.E., and Walker, J.C. (2002). BAK1, an Arabidopsis LRR receptor-like protein kinase, interacts with BRI1 and modulates brassinosteroid signaling. Cell *110*, 213-222.

Li, J., Zhao-Hui, C., Batoux, M., Nekrasov, V., Roux, M., Chinchilla, D., Zipfel, C., and Jones, J.D.G. (2009). Specific ER quality control components required for biogenesis of the plant innate immune receptor EFR. Proceedings of the National Academy of Sciences of the United States of America *106*, 15973-15978.

Li, J.M., and Chory, J. (1997). A putative leucine-rich repeat receptor kinase involved in brassinosteroid signal transduction. Cell *90*, 929-938.

Liebrand, T.W.H., van den Burg, H.A., and Joosten, M. (2014). Two for all: receptor-associated kinases SOBIR1 and BAK1. Trends in Plant Science *19*, 123-132.

Liu, C.Y., Wong, H.N., Schauerte, J.A., and Kaufman, R.J. (2002). The protein kinase/endoribonuclease IRE1 alpha that signals the unfolded protein response has a luminal N-terminal ligand-independent dimerization domain. J Biol Chem *277*, 18346-18356.

Liu, T.T., Liu, Z.X., Song, C.J., Hu, Y.F., Han, Z.F., She, J., Fan, F.F., Wang, J.W., Jin, C.W., Chang, J.B., *et al.* (2012). Chitin-Induced Dimerization Activates a Plant Immune Receptor. Science *336*, 1160-1164.

Liu, Y., and Li, J. (2014). Endoplasmic reticulum-mediated protein quality control in Arabidopsis. Frontiers in plant science *5*, 162.

Lu, D.P., Lin, W.W., Gao, X.Q., Wu, S.J., Cheng, C., Avila, J., Heese, A., Devarenne, T.P., He, P., and Shan, L.B. (2011). Direct Ubiquitination of Pattern Recognition Receptor FLS2 Attenuates Plant Innate Immunity. Science *332*, 1439-1442.

Lu, X., Tintor, N., Mentzel, T., Kombrink, E., Boller, T., Robatzek, S., Schulze-Lefert, P., and Saijo, Y. (2009). Uncoupling of sustained MAMP receptor signaling from early outputs in an Arabidopsis endoplasmic reticulum glucosidase II allele. Proceedings of the National Academy of Sciences of the United States of America *106*, 22522-22527.

Ma, W., Ali, R., and Berkowitz, G.A. (2006). Characterization of plant phenotypes associated with loss-of-function of AtCNGC1, a plant cyclic nucleotide gated cation channel. Plant Physiology and Biochemistry *44*, 494-505.

Ma, Y., Walker, R.K., Zhao, Y.C., and Berkowitz, G.A. (2012). Linking ligand perception by PEPR pattern recognition receptors to cytosolic Ca2+ elevation and downstream immune signaling in plants. Proceedings of the National Academy of Sciences of the United States of America *109*, 19852-19857.

Martinez-Atienza, J., Van Ingelgem, C., Roef, L., and Maathuis, F.J. (2007). Plant cyclic nucleotide signaling. Plant Signal Behav *2*, 540-543.

Maser, P., Thomine, S., Schroeder, J.I., Ward, J.M., Hirschi, K., Sze, H., Talke, I.N., Amtmann, A., Maathuis, F.J.M., Sanders, D., *et al.* (2001). Phylogenetic relationships within cation transporter families of Arabidopsis. Plant Physiology *126*, 1646-1667.

Meng, X., Chen, X., Mang, H., Liu, C., Yu, X., Gao, X., Torii, Keiko U., He, P., and Shan, L. (2015). Differential Function of Arabidopsis SERK Family Receptor-like Kinases in Stomatal Patterning. Current Biology.

Meng, X.Z., Zhou, J.G., Tang, J., Li, B., de Oliveira, M.V.V., Chai, J.J., He, P., and Shan, L.B. (2016). Ligand-Induced Receptor-like Kinase Complex Regulates Floral Organ Abscission in Arabidopsis. Cell Reports *14*, 1330-1338.

Monaghan, J., and Zipfel, C. (2012). Plant pattern recognition receptor complexes at the plasma membrane. Current Opinion in Plant Biology *15*, 349-357.

Nam, K.H., and Li, J.M. (2002). BRI1/BAK1, a receptor kinase pair mediating brassinosteroid signaling. Cell *110*, 203-212.

Nawaz, Z., Kakar, K.U., Saand, M.A., and Shu, Q.-Y. (2014). Cyclic nucleotide-gated ion channel gene family in rice, identification, characterization and experimental analysis of expression response to plant hormones, biotic and abiotic stresses. BMC genomics *15*, 853.

Nekrasov, V., Li, J., Batoux, M., Roux, M., Chu, Z.H., Lacombe, S., Rougon, A., Bittel, P., Kiss-Papp, M., Chinchilla, D., *et al.* (2009). Control of the pattern-recognition receptor EFR by an ER protein complex in plant immunity. Embo Journal *28*, 3428-3438.

Newton, R.P., and Smith, C.J. (2004). Cyclic nucleotides. Phytochemistry *65*, 2423-2437.

Olvera-Carrillo, Y., Van Bel, M., Van Hautegem, T., Fendrych, M., Huysmans, M., Simaskova, M., van Durme, M., Buscaill, P., Rivas, S., Coll, N.S., *et al.* (2015). A Conserved Core of Programmed Cell Death Indicator Genes Discriminates

Developmentally and Environmentally Induced Programmed Cell Death in Plants. Plant Physiology *169*, 2684-2699.

Pattison, R.J., and Amtmann, A. (2009). N-glycan production in the endoplasmic reticulum of plants. Trends in plant science *14*, 92-99.

Postel, S., Kufner, I., Beuter, C., Mazzotta, S., Schwedt, A., Borlotti, A., Halter, T., Kemmerling, B., and Nurnberger, T. (2010). The multifunctional leucine-rich repeat receptor kinase BAK1 is implicated in Arabidopsis development and immunity. European Journal of Cell Biology *89*, 169-174.

Qi, Z., Verma, R., Gehring, C., Yamaguchi, Y., Zhao, Y.C., Ryan, C.A., and Berkowitz, G.A. (2010). Ca2+ signaling by plant Arabidopsis thaliana Pep peptides depends on AtPepR1, a receptor with guanylyl cyclase activity, and cGMP-activated Ca2+ channels. Proceedings of the National Academy of Sciences of the United States of America *107*, 21193-21198.

Ranf, S., Gisch, N., Schaffer, M., Illig, T., Westphal, L., Knirel, Y.A., and Sanchez-Carballo, P.M. (2015). A lectin S-domain receptor kinase mediates lipopolysaccharide sensing in Arabidopsis thaliana. *16*, 426-433.

Roberts, M., Tang, S.J., Stallmann, A., Dangl, J.L., and Bonardi, V. (2013). Genetic Requirements for Signaling from an Autoactive Plant NB-LRR Intracellular Innate Immune Receptor. Plos Genetics *9*, 15.

Roux, M., Schwessinger, B., Albrecht, C., Chinchilla, D., Jones, A., Holton, N., Malinovsky, F.G., Tor, M., de Vries, S., and Zipfel, C. (2011). The Arabidopsis Leucine-Rich Repeat Receptor-Like Kinases BAK1/SERK3 and BKK1/SERK4 Are Required for Innate Immunity to Hemibiotrophic and Biotrophic Pathogens. Plant Cell *23*, 2440-2455.

Saijo, Y., Tintor, N., Lu, X.L., Rauf, P., Pajerowska-Mukhtar, K., Haweker, H., Dong, X.N., Robatzek, S., and Schulze-Lefert, P. (2009). Receptor quality control in the endoplasmic reticulum for plant innate immunity. Embo Journal *28*, 3439-3449.

Schulze, B., Mentzel, T., Jehle, A.K., Mueller, K., Beeler, S., Boller, T., Felix, G., and Chinchilla, D. (2010). Rapid Heteromerization and Phosphorylation of Ligand-activated

Plant Transmembrane Receptors and Their Associated Kinase BAK1. J Biol Chem *285*, 9444-9451.

Schuurink, R.C., Shartzer, S.F., Fath, A., and Jones, R.L. (1998). Characterization of a calmodulin-binding transporter from the plasma membrane of barley aleurone. Proceedings of the National Academy of Sciences of the United States of America *95*, 1944-1949.

Schwessinger, B., and Ronald, P.C. (2012). Plant Innate Immunity: Perception of Conserved Microbial Signatures. Annual Review of Plant Biology, Vol 63 *63*, 451-482.

Schwessinger, B., Roux, M., Kadota, Y., Ntoukakis, V., Sklenar, J., Jones, A., and Zipfel, C. (2011). Phosphorylation-Dependent Differential Regulation of Plant Growth, Cell Death, and Innate Immunity by the Regulatory Receptor-Like Kinase BAK1. Plos Genetics *7*, 17.

Shen, Y.P., and Diener, A.C. (2013). Arabidopsis thaliana RESISTANCE TO FUSARIUM OXYSPORUM 2 Implicates Tyrosine-Sulfated Peptide Signaling in Susceptibility and Resistance to Root Infection. Plos Genetics *9*, 16.

Shih, H.W., DePew, C.L., Miller, N.D., and Monshausen, G.B. (2015). The Cyclic Nucleotide-Gated Channel CNGC14 Regulates Root Gravitropism in Arabidopsis thaliana. Curr Biol *25*, 3119-3125.

Shiu, S.-H., and Bleecker, A.B. (2001). Receptor-like kinases from Arabidopsis form a monophyletic gene family related to animal receptor kinases. Proceedings of the National Academy of Sciences *98*, 10763-10768.

Shiu, S.H., and Bleecker, A.B. (2003). Expansion of the receptor-like kinase/Pelle gene family and receptor-like proteins in Arabidopsis. Plant Physiol *132*, 530-543.

Shpak, E.D., McAbee, J.M., Pillitteri, L.J., and Torii, K.U. (2005). Stomatal patterning and differentiation by synergistic interactions of receptor kinases. Science *309*, 290-293.

Stenvik, G.E., Tandstad, N.M., Guo, Y., Shi, C.L., Kristiansen, W., Holmgren, A., Clark, S.E., Aalen, R.B., and Butenko, M.A. (2008). The EPIP peptide of INFLORESCENCE DEFICIENT IN ABSCISSION is sufficient to induce abscission in

Arabidopsis through the receptor-like kinases HAESA and HAESA-LIKE2. Plant Cell *20*, 1805-1817.

Strasser, R. (2016). Plant protein glycosylation. Glycobiology.

Sun, T.J., Zhang, Q., Gao, M.H., and Zhang, Y.L. (2014). Regulation of SOBIR1 accumulation and activation of defense responses in bir1-1 by specific components of ER quality control. Plant Journal *77*, 748-756.

Tang, J., Han, Z., Sun, Y., Zhang, H., Gong, X., and Chai, J. (2015). Structural basis for recognition of an endogenous peptide by the plant receptor kinase PEPR1. Cell Res *25*, 110-120.

Tunc-Ozdemir, M., Rato, C., Brown, E., Rogers, S., Mooneyham, A., Frietsch, S., Myers, C.T., Poulsen, L.R., Malho, R., and Harper, J.F. (2013a). Cyclic Nucleotide Gated Channels 7 and 8 Are Essential for Male Reproductive Fertility. Plos One *8*, 8.

Tunc-Ozdemir, M., Tang, C., Ishka, M.R., Brown, E., Groves, N.R., Myers, C.T., Rato, C., Poulsen, L.R., McDowell, S., Miller, G., *et al.* (2013b). A Cyclic Nucleotide-Gated Channel (CNGC16) in Pollen Is Critical for Stress Tolerance in Pollen Reproductive Development. Plant Physiology *161*, 1010-1020.

von Numers, N., Survila, M., Aalto, M., Batoux, M., Heino, P., Palva, E.T., and Li, J. (2010). Requirement of a Homolog of Glucosidase II beta-Subunit for EFR-Mediated Defense Signaling in Arabidopsis thaliana. Molecular Plant *3*, 740-750.

Wang, G.D., Ellendorff, U., Kemp, B., Mansfield, J.W., Forsyth, A., Mitchell, K., Bastas, K., Liu, C.M., Woods-Tor, A., Zipfel, C., *et al.* (2008a). A genome-wide functional investigation into the roles of receptor-like proteins in Arabidopsis. Plant Physiology *147*, 503-517.

Wang, J., Li, H., Han, Z., Zhang, H., Wang, T., Lin, G., Chang, J., Yang, W., and Chai, J. (2015a). Allosteric receptor activation by the plant peptide hormone phytosulfokine. Nature *525*, 265-268.

Wang, Q., Groenendyk, J., and Michalak, M. (2015b). Glycoprotein Quality Control and Endoplasmic Reticulum Stress. Molecules *20*, 13689-13704.

Wang, S., Gu, Y.N., Zebell, S.G., Anderson, L.K., Wang, W., Mohan, R., and Dong, X.N. (2014). A Noncanonical Role for the CKI-RB-E2F Cell-Cycle Signaling Pathway in Plant Effector-Triggered Immunity. Cell Host & Microbe *16*, 787-794.

Wang, T., Liang, L., Xue, Y., Jia, P.F., Chen, W., Zhang, M.X., Wang, Y.C., Li, H.J., and Yang, W.C. (2016). A receptor heteromer mediates the male perception of female attractants in plants. Nature.

Wang, X.F., Kota, U., He, K., Blackburn, K., Li, J., Goshe, M.B., Huber, S.C., and Clouse, S.D. (2008b). Sequential transphosphorylation of the BRI1/BAK1 receptor kinase complex impacts early events in brassinosteroid signaling. Developmental Cell *15*, 220-235.

Wang, Y.F., Munemasa, S., Nishimura, N., Ren, H.M., Robert, N., Han, M., Puzorjova, I., Kollist, H., Lee, S., Mori, I., *et al.* (2013). Identification of Cyclic GMP-Activated Nonselective Ca2+-Permeable Cation Channels and Associated CNGC5 and CNGC6 Genes in Arabidopsis Guard Cells. Plant Physiology *163*, 578-590.

Wu, S., Shan, L., and He, P. (2014). Microbial signature-triggered plant defense responses and early signaling mechanisms. Plant Sci *228C*, 118-126.

Wu, W.Z., Wu, Y.J., Gao, Y., Li, M.Z., Yin, H.J., Lv, M.H., Zhao, J.X., Li, J., and He, K. (2015). Somatic embryogenesis receptor-like kinase 5 in the ecotype Landsberg erecta of Arabidopsis is a functional RD LRR-RLK in regulating brassinosteroid signaling and cell death control. Frontiers in Plant Science *6*, 16.

Ye, J., Rawson, R.B., Komuro, R., Chen, X., Dave, U.P., Prywes, R., Brown, M.S., and Goldstein, J.L. (2000). ER stress induces cleavage of membrane-bound ATF6 by the same proteases that process SREBPs. Molecular Cell *6*, 1355-1364.

Yeh, Y.H., Chang, Y.H., Huang, P.Y., Huang, J.B., and Zimmerli, L. (2015). Enhanced Arabidopsis pattern-triggered immunity by overexpression of cysteine-rich receptor-like kinases. Frontiers in plant science *6*, 322.

Yoshioka, K., Moeder, W., Kang, H.G., Kachroo, P., Masmoudi, K., Berkowitz, G., and Klessig, D.F. (2006). The chimeric Arabidopsis CYCLIC NUCLEOTIDE-GATED ION CHANNEL11/12 activates multiple pathogen resistance responses. Plant Cell *18*, 747-763.

Yu, I.C., Parker, J., and Bent, A.F. (1998). Gene-for-gene disease resistance without the hypersensitive response in Arabidopsis dnd1 mutant. Proceedings of the National Academy of Sciences of the United States of America *95*, 7819-7824.

Yuen, C.C.Y., and Christopher, D.A. (2013). The group IV-A cyclic nucleotide-gated channels, CNGC19 and CNGC20, localize to the vacuole membrane in Arabidopsis thaliana. Aob Plants *5*, 14.

Zhang, Q., Sun, T.J., and Zhang, Y.L. (2015). ER Quality Control Components UGGT and STT3a Are Required for Activation of Defense Responses in Bir1-1. Plos One *10*, 10.

Zhang, W.G., Fraiture, M., Kolb, D., Loffelhardt, B., Desaki, Y., Boutrot, F.F.G., Tor, M., Zipfel, C., Gust, A.A., and Brunner, F. (2013). Arabidopsis RECEPTOR-LIKE PROTEIN30 and Receptor-Like Kinase SUPPRESSOR OF BIR1-1/EVERSHED Mediate Innate Immunity to Necrotrophic Fungi. Plant Cell *25*, 4227-4241.

Zhang, Y.X., Yang, Y.A., Fang, B., Gannon, P., Ding, P.T., Li, X., and Zhang, Y.L. (2010). Arabidopsis snc2-1D Activates Receptor-Like Protein-Mediated Immunity Transduced through WRKY70. Plant Cell *22*, 3153-3163.

Zhang, Z.B., Wu, Y.L., Gao, M.H., Zhang, J., Kong, Q., Liu, Y.A., Ba, H.P., Zhou, J.M., and Zhang, Y.L. (2012). Disruption of PAMP-Induced MAP Kinase Cascade by a Pseudomonas syringae Effector Activates Plant Immunity Mediated by the NB-LRR Protein SUMM2. Cell Host & Microbe *11*, 253-263.

Zhou, L.M., Lan, W.Z., Jiang, Y.Q., Fang, W., and Luan, S. (2014). A Calcium-Dependent Protein Kinase Interacts with and Activates A Calcium Channel to Regulate Pollen Tube Growth. Molecular Plant *7*, 369-376.

Zipfel, C., Kunze, G., Chinchilla, D., Caniard, A., Jones, J.D.G., Boller, T., and Felix, G. (2006). Perception of the bacterial PAMP EF-Tu by the receptor EFR restricts Agrobacterium-mediated transformation. Cell *125*, 749-760.